

<b>REPORT DOCUMENTATION PAGE</b>				<i>Form Approved</i> OMB No. 0704-0188	
The public reporting burden for this collection of information is estimated to average 1 hour per response, including the time for reviewing instructions, searching existing data sources, gathering and maintaining the data needed, and completing and reviewing the collection of information. Send comments regarding this burden estimate or any other aspect of this collection of information, including suggestions for reducing the burden, to Department of Defense, Washington Headquarters Services, Directorate for Information Operations and Reports (0704-0188), 1215 Jefferson Davis Highway, Suite 1204, Arlington, VA 22202-4302. Respondents should be aware that notwithstanding any other provision of law, no person shall be subject to any penalty for failing to comply with a collection of information if it does not display a currently valid OMB control number. <b>PLEASE DO NOT RETURN YOUR FORM TO THE ABOVE ADDRESS.</b>					
<b>1. REPORT DATE (DD-MM-YYYY)</b> 26-06-2014		<b>2. REPORT TYPE</b> Final		<b>3. DATES COVERED (From - To)</b> 11-Sep-2011 to 20 Mar-2014	
<b>4. TITLE AND SUBTITLE</b>  Research of Ionospheric Scintillation in Asia (RISA)				<b>5a. CONTRACT NUMBER</b> FA2386-11-1-4087	
				<b>5b. GRANT NUMBER</b>  Grant AOARD-114087	
				<b>5c. PROGRAM ELEMENT NUMBER</b> 61102F	
<b>6. AUTHOR(S)</b>  Dr Nitin Kumar Tripathi				<b>5d. PROJECT NUMBER</b>	
				<b>5e. TASK NUMBER</b>	
				<b>5f. WORK UNIT NUMBER</b>	
<b>7. PERFORMING ORGANIZATION NAME(S) AND ADDRESS(ES)</b> Asian Institute of Technology Asian Institute of Technology Pathumthani, Bangkok 12120 Thailand				<b>8. PERFORMING ORGANIZATION REPORT NUMBER</b>  N/A	
<b>9. SPONSORING/MONITORING AGENCY NAME(S) AND ADDRESS(ES)</b>  AOARD UNIT 45002 APO AP 96338-5002				<b>10. SPONSOR/MONITOR'S ACRONYM(S)</b>  AFRL/AFOSR/IOA(AOARD)	
				<b>11. SPONSOR/MONITOR'S REPORT NUMBER(S)</b> AOARD-114087	
<b>12. DISTRIBUTION/AVAILABILITY STATEMENT</b> Distribution A: Approved for public release. Distribution is unlimited.					
<b>13. SUPPLEMENTARY NOTES</b>					
<b>14. ABSTRACT</b> The RISA (Research of Ionospheric Scintillation in Asia) project advanced Ionospheric studies in South-East Asia using space-geodetic systems, in particular by analyzing data acquired using dedicated or available GNSS (Global Navigation Satellite Systems) networks. This project also used activities carried out in the framework of the SCINDA (Scintillation Network Decision Aid) project, which is being implemented by Air Force Research Laboratory in South-East Asia. RISA has investigated the effects of ionospheric scintillation in distributed GNSS networks in Thailand and vicinity and the potential correlation with extreme space weather events. New stations in Asian Institute of Technology, Bangkok; Chiang Mai University, and Phuket have been installed and connected to main SCINDA network. RISA collaborated with International Civil Aviation Organization (ICAO), Boston College, University of California Los Angeles and AMBER projects. This has given an opportunity to develop an intensive research base on impact of solar radiations on Ionosphere as well as Geomagnetism.					
<b>15. SUBJECT TERMS</b> Ionospheric Irregularities, GPS, Global Navigation satellite Systems(GNSS), SCINDA					
<b>16. SECURITY CLASSIFICATION OF:</b>			<b>17. LIMITATION OF ABSTRACT</b>	<b>18. NUMBER OF PAGES</b>	<b>19a. NAME OF RESPONSIBLE PERSON</b> Ingrid J. Wysong, Ph.D.
<b>a. REPORT</b>	<b>b. ABSTRACT</b>	<b>c. THIS PAGE</b>			<b>19b. TELEPHONE NUMBER (Include area code)</b>
U	U	U	SAR	99	+81-3-5410-4409

Report Documentation Page			Form Approved OMB No. 0704-0188		
Public reporting burden for the collection of information is estimated to average 1 hour per response, including the time for reviewing instructions, searching existing data sources, gathering and maintaining the data needed, and completing and reviewing the collection of information. Send comments regarding this burden estimate or any other aspect of this collection of information, including suggestions for reducing this burden, to Washington Headquarters Services, Directorate for Information Operations and Reports, 1215 Jefferson Davis Highway, Suite 1204, Arlington VA 22202-4302. Respondents should be aware that notwithstanding any other provision of law, no person shall be subject to a penalty for failing to comply with a collection of information if it does not display a currently valid OMB control number.					
1. REPORT DATE <b>17 JUL 2014</b>		2. REPORT TYPE <b>Final</b>		3. DATES COVERED <b>11-09-2011 to 20-03-2014</b>	
4. TITLE AND SUBTITLE <b>Research of Ionospheric Scintillation in Asia (RISA)</b>			5a. CONTRACT NUMBER <b>FA2386-11-1-4087</b>		
			5b. GRANT NUMBER		
			5c. PROGRAM ELEMENT NUMBER <b>61102F</b>		
6. AUTHOR(S) <b>Nitin Kumar Tripathi</b>			5d. PROJECT NUMBER		
			5e. TASK NUMBER		
			5f. WORK UNIT NUMBER		
7. PERFORMING ORGANIZATION NAME(S) AND ADDRESS(ES) <b>Asian Institute of Technology, Asian Institute of Technology, Pathumthani, Bangkok 12120, Thailand, NA, NA</b>			8. PERFORMING ORGANIZATION REPORT NUMBER <b>N/A</b>		
9. SPONSORING/MONITORING AGENCY NAME(S) AND ADDRESS(ES) <b>AOARD, UNIT 45002, APO, AP, 96338-5002</b>			10. SPONSOR/MONITOR'S ACRONYM(S) <b>AFRL/AFOSR/IOA(AOARD)</b>		
			11. SPONSOR/MONITOR'S REPORT NUMBER(S) <b>AOARD-114087</b>		
12. DISTRIBUTION/AVAILABILITY STATEMENT <b>Approved for public release; distribution unlimited</b>					
13. SUPPLEMENTARY NOTES					
14. ABSTRACT <b>The RISA (Research of Ionospheric Scintillation in Asia) project advanced Ionospheric studies in South-East Asia using space-geodetic systems, in particular by analyzing data acquired using dedicated or available GNSS (Global Navigation Satellite Systems) networks. This project also used activities carried out in the framework of the SCINDA (Scintillation Network Decision Aid) project, which is being implemented by Air Force Research Laboratory in South-East Asia. RISA has investigated the effects of ionospheric scintillation in distributed GNSS networks in Thailand and vicinity and the potential correlation with extreme space weather events. New stations in Asian Institute of Technology, Bangkok; Chiang Mai University, and Phuket have been installed and connected to main SCINDA network. RISA collaborated with International Civil Aviation Organization (ICAO), Boston College, University of California Los Angeles and AMBER projects. This has given an opportunity to develop an intensive research base on impact of solar radiations on Ionosphere as well as Geomagnetism.</b>					
15. SUBJECT TERMS <b>Ionospheric Irregularities, GPS, Global Navigation satellite Systems(GNSS), SCINDA</b>					
16. SECURITY CLASSIFICATION OF:			17. LIMITATION OF ABSTRACT <b>Same as Report (SAR)</b>	18. NUMBER OF PAGES <b>99</b>	19a. NAME OF RESPONSIBLE PERSON
a. REPORT <b>unclassified</b>	b. ABSTRACT <b>unclassified</b>	c. THIS PAGE <b>unclassified</b>			



# FINAL PROJECT REPORT

for AOARD GrantFA2386-11-1-4087

## **Research of Ionospheric Scintillation in Asia (RISA)**

Period of Performance: 1 September 2011 – 20 March 2014

March 2014



Final Report for AOARD Grant FA2386-11-1-4087

**Title of Project:** Research of Ionospheric Scintillation in Asia (RISA)

**Key Researchers**

1. Nitin Kumar Tripathi, Principal Investigator
2. Durairaju Kumaran Raju,
3. Rui Manuel da Silva Fernandes

**Affiliation & Address of Researchers:**

1. School of Engineering and Technology, Asian Institute of Technology  
P.O. Box 4, Klong Luang, Pathumthani 12120, THAILAND  
Phone: +66 (0) 2524-6392, Fax: +66 (0) 2524-5597; Email: [nitinkt@ait.ac.th](mailto:nitinkt@ait.ac.th)
2. Tropical Marine Science Institute, National University of Singapore 18, Kent  
Ridge Road, 119227, Singapore Phone: +6565165691; Fax: +6568721455;  
Email: [tmsdkr@nus.edu.sg](mailto:tmsdkr@nus.edu.sg)
3. Space & Earth Geodetic Analysis Laboratory, University of Beira Interior, R.  
Marquês d'Ávila e Bolama, 6201-001 Covilhã, Portugal. Phone:  
+351275319891; Fax: +351275319891 Email: [rmanuel@di.ubi.pt](mailto:rmanuel@di.ubi.pt)

Period of Performance: 1 September 2011 – 20 March 2014

## Abstract

The RISA (Research of Ionospheric Scintillation in Asia) project contributed to the development of Ionospheric studies in South-East Asia using space-geodetic systems, in particular by analyzing data acquired using dedicated or available GNSS (Global Navigation Satellite Systems) networks.

This project contributed directly towards the current activities carried out in the framework of the SCINDA (Scintillation Network Decision Aid) project, which is being implemented by AFRL (Air Force Research Laboratory) in South-East Asia. RISA has investigated the effects of ionospheric scintillation in distributed GNSS networks in Thailand and vicinity and the potential correlation with extreme space weather events.

RISA was also able to conduct visits to possible locations in few countries and supported extension of SCINDA network. This also helped in developing interaction with other network of SCINDA GNSS stations in the region. New stations in Asian Institute of Technology, Bangkok; Department of Geography, Chiang Mai University, Chiang Mai-Thailand and Prince of Songkhla University, Phuket have been installed and connected to main SCINDA network.

RISA could contribute towards improving the scientific knowledge on ionosphere research and GNSS data processing of the partners that are collaborating with AFRL in the region. This has also contributed towards doctoral research of two students. These students also helped in maintaining the stations and developing scientific output.

RISA also supported the Thailand stations to develop international collaborations with International Civil Aviation Organization (ICAO), Boston College, University of California Los Angeles and AMBER projects. This has given an opportunity to develop an intensive research base on impact of solar radiations on Ionosphere as well as Geomagnetism.



## Acronyms

AIT	Asian Institute of Technology
AFRL	Air Force Research Laboratory
AMBER	African Meridian B-Field Education and Research
CHGM	Chiang Mai
CMU	Chiang Mai University
Dst-Index	Disturbance Storm Time- Index
EIA	Equatorial Ionospheric Anomaly
GAGAN	GPS-Aided Geo-Augmented Navigation
GPS	Global Positioning System
GNSS	Global Navigation Satellite System
LT	Local Time
NASA	National Aeronautics and Space Administration
QZSS	Quasi-Zenith Satellite System
IPP	Ionospheric Pierce Point
IRI	International Reference Ionosphere
PMBC	Phuket Marine Biological Centre
RISA	Research of Ionospheric Scintillations in Asia
SCINDA	Scintillation Network Decision Aid
SEGAL	Space & Earth Geodetic Analysis Laboratory
S <sub>4</sub>	Scintillation Index
TEC	Total Electron Content
TECU	Total Electron Content Unit
UT	Universal Time

# Content

S.No	Title	Page No.
	<a href="#">Abstract</a>	iii
	<a href="#">Acronyms</a>	iv
1.	<a href="#">Introduction</a>	1
2.	<a href="#">Objectives</a>	1
3.	<a href="#">Scope of the Work</a>	1
4.	<a href="#">System Development and Setup</a>	2
	4.1 <a href="#">GPS SCINDA stations in Thailand</a>	2
	4.2 <a href="#">GPS SCINDA station at AIT, Bangkok</a>	7
	4.3 <a href="#">GPS SCINDA station at CMU, Chiang Mai</a>	10
	4.4 <a href="#">AMBER Stations in Thailand</a>	12
5.	<a href="#">Survey for Extending SCINDA Stations</a>	19
	5.1 <a href="#">Phuket, Thailand</a>	19
	5.2 <a href="#">Dili, Timor-Leste</a>	21
	5.3 <a href="#">Philippines</a>	24
6.	<a href="#">Research Interactions and Collaborations</a>	27
	6.1 <a href="#">ICAO</a>	27
	6.2 <a href="#">Manila Observatory</a>	27
	6.3 <a href="#">Electronic Navigation Research institute (ENRI), Japan</a>	27
7.	<a href="#">Ionospheric Scintillation Research Carried Out</a>	28
	7.1 <a href="#">International Reference Ionosphere Model</a>	29
	7.2 <a href="#">Diurnal mean variations of the GPS TEC, IRI-TEC</a>	30
	7.3 <a href="#">Severe Space Weather Events of March 2012</a>	38
	7.4 <a href="#">Higher Order Ionospheric effects in GPS Positioning</a>	45
8.	<a href="#">List of Publications and Student Research Support</a>	75
9.	<a href="#">Conclusion</a>	79
10.	<a href="#">Future Recommendations</a>	81
	<a href="#">References</a>	82
	<a href="#">Appendix-A: Photo of Monitor in RISA Project Room</a>	
	<a href="#">Appendix-B: Workshop on Ionospheric Scintillations Monitoring using GPS</a>	
	<a href="#">Appendix-C: Visit of Dr. Ingrid Wysong, AOARD for RISA project meeting in 2013.</a>	
	<a href="#">Appendix-D: Summary Meeting with Dr. Susumo SAITO at NUS, Singapore.</a>	

## **1. Introduction**

Equatorial regions suffer errors in positioning by GPS during solar activities. This is caused by influence of solar currents affecting the total electron contents and cause scintillations in the ionosphere.

This project aimed at contributing directly to the current activities carried out in the framework of the SCINDA (Scintillation Network Decision Aid) project, which is being implemented by AFRL (Air Force Research Laboratory) in South-East Asia. RISA will investigate the effects of scintillation in dense GNSS networks. Additionally, RISA has contributed to densify and maintain the network of SCINDA GNSS stations being currently installed in the region. Finally, the activities under RISA could improve the scientific knowledge on ionosphere research and GNSS data processing of the partners that are collaborating with AFRL in the region.

## **2. Objectives**

*Major objectives of RISA project were to support the installation and maintenance of SCINDA systems in SE Asia and study the influence of scintillation events in positioning.*

## **3. Scope of the Work**

The development of scientific knowledge on the Ionosphere and on GNSS data processing by the Asian partners was one of the main interests of the RISA project. AIT, National University of Singapore and SEGAL-Portugal played active roles on these topics by supporting post graduate programmes at AIT (host institute). Few meetings and workshops were conducted related to Ionosphere-focused meeting in order to promote Ionospheric research among interested Asian institutions.

## 4. System Development and Setup

### 4.1 GPSSCINDA Stations in Thailand

The Scintillation Network and Decision Aid (SCINDA) is a network of ground based receivers that monitors scintillations at the UHF and L-band frequencies caused by electron density irregularities in the equatorial ionosphere. Established by the Air Force Research Laboratory (AFRL) to provide regional specification and short term forecasts of scintillation to operational users in real time. The SCINDA ground stations are generally positioned between the ionization crests of the Appleton anomaly, as these locations experience the strongest global levels of scintillation. Figure 4.1 shows the GPS SCINDA stations that were established worldwide.

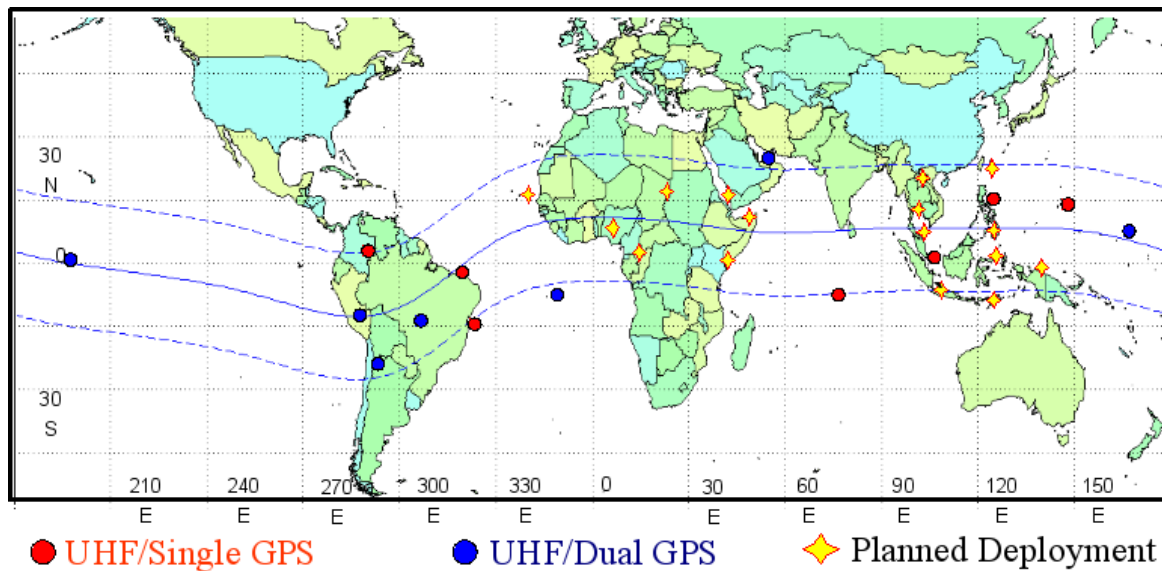


Figure 4.1 GPS-SCINDA worldwide sites

Source: "The GPS Segment of the AFRL-SCINDA Global Network and the Challenges of Real-Time TEC Estimation in the Equatorial Ionosphere" by Charles S. Carrano and Keith M. Groves.

The word "scintillation" typically refers to rapid amplitude and phase fluctuations in a received electromagnetic wave. The cause may be diffractive when electromagnetic waves are scattered in an irregular medium composed of many small changes in the refractive index. The fluctuations in the signal intensity are quantified by the scintillation intensity index  $S_4$  which is defined as follows:

$$S_4 = \frac{\sqrt{\langle I^2 \rangle - \langle I \rangle^2}}{\langle I \rangle}, \quad (1)$$

Where:  $\langle I \rangle$  = mean of the signal intensity.

$S_4$  = the ratio of the standard deviation of the signal intensity to the mean of the signal intensity, calculated for a one minute period based on a 50 Hz sampling rate.

The scintillation index may be interpreted as the fractional fluctuation of the signal ( $S_4 = 0.0$  indicates no modulation whereas  $S_4 = 1.0$  indicates 100% modulation).

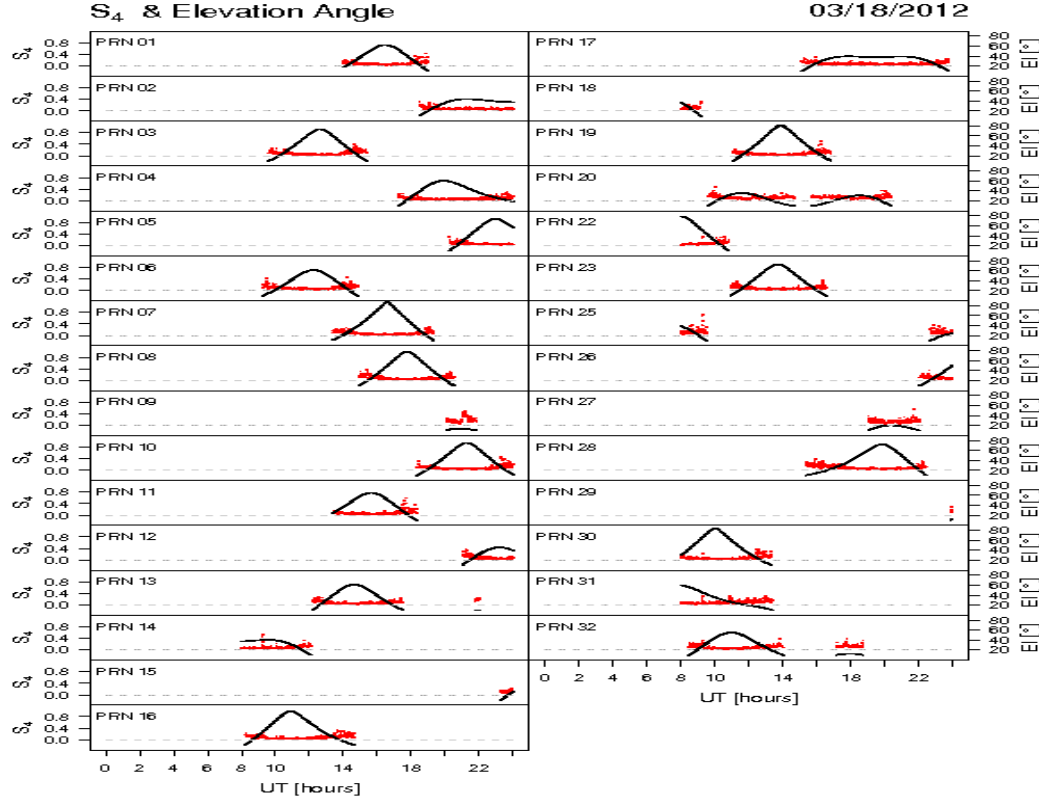


Figure 4.2 S4 & Elevation angle data on 18<sup>th</sup> March, 2012.

The total electron content (TEC), one of the most important parameters for studying the characteristics of the ionosphere, is defined as the integral of the electron number density along the signal path from a satellite to a receiver (Carrano et al., 2006), where 1 TEC unit= $10^{16}$  electrons/m<sup>2</sup>. TEC is computed from the combined L1 (1,575 MHz) and L2 (1,228 MHz) pseudo ranges and carrier phase of GPS signal. The phase and group velocities of signals from satellites are affected as TEC varies. Estimation of the absolute TEC using GPS involves two steps: 1). levelling the phases to the pseudorange gives the relative TEC,

$$TEC_R = TEC_\emptyset + \langle TEC_R - TEC_\emptyset \rangle \quad (2)$$

where  $TEC_\emptyset$  is the differential carrier phase.

and 2). the estimation or removal of instrumental biases (calibration) gives the absolute TEC given by:

$$TEC = TEC_R - (B_R + B_S), \quad (3)$$

Where  $B_R$  and  $B_S$  are the receiver differential code bias (ns) and satellite differential code bias (ns), respectively (Groves and Carrano et al., 2009). The GPS-SCINDA software computes relative TEC (uncalibrated slant TEC) as well as the differential phase and differential pseudo-range among other ionospheric statistics that can be used to get a more precise TEC in post-processing.



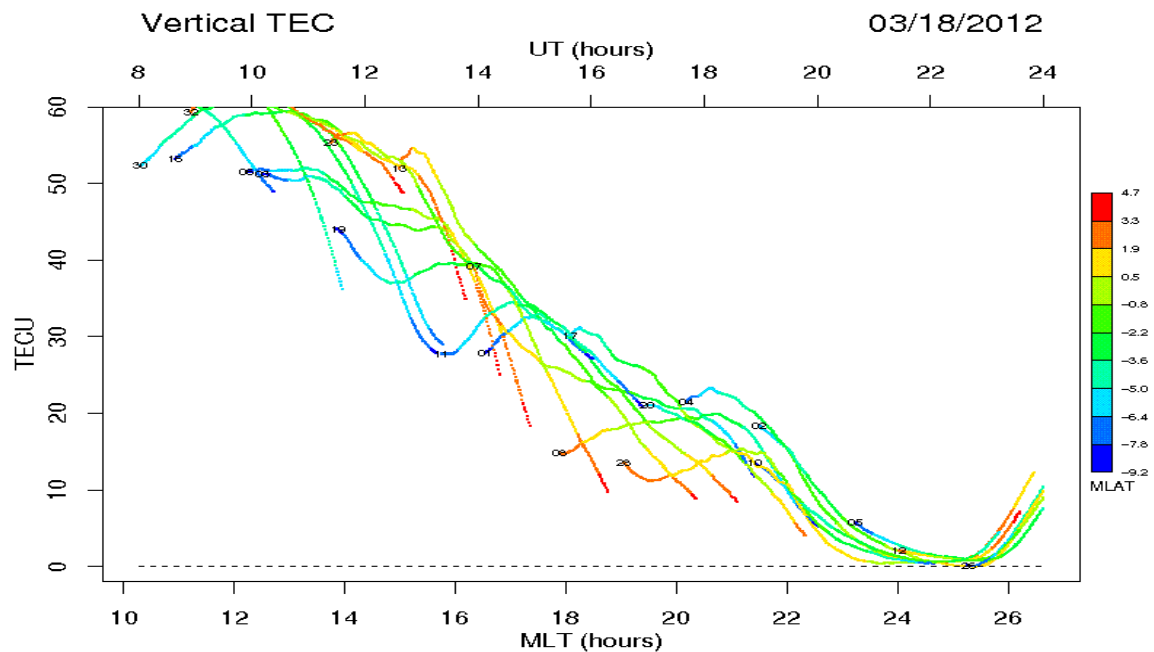


Figure 4.3 Vertical TEC data on 18<sup>th</sup> March, 2012

The GPS-SCRIPT package avails automated data delivery services, data management and is used for performing data backups onto CDROM or DVD media. The GPS-SCINDA derived parameters were recorded at 50Hz sampling rate and an average was made over every sixty (60) seconds and stored in a compressed file. The types of files generated by a GPS SCINDA are differentiated according to their filename extensions.

Literature reviews on scintillation and GNSS can be broadly classified into monitoring and modelling studies and analysis of the both. The Scintillation Network and Decision Aid (SCINDA) is a network of ground based receivers that monitors scintillations at the UHF and L-band frequencies caused by electron density irregularities in the equatorial ionosphere. Established by the Air Force Research Laboratory (AFRL) to provide regional specification and short term forecasts of scintillation to operational users in real time. The SCINDA ground stations are generally positioned between the ionization crests of the Appleton anomaly, as these locations experience the strongest global levels of scintillation (Groves et al., 1997). As a result, large quantities of data sets have become available for analysis. By 2001, the SCINDA network had grown and with it, the knowledge of scintillation impacts on GPS. (Thomas et al. 2001) presented findings from the Pacific sector. In addition to annual summary plots of scintillation levels at Marak Parak and Parepare showing the seasonal and diurnal peaks, he presented regional correlation data that showed if any satellite in the region experienced  $S4 > 0.6$  on at least one link during the night, “there was a mean probability of 75% that the other stations in the network will have at least one link which also records scintillation above  $S4 = 0.6$  on that night”. He also presented the number of satellite links surviving during scintillation episodes, finding that up to 40% of the links were affected under moderate scintillation ( $S4 > 0.6$ ), and over 90% for weak scintillation ( $S4 > 0.3$ ), markedly higher than earlier estimates. In his estimation, this not severe enough to significantly hamper navigation because the episodes were short lived.

Additionally, in-situ measurements of plasma irregularities have continued and will expand with the anticipated launch of the Communication/Navigation Outage Forecasting System (C/NOFS) (La Beaujardiere et al., 2004). (Thomas et al. 2004) studied GPS precision

degradation in the Pacific sector caused by scintillation during the 1998-2002 portion of the solar cycle. Errors up to 30 m were discovered, with an “underlying seasonal modulation from about 5 m to 15 m”. (J B Ackah et al. 2011) presented the diurnal, seasonal and annual variations of TEC and S4 in Abidjan station. Various other authors presented similar kinds of works at different geographic locations using GPS-SCINDA stations data. Many a studies have been conducted on the effect of extreme space weather events like geomagnetic storms, solar flares, storms and solar maximum and minimum on GNSS signals. Also the effects of solar eclipse, equinoxes and solstices have been keenly monitoring and were analyzed by so far.

Eranna et al. (2010) studied on 50 geomagnetic storms during the period 2005-06 at the low latitude near equatorial station Anantapur and found that the scintillations occur occasionally on the storm date and frequently on the subsequent on both sides of storm days. The magnetic storms produces magnetic disturbances throughout the world are generally characterized by using various magnetic indices like Kp, Ap and DST indices. The Kp index will have a value between 0 and 9 assigned to a certain level of disturbance according to the observed global fluctuations in the magnetic field during a 3 hour interval of universal time (UT). Groves presented some findings regarding scintillation and L-band satellites through 1996. Early data from GPS receivers indicated signal fades exceeding 15 dB were possible and more than one GPS satellite could potentially be dropped during a scintillation event. His follow-up 1997 paper (Groves et al., 1997) described the SCINDA network and the temporal and spatial variations of L-band scintillation in the Atlantic and America sector, along the magnetic dip equator as well as under the anomaly crest.

Additionally, the solar cycle had reached its peak, providing 29 additional fodder for comparisons. Datta-Barua et al. (2003) compared the scintillation impacts on single and dual-frequency GPS users. They found both susceptible to impacts from equatorial scintillation, with the L2 frequency more prone to interruptions. They also note if L2 is lost, dual frequency users can substitute the ionospheric model available to single frequency users and essentially obtain the same precision and availability as L1 users. Thomas et al. (2004) studied GPS precision degradation in the Pacific sector caused by scintillation during the 1998-2002 portion of the solar cycle. Errors up to 30 m were discovered, with an “underlying seasonal modulation from about 5 m to 15 m”. At the same time SCINDA was gaining momentum, serious efforts at modelling ionospheric scintillation produced the WideBand MODel (WBMOD) in 1995. WBMOD is based on climatology and the one-degree phase screen model (Rino et al., 1979). Naturally, comparisons between predicted and observed conditions began. In 1999, Knight et al. (1999) compared predictions with observations in the Pacific sector. They found good agreement between modeled and predicted observations. A similar study by Cervera et al. (2001) supported the earlier work for periods of low sunspot activity, except WBMOD ended scintillation prematurely at night. Few found WBMOD performed poorly during solar maximum at the equatorial stations, underestimating scintillation in some cases by an order of magnitude. WBMOD also predicted the end of nightly scintillation two hours earlier than was observed. Since many weapons systems rely on GPS, a logical step was to investigate the impact of scintillation on various weapons systems. In a modeling study of B-1B and F-15E weapons platforms, Evans (2005) demonstrated that scintillation degrades accuracy and can, if occurring in conjunction with jamming, render GPS unavailable. In the intervening years since Thomas et al. (2001), more has been learned about scintillation and GPS. Thomas’ original exploration and particular presentation, however, was never expanded to include other sites or years. Thomas et al. [2001] wrote “It is desirable to have a more rigorous statistical analysis of the S4

database for specific S4 thresholds, for example, as a function of local solar time and day or month of the year.”

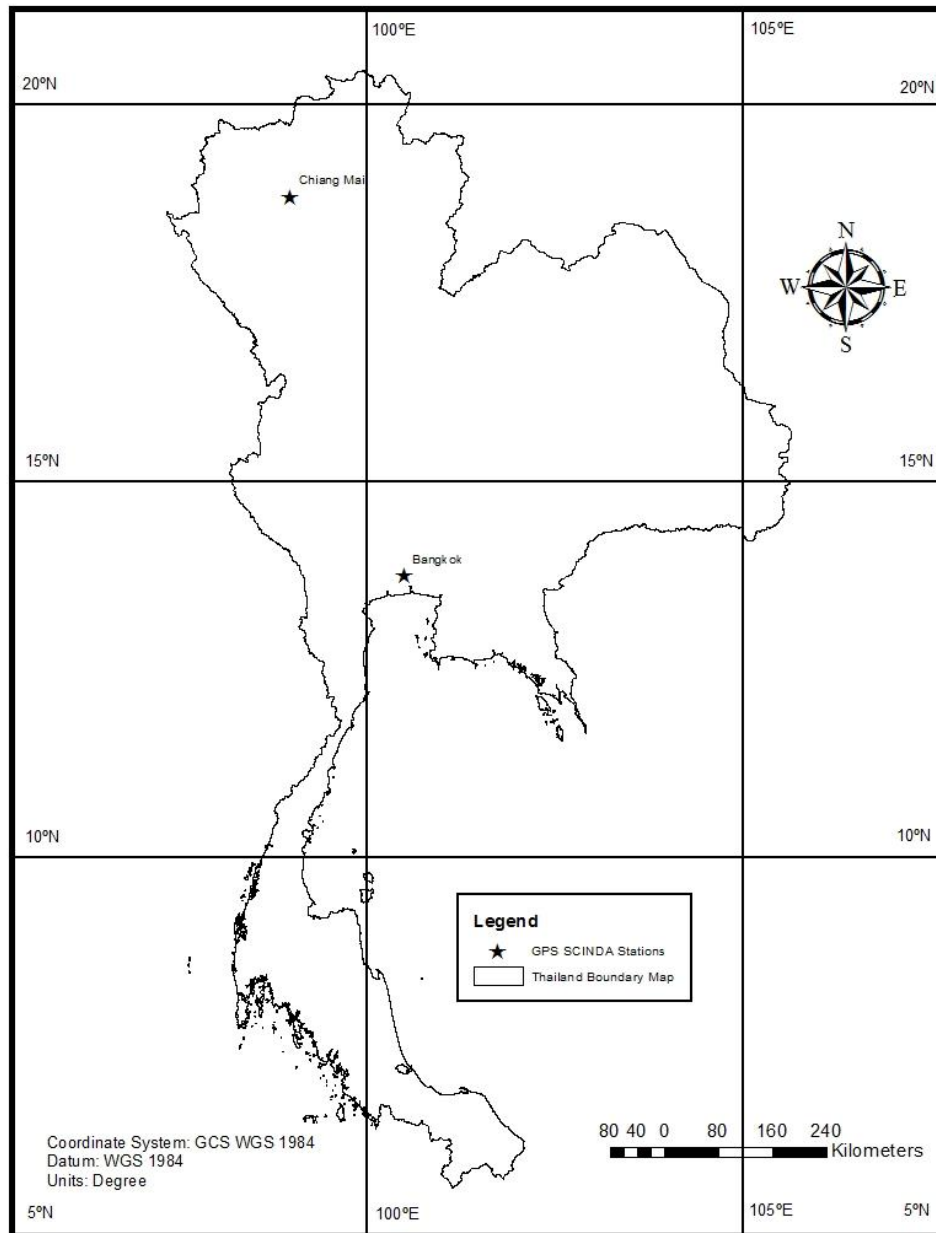


Figure 4.4. Geographic locations of GPS SCINDA stations setup during RISA Project in Thailand.

Two GPS SCINDA stations were installed under this project one at Asian Institute of Technology, (*AIT*,  $14.079^{\circ}N$ ,  $100.612^{\circ}E$ ) and other at Chiang Mai University, (*CHGM*,  $18.480^{\circ}N$ ,  $98.570^{\circ}E$ ), Thailand. Figure 4.4 shows the geographic location of these two stations. These two stations are separated by 657 km in the equatorial anomaly region. The GPSSCINDAsystem consists of a GPS receiver, a GPS antenna, the GPSSCINDAdata collectionsoftware and a computer running the LINUX operating system with access to the Internet. A schematicof the setup is shown in Figure 4.5 below.

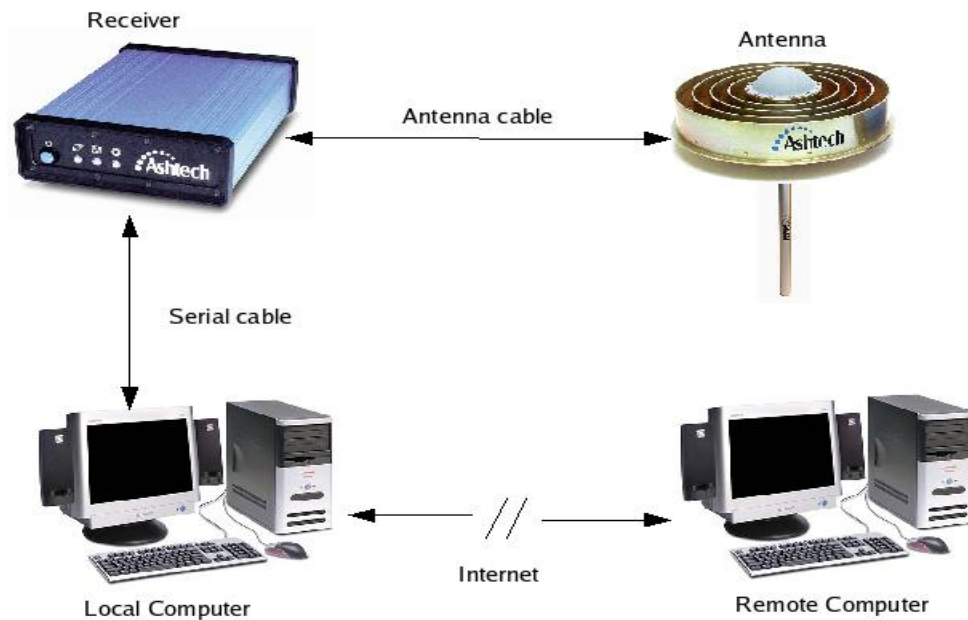


Figure 4.5: GPS SCINDA Station set up

The GPS antenna should be mounted on a pole in clear view of the sky, with a minimum of obstructions nearby (in particular, metallic objects and power lines should be avoided). The antenna is connected to the receiver using the supplied antenna cable. A specialized serial cable connects the GPS receiver to the local computer via its serial port interface. While the system is operating, the receiver tracks the constellation of visible GPS satellites.

The GPSSCINDA software running on the local computer records the stream of data from the receiver and computes postprocessed parameters such as  $S_4$  and TEC, and displays them along with information about which satellites the receiver is tracking on the computer screen. A collection of scripts, written in Perl, is run on the local computer to automatically deliver the postprocessed parameters to the remote computer over the Internet every fifteen minutes. The system is designed so that once properly configured, these tasks are performed automatically without requiring the assistance of an operator. Figure 4.6 shows the SCINDA hardware setup at AIT. A similar setup has been done at Chiang Mai University as well.

## 4.2 GPS SCINDA Station at AIT, Bangkok

As a part of SCINDA's expansion mainly over the equatorial region, a station at Bangkok was established during July 2010.

Person In-charge of AIT station is : Prof. Nitin K. Tripathi of Department of Remote Sensing and GIS in School of engineering and Technology.

It became operational for logging data 24 hours since July 2010 to middle of October 2011. Due to devastating floods of Thailand in October 2011, AIT's SCINDA station was shut down till March 2012. AIT had 2.5 m of water for almost 2 months and was shut down. Since

restored after floods, this station is perfectly in operation with satisfactory data archive. Figure 4.6 shows the hardware setup of SCINDA station at Asian Institute of Technology, Bangkok. The data availability period has been shown in the Table 4.1 for AIT station.

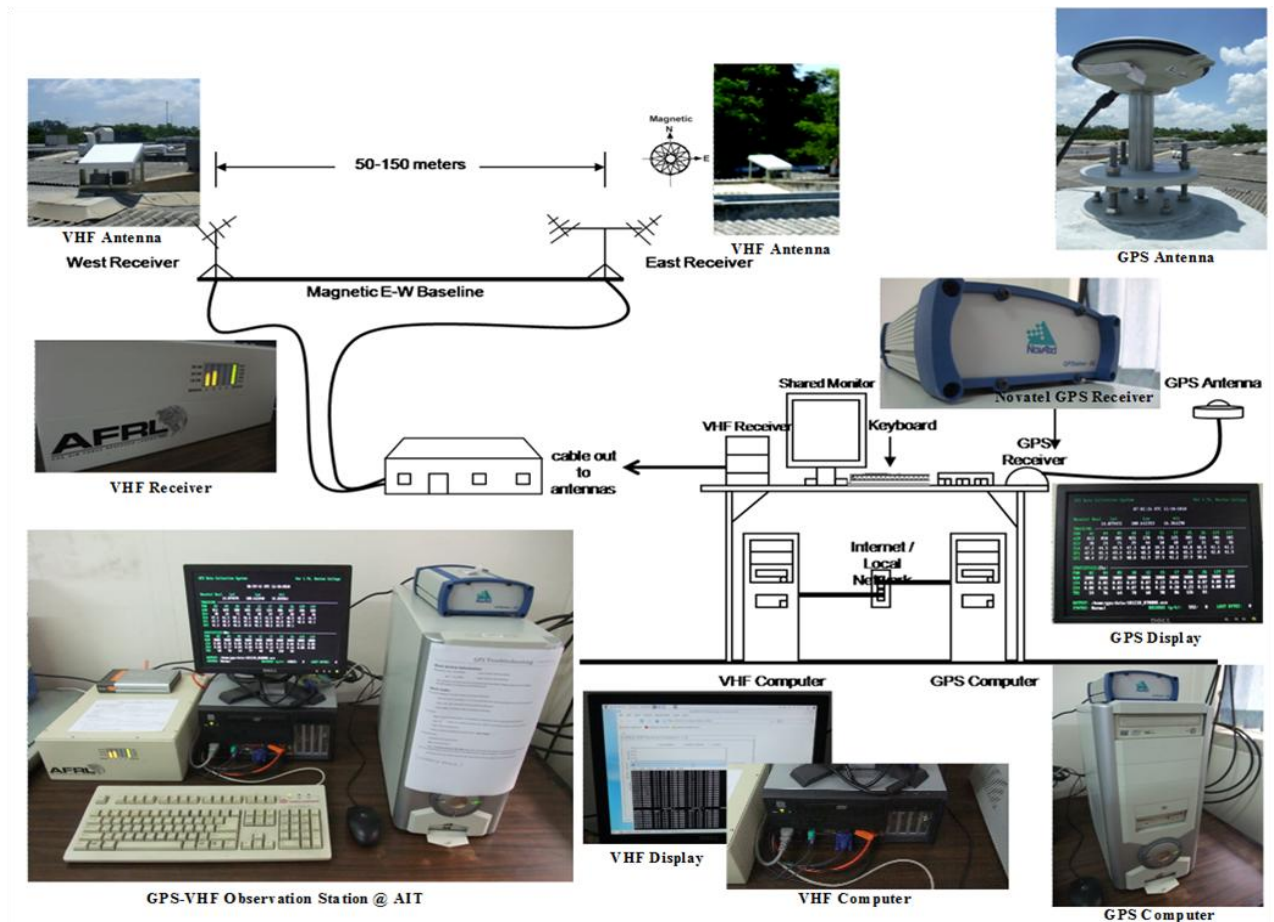


Figure 4.6: SCINDA hardware setup at Asian Institute of Technology, Bangkok.

Table 4.1 Data Availability at AIT station

Year	AIT Bangkok
2010	8 <sup>th</sup> July – 5 <sup>th</sup> Aug 14 <sup>th</sup> Aug – 24 <sup>th</sup> Dec 28 <sup>th</sup> Dec – 28 <sup>th</sup> Dec
2011	3 <sup>rd</sup> Jan – 19 <sup>th</sup> Feb 24 <sup>th</sup> Feb – 4 <sup>th</sup> Mar 6 <sup>th</sup> Mar – 28 <sup>th</sup> Apr 30 <sup>th</sup> Apr – 10 <sup>th</sup> June 13 <sup>th</sup> June – 11 <sup>th</sup> Aug 15 <sup>th</sup> Aug – 18 <sup>th</sup> Sept 20 <sup>th</sup> Sept – 20 <sup>th</sup> Sept 28 <sup>th</sup> Sept – 21 <sup>st</sup> Oct
2012	2 <sup>nd</sup> Mar – 25 <sup>th</sup> Mar 28 <sup>th</sup> Mar – 5 <sup>th</sup> Apr 15 <sup>th</sup> Apr – 18 <sup>th</sup> Apr 24 <sup>th</sup> Apr – 10 <sup>th</sup> May 18 <sup>th</sup> May – 24 <sup>th</sup> May 26 <sup>th</sup> May – 30 <sup>th</sup> Nov 2 <sup>nd</sup> Dec – 3 <sup>rd</sup> Dec 5 <sup>th</sup> Dec – 9 <sup>th</sup> Dec
2013	16 <sup>th</sup> Jan – 16 <sup>th</sup> Feb 18 <sup>th</sup> Feb – 22 <sup>nd</sup> Feb 26 <sup>th</sup> Feb – till

### 4.3 GPS SCINDA station at CMU, Chiang Mai

Another SCINDA station was established in northern part of Thailand, located in Chiang Mau University, Chiang Mai.

Person In-Charge of this station is: Dr. (Ms.) Arisara Charoenpanyanet of Department of Geography in Chiang Mai University.

This station started its operations from 13<sup>th</sup> July, 2010. Table 4.2 illustrates the data availability period for the CMU station. A breakdown in operations took place from December 2012, due to GPS antenna malfunction. A new antenna will be deployed soon in Chiang Mai to continue its operations.

Table 4.2 Data Availability at CMU station

Year	Chiang Mai
2010	13 <sup>th</sup> July – 31 <sup>st</sup> Dec
2011	1 <sup>st</sup> Jan – 8 <sup>th</sup> Feb 11 <sup>th</sup> Feb – 25 <sup>th</sup> June 24 <sup>th</sup> July – 3 <sup>rd</sup> Aug 8 <sup>th</sup> Aug – 14 <sup>th</sup> Nov 19 <sup>th</sup> Nov – 31 <sup>st</sup> Dec
2012	1 <sup>st</sup> Jan – 4 <sup>th</sup> May 8 <sup>th</sup> May – 3 <sup>rd</sup> Sept 29 <sup>th</sup> Sept – 11 <sup>th</sup> Nov 26 <sup>th</sup> Nov – 6 <sup>th</sup> Dec
2013	No Data as the GPS antenna failed



Regarding the operations of this SCINDA station located at Chiang Mai, there has been a data outage since November, 2012. And this issue was raised from the GPS firmware and server hardware.



Figure 4.7 GPS- Antenna located in Chiang Mai University.

RISA team has sent Mr. Sanit Arunpold of AIT to Chiang Mai to troubleshoot the system and to find out the possible solutions during 20<sup>th</sup> -22<sup>nd</sup> November, 2013. The team has examined the system and updated the firmware but problem still persisted. Finally they found that GPS antenna shell was filled with water which was the main reason for underperformance of the system. This was cross checked by using the CMU's antenna in AIT site. This was reported and briefed to Boston College team and requested to ship a new antenna. A new antenna has been shipped on 11<sup>th</sup> April 2014.

Our team will go to Chiang Mai and will install new antenna and will make sure to continue the operations of the SCINDA system. Figure 4.7 shows the updating process of GPS firmware which was done during the check up and maintenance of CMU system.



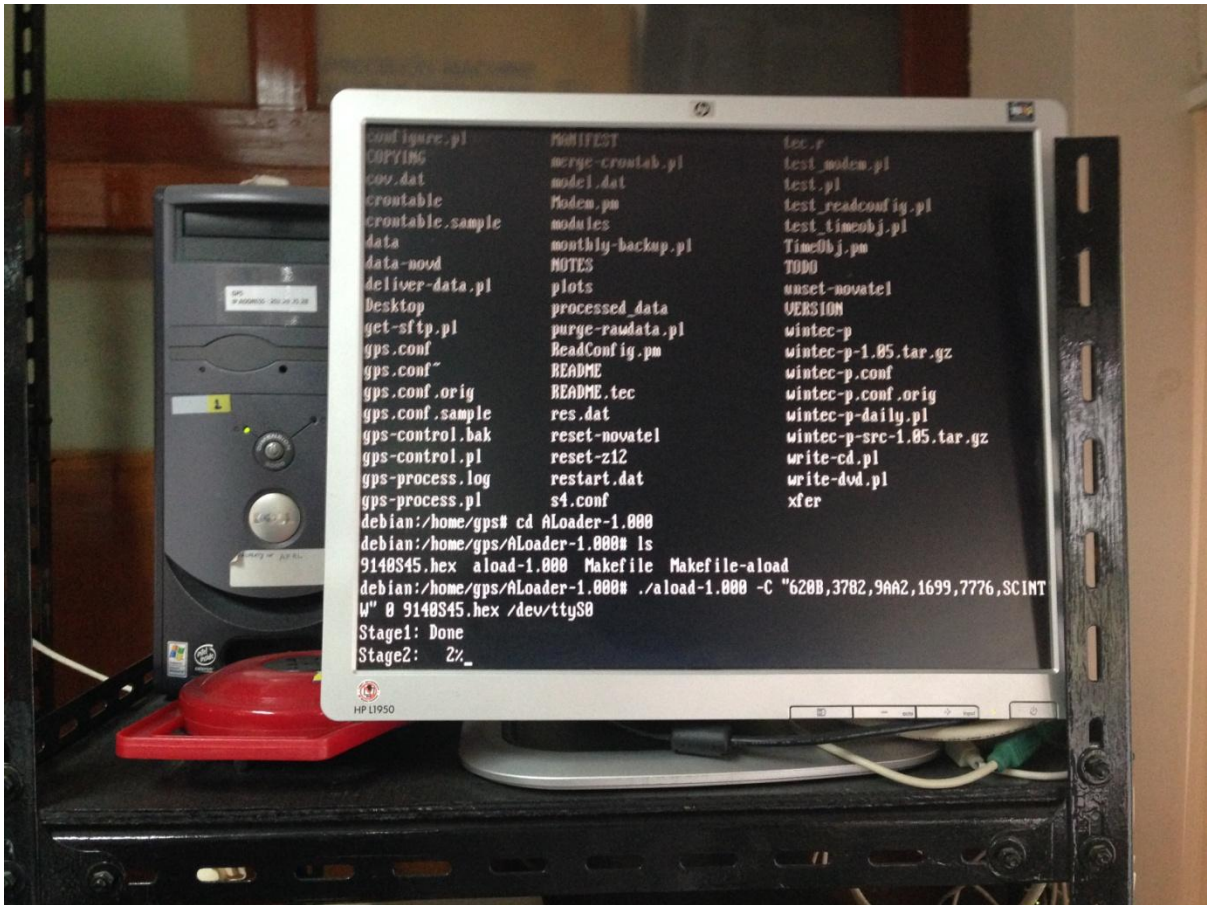


Figure 4.8: Updating process of Novatel GPS receiver firmware

#### 4.4 AMBER Stationsin Thailand

Off late it has been recognized that the observation of ionospheric processes over African continent is the best opportunity for new science. In order to have a complete global understanding of equatorial ionosphere motions, deployment of ground-base magnetometers in Africa is essential. Today over 30 new instrument installations are either installed or in process, and the NASA funded AMBER (African Meridian B-Field Education and Research) magnetometer array is one of those deployed in Africa. After the successful installations of stations in Africa, it has been decided to extend the network across the globe near equatorial region for further research and studies. The figure below shows the current and proposed stations of AMBER network.

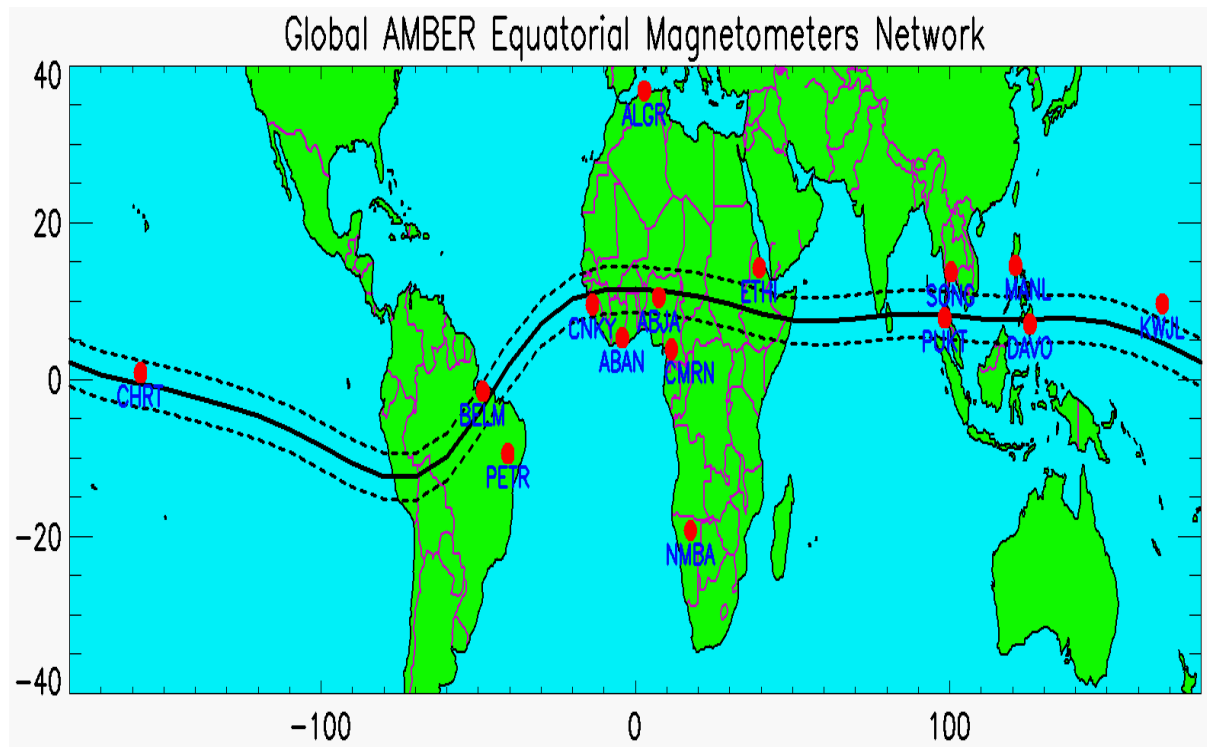


Figure 4.9 Global AMBER Equatorial Magnetometers Network

This AMBER network has given an opportunity to set up 2 magnetometer stations in Thailand. One at Asian Institute of Technology, Bangkok and another at Prince Songkla University, Phuket. Our team was involved in establishing both stations in Thailand. Our team had a visit to Prince Songkla University, Phuket during 6<sup>th</sup> -9<sup>th</sup> April, 2014 for installation of magnetometer. An appropriate location was selected which was away from regular traffic and pedestrians. Below pictures shows the activities carried out in Phuket during installation.













Figure 4.10 Installation of Magnetometer station at Prince Songkla University (PSU), Phuket

GPS Antenna was installed with the magnetometer sensor to set the timing of the instrument. Another GPS antenna was installed for setting up SCINDA station at Phuket. The magnetometer has been successfully installed and data has been tested and verified. Data is archiving and plots can be available at <http://magnetometers.bc.edu/index.php/78-magnetometers/78-home> . Another station was established at Asian Institute of Technology, Bangkok, where SCINDA station was already present. Below figures shows the installation activities carried out at Bangkok. This work has been carried on 10<sup>th</sup> -11<sup>th</sup> April, 2014 at AIT, Bangkok. The data archived and plots can be available from the above mentioned web link.







Figure 4.11 Installation of Magnetometer station at AIT, Bangkok

## **5. Survey for Extending SCINDA stations**

RISA team has visited various geographic locations to position more SCINDA stations across the globe. This section includes the summary of field visits to East-Timor and Sri Lanka for extending station network.

This following tasks describes the activities performed in the framework of the mission carried out as part of the densification and maintenance of the SCINDA network in South East Asia. This mission took place between 3<sup>rd</sup> and 22<sup>nd</sup> February 2012 and it was divided in three parts.

### **5.1 Phuket, Thailand (4<sup>th</sup> – 5<sup>th</sup> February)**

The objectives of the visit to Phuket were two:

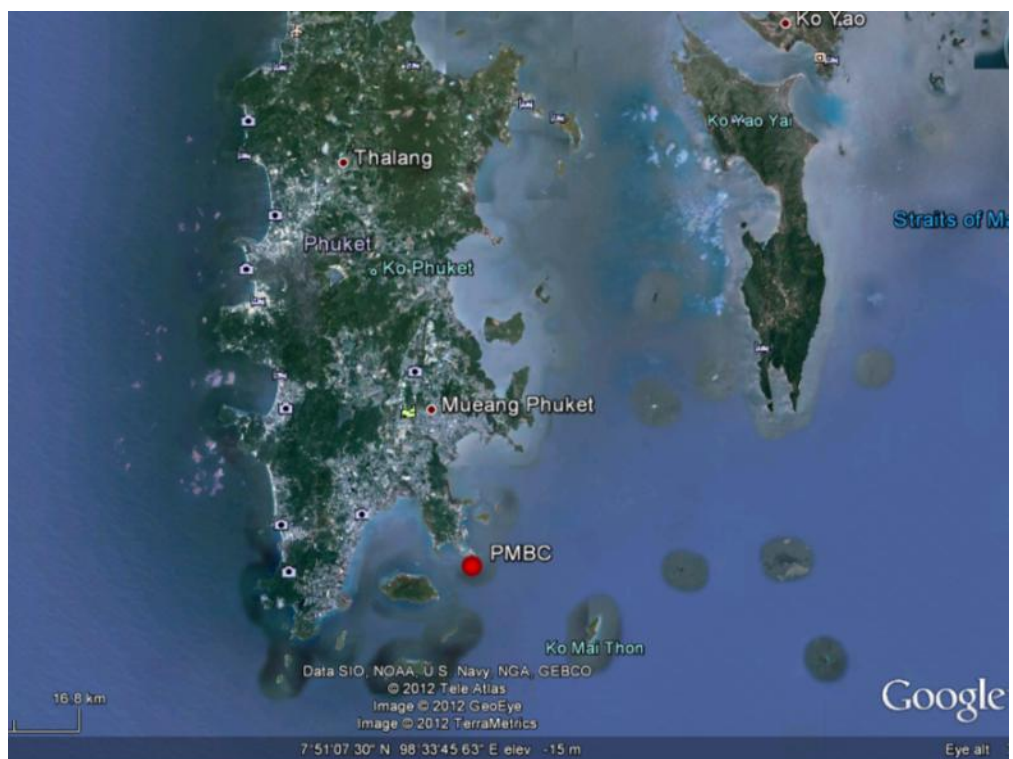
- a) First project meeting between all the collaborators: NitinTarpahi (NT), D.K. Raju (DR), Rui Fernandes (RF), and SanitArunpold (SA) in order to define the work plan for the next six months. The minutes of the meeting are included in annex.
- b) Survey of the potential location for a SCINDA site at the Phuket Marine Biological Center (PMBC). There was a meeting with the Director of the Center (Dr. WannakiatThuthimsang), who shows the complete availability to collaborate in the project. They are willing to provide all conditions for the installation of the equipment. Dr. Nitin can prepare a MoU with them.

There are some doubts concerning the installation of the VHF system since there is an antenna that might interfere with it and the maximum distance that can be reached between the two VHF antennas is around 50m.

The details about the conditions of the location are available in two movies located at: <http://youtu.be/3m-8XXbVTBs> and <http://youtu.be/UC275A3MkG4>.

Approximate geographical location can be observed in the next GE figures:





## 5.2 Dili, Timor-Leste (7<sup>th</sup> – 11<sup>th</sup> February)

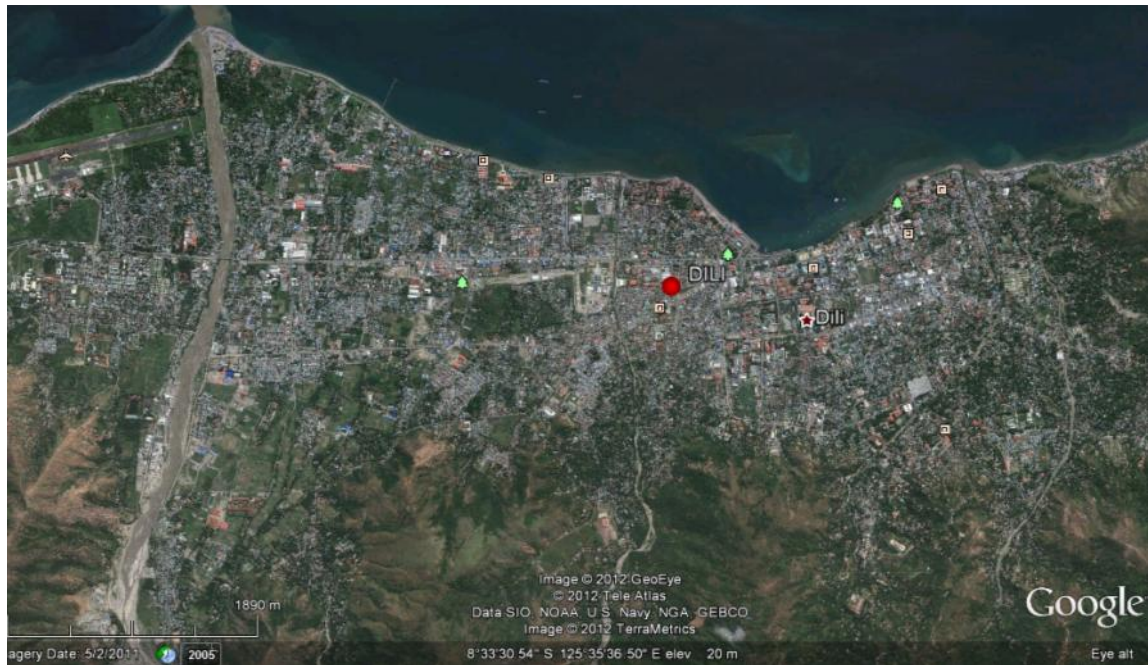
The goal of the mission to Dili was to install a new GPS SCINDA station. It was carried out by DR and RF.

The local partners are the Land Authority that supports the installation and will be responsible for the maintenance of the station. The Point of Contact is Mr. RomãoGuterres (totoromi@yahoo.co.id).

The following GE figures show the approximate geographical location of the DILI station. The antenna is located in the roof top of the National Directorate of Registry and Notary building, just opposite to the building of the National Land Authority (DNTP).







The following pictures describe the installation setup of the station:





**View of the DNTP building from the antenna**

The station was commissioned and tested. It is working but it should be considered to improve the reliability of the power supply (solar panels) due to the present existing conditions in Dili.

### **5.3 Philippines (12<sup>th</sup> – 19<sup>th</sup> February)**

The goal of the mission to Philippines was to evaluate the present conditions of the existing SCINDA stations in Philippines (Davao, Manila, and Baguio). It was carried out by RF.

#### *Davao*

The station was not transmitting data due to communication problems. Therefore, the main goal was to try to recover the historical data, what has been done. However, we noticed that the communication issues could be solved and in this moment the station is already transmitting the data automatically to the SCINDA server at Boston.

#### *Manila*

The SCINDA systems (GPS and VHF) are located in a very noisy environment since they are surrounded by several mobile network antennas. In addition, the GPS computer is not working properly – it turns off after 15-20 minutes of operation. Its replacement is necessary. The VHF system is also not working properly. It was suggested to relocate the system to the roof top of the Manila Observatory. The azimuth of the building is on E-W direction and this would definitely improve the quality of the site. The local partners are willing to support this recommendation. The next two pictures show the present environment and the building for the relocation.



### *Baguio*

The situation in Baguio needs to be improved in terms of hardware and local support. SCINDA PIs (Ron Caton and Keith Groves) are already aware of the situation and even suggested if RISA can contribute in near future to solve the issues. Namely, the GPS station needs to be replaced (since the receiver is damaged) and also it needs to be relocated in order to also be used for other applications since the present position of the antenna strongly suffers from instability and multi-path. The suggestion is to relocate the computers nearby the guest house managed by Manila Observatory. Next pictures illustrate the issues with the present situation and the suggested new location.





## **6. Research Interactions and Collaborations**

RISA has given a brilliant opportunity to interact with various research groups working on ionosphere and GNSS.

### **6.1 International Civil Aviation Organisation**

RISA team has attended two days Conference on “Ionospheric Study Task Force” at “International Civil Aviation Organization” Bangkok affiliated to “United Nations” during 15<sup>th</sup> -17<sup>th</sup> October 2012. This conference was attended by various countries aviation agencies. During this conference, we organised a 1 day workshop on 17<sup>th</sup> October 2012 with members of the conference at AIT. The meeting discussed the possibilities of data sharing and modelling the ionospheric data for regional forecast, which will be beneficial for aviation companies.

Also we got the opportunity to meet with Indian project GAGAN, team members as well.

### **6.2 Manila Observatory, Philippines**

Under the framework of RISA project to explore the possible technical collaboration with Manila Observatory two day visit was planned during 19 – 20 June, 2013 to discuss about the technical cooperation on ionosphere data interpretation and analysis. The meeting with Manila Observatory was successful and areas of co-operation were identified on data reception from sensors such as Magnetometer, interpretation and tools and techniques for data analysis.

### **6.3 Electronic Navigation Research institute (ENRI), Japan**

Dr. Susumu Saito of Electronic Navigation Research institute (ENRI), Japan lead investigator for GBAS project (GNSS based aviation navigation) visited Tropical Marine Science Institute, NUS on 11<sup>th</sup> February 2013. AIT researchers were also invited to participate in the meeting as part of Dr Susumu visit. The interaction with Dr Susumu on the ongoing research on ionosphere and future collaborations with ENRI group for further enriching our research goals were discussed in detail. Dr Susumu was kind enough on providing expert advice on the scientific research work and also shared some of the analytical tools that can improve the results. The minutes of the meetings with Dr Susumu enclosed in the Appendix-D.



## 7.0 Ionospheric Scintillation Research Carried Out

The equatorial and low latitude ionosphere is always a keen of interest for many researchers across the world. Due to its illustrative features in density and temperature, such as the equatorial ionization anomaly (EIA), the plasma fountain, equatorial electrojet, etc. The horizontal orientation of the geomagnetic field lines at the equator and the shift between the geographic and geomagnetic equator is known to be responsible for these observed features and their longitudinal variations. EIA is characterized by trough at the geomagnetic equator and two peaks (crests) on either side of the equator at about  $15^\circ$  magnetic latitudes (Appleton et al., 1946). Mitra et al., (1946) suggested that the trough exists because plasma produced by photo ionization at great heights over the magnetic equator diffuses downwards and outwards to the north and south leaving depletion at the equator. This leads to the formation of ionization crests on either side of the magnetic equator. Martyn et al., (1947) offered the explanation that the mutually perpendicular east-west electric field and north-south geomagnetic field give rise to an upward electrodynamic ( $\mathbf{E} \times \mathbf{B}$  [ $\mathbf{E}$  being the electric field and  $\mathbf{B}$  the magnetic field intensity]) drift of plasma during the daytime.

Global Positioning System (GPS) observations by dual frequency receivers can be utilized to calculate the estimates of GPS derived ionospheric Total Electron Content (GPS-TEC). GPS-TEC is an important constraint for characterization of the ionosphere and has been proposed as an input to an assimilative model of the ionosphere (Misra et al., 2006). The expansion and variation of the anomaly in electron density is reflected in TEC as the F region forms the largest part of TEC. TEC is a measure of the total number of electrons in a cylinder with a cross section of  $1 \text{ m}^2$  centered on the line of sight from the transmitter on a satellite to a terrestrial receiver (Bhuyan et al., 2007). Due to dispersive medium of ionosphere it causes a frequency dependent time delay and phase shift on radio frequency waves passing through it. The relative ionospheric delay of the signal is proportional to the total electron content along the ray path (Theodore et al., 1999). The TEC measured along the line of sight of the satellite signal, called the slant TEC, is then converted to the vertical TEC at the Ionospheric Pierce Point (IPP) i.e., the points where the ray paths intersect the shell model of the ionosphere. Vertical TEC (VTEC) is considered as more compact parameter to characterize the TEC over a given receiver position. The TEC serves as a good indicator for the geographical distribution of the ionization of the earth's ionosphere. The TEC data is continuous and can be used to study long term characteristics and the variations of the ionosphere on a wide range of timescales: diurnal, day to day, seasonal, annual, solar cycle and long term (Luhr et al., 2010; Xu et al., 2012). In the last decade, several research works have been carried out on the diurnal, seasonal and annual variations of TEC in low latitude region (Mendes da Costa et al., 2004; Ezquer et al., 2004; Rama Rao et al., 2006; Chauhan et al., 2010; Xu et al., 2012). And many offered comparison results of the measured TEC data obtained from different resources at various locations with various models, such as the IRI models (Bilitza et al., 1998; Jakowski et al., 1998; Ezquer et al., 1998, 2004; Huang et al., 2001; Jodogne et al., 2004; Mosert et al., 2004).

Also, extreme space weather caused by intense solar storms or activities affects the ionosphere by increasing ionization. Irregularities related to rapid spatial and temporal fluctuations in the density of charged particles causes errors in GNSS signals worldwide. The ionosphere is the source of the largest error in the pseudo-range derived from GNSS

observations. Fluctuations in the ionization level during space weather storms can increase the errors in position estimation derived from GNSS observations. One of the first known effects of space weather is the fluctuations in the amplitude and phase of radio signals that transit the ionosphere caused by the irregularity of electron density in the ionosphere (Hey et al., 1946). The principal manifestation of a disturbed ionosphere on GPS signals is ionospheric scintillation, which if sufficiently intense to degrade the signal quality, increases the error in the position estimate, or causes loss of lock on the satellite signal.

## **7.1 International Reference Ionosphere Model**

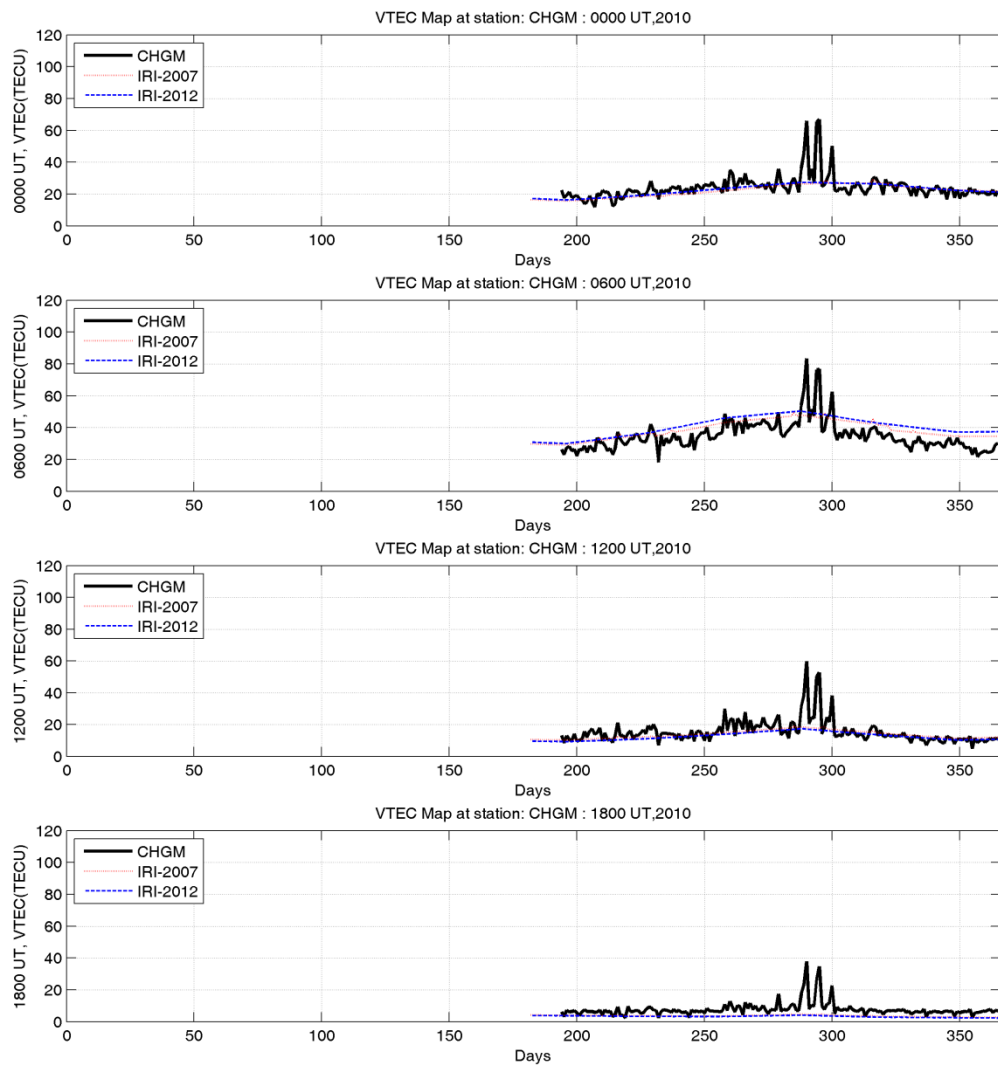
In order to establish an international standard for the specification of ionospheric parameters based on all worldwide available data from both satellite and ground station observations, the International Reference Ionosphere (IRI) project was initiated by the Committee on Space Research (COSPAR) and by the International Union of Radio Science (URSI) in the late 1960's. COSPAR and URSI specifically asked for an empirical IRI model to avoid the uncertainties developing in the theoretical understanding of ionospheric processes and coupling to the regimes below and above. The International Reference Ionosphere, IRI, is an internationally accepted standard model for the measurement of ionospheric parameters. It is pack of various parameters which can derive e.g., electron density, total electron content, electron and ion temperature, ion composition as a function of geographic location, time (LT or UT), height and sunspot number for magnetically quiet days. The IRI model has advanced over time and many significant enhancements have been made through the addition of data available from all the ground stations across the world as well as from satellite observations (Bilitza et al., 2003). More information on the IRI project, including information on the IRI Newsletter and the IRI electronic mailer, can be found on the IRI homepage at <http://IRI.gsfc.nasa.gov/>.

Earlier, model inputs have been mostly from mid-latitudes and the model estimates have explained the ionospheric factors from these regions very well. On the other hand, for equatorial and low mid-latitude regions, many researchers have stated non-compatibility of the earlier model versions. This is due to under or over estimation of TEC for these areas (Scida et al., 2009; Bhuyan and Borah, 2007; Mosert et al., 2007). The IRI-2007 version, for the first time included a model for the occurrence probability of spread F, a characteristic observation which occurs near the magnetic equator during night time (Bilitza and Reinisch, 2008). The IRI-2007 model has been verified in various equatorial and low latitude regions and a good concurrence, in certain parameters, has been recorded between modelled TEC and that acquired from both satellite measurements and ground based GPS receivers (Adewale et al., 2012; Olwendo et al., 2012; Sethi et al., 2011). And recently IRI model was upgraded to IRI-2012 version. This has come up with additional number of indices used by the model namely, 3-hour  $A_p$ -Index, daily  $A_p$ -Index, 3-h  $K_p$ -Index and 81 day Solar Radio Flux F107\_81D.

## 7.2 Diurnal mean variation of the GPS TEC, TEC from the IRI-2007 and IRI-2012 models

Figure 5 a & 5 b shows the comparison between the diurnal median values of GPS TEC, IRI-2007 and IRI-2012 (in TEC units of  $10^{16}/\text{m}^2 = 1\text{TECU}$ ) at Chiang Mai (CHGM) and AITB stations from August 2010 to December 2010, a period of increasing solar activity. Each curve shows the variation of TEC versus the hours representing different times of the day, including 0000 UT (+7 hours LT, sunrise), 0600 UT (midday), 1200UT (post sunset) and 1800UT (midnight) respectively. The black solid line denotes GPS TEC from the observation of the station, dotted red line is the IRI-2007 and dotted blue line is the IRI-2012 predictions respectively.

From figure 5 a it is inferred that both IRI models have shown good agreement with the GPS TEC data during 0000UT. While for 0600UT, models have overestimated TEC values than actual. For 1200UT, IRI-2007 values were observed more than IRI-2012 and were in good agreement with GPS TEC data. But during 1800UT i.e., 0100LT both the models underestimated TEC values. From figure 5 b it can be observed that similar trend has been followed by both model for AITB station as well. Thus from July-December 2010 data confirms that both the models have shown underestimation and overestimation during 0100 LT and 1300 LT for maximum number of days in the year for both stations. Also, maximum TEC values were recorded during 1300LT from the GPS station. A peak is quite evident during 284<sup>th</sup> day for CHGM station which was due to geomagnetic storm on October 11<sup>th</sup> 2010, which was not predicted by both the models. This peak due to storm is not observed at AITB station. Enhancements in TEC during night time were not predicted by the models which were predominant over AITB than at CHGM station. Average highest diurnal TEC value observed from GPS-TEC was 51 and 40 TECU during noon time and lowest being 4 TECU during early morning hours for CHGM and AITB respectively.



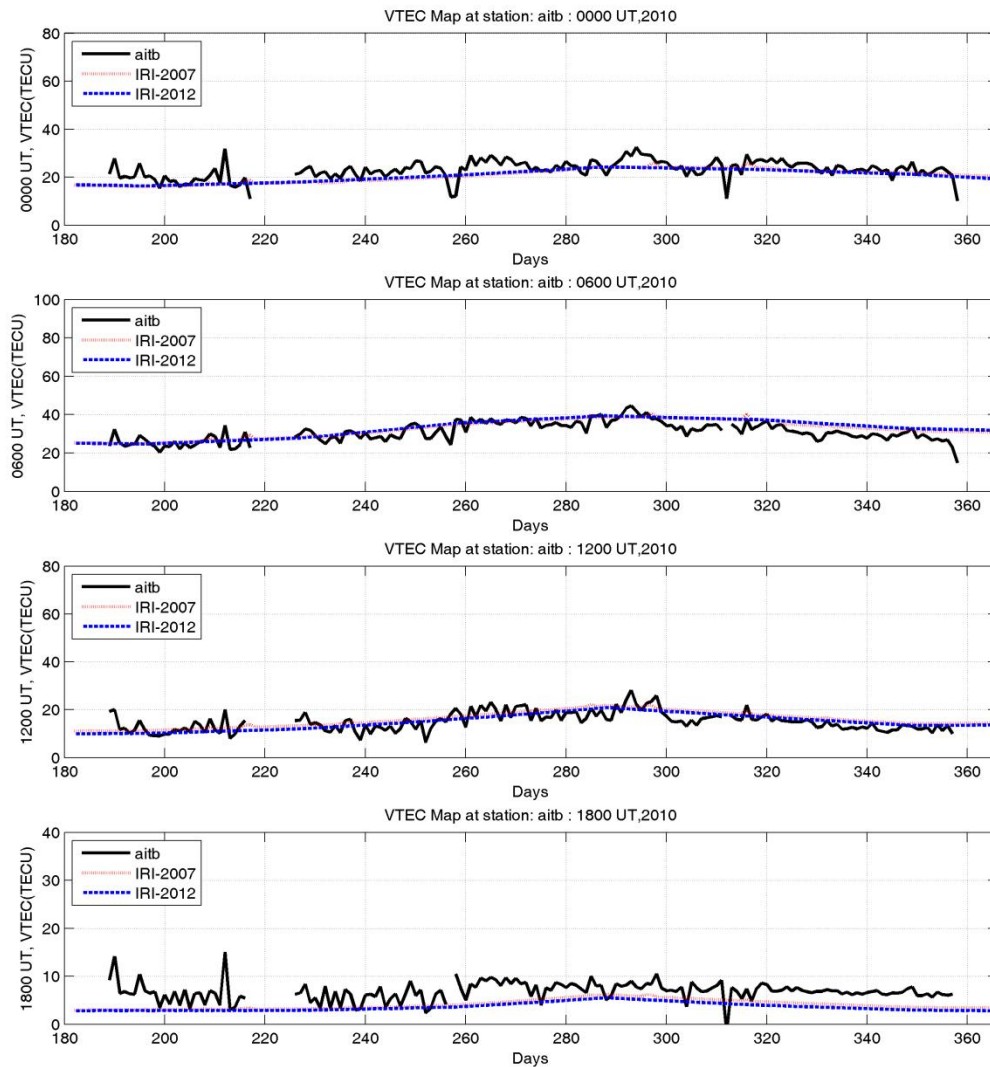
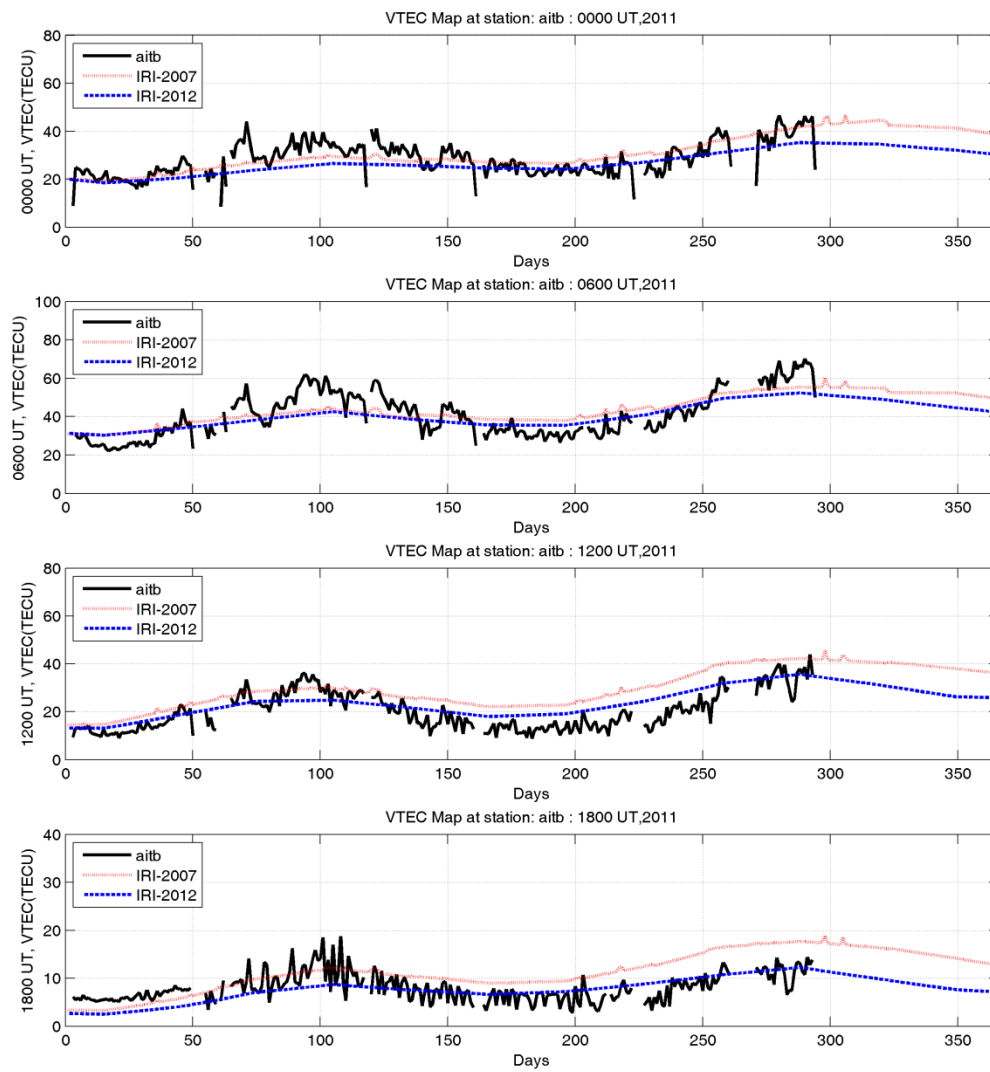


Figure 5 a &5b: Diurnal mean variation of the GPS TEC, TEC from the IRI-2007 model and TEC from the IRI-2012 model, from August, 2010 -December, 2010 at CHGM and AITB respectively.

Figure 6 a &6 b gives the comparison of GPS derived TEC with models derived values for the year 2011 for CHGM and AITB respectively. It can be inferred that due to increase of solar activity and approaching of solar cycle 24, the TEC values showed an increase. During sunrise both the models have shown good correlation with TEC data from GPS stations. But during noon time, both IRI-TEC values show underestimation and overestimation during equinox and solstice seasons, respectively for both stations. And for post sunset IRI-2012 has shown little underestimation whereas IRI-2007 has deviated much more than observed TEC. During midnight IRI-2012 model has shown good agreement with observed values than IRI-2007 model. Thus, it can be clearly seen that for 2011 data, both models have overestimated and underestimated during solstice and equinox respectively. The equinoctial months (March and April) have got particularly high TEC values greater than 60 and 45 TECU, whereas the solstice months (June and July) have maximum values that are lower than 40 TECU for

CHGM and AITB respectively. The observed maximum values of TEC have been attributed to the solar EUV ionization coupled with the upward vertical ExB drift (Bolaji et al. (2012)). In 2011, severe events were occurred during September and October which influenced the TEC values of CHGM but were unpredicted by IRI models. There was a data outage due to floods from October, 2011 to February, 2012. A wave like trend can be observed from the plots, which gives a clear understanding of TEC characteristics. During 50-100 days TEC values increases and reach to a peak and then slowly decreases during 150-200 days. This trend is due to the effect of seasonal variations on the Earth.

Figure 7 a & 7 b shows the data for the year 2012 for CHGM and AITB respectively. From the plot it is clearly stated that TEC values observed from CHGM station has exhibited more compared to previous years and the average value during noontime has peaked from 51 TECU in 2010 to 80 TECU in 2012 respectively. Same applied to AITB as well, from 45 TECU in 2010 to 70 TECU in 2012 respectively. From figure 7 a & b it is observed that IRI-2007 model has totally failed to predict the right values for the TEC by predicting severe overestimation, whereas on the other hand IRI-2012 has been observed to be in good agreement with TEC data. Due to expected peak of solar cycle, the overall observed values of TEC have been increased and have become intense. Number of sunspots also increased, compared to previous year which also resulted in increase in number of severe events. TEC depletions and enhancements were observed during these severe events dates. March 2012 was the most intense month of the whole study. Bhattacharya et al. (2009) studied the diurnal variation of the ionospheric time delay at Bhopal (lat  $23^{\circ}12'N$ ; lon  $77^{\circ}36'E$ ), an equatorial anomaly region, and reported that the diurnal variation was maximum during the equinoctial months. This is in agreement with our study since ionospheric time delay is directly proportional to TEC along the path of propagation.



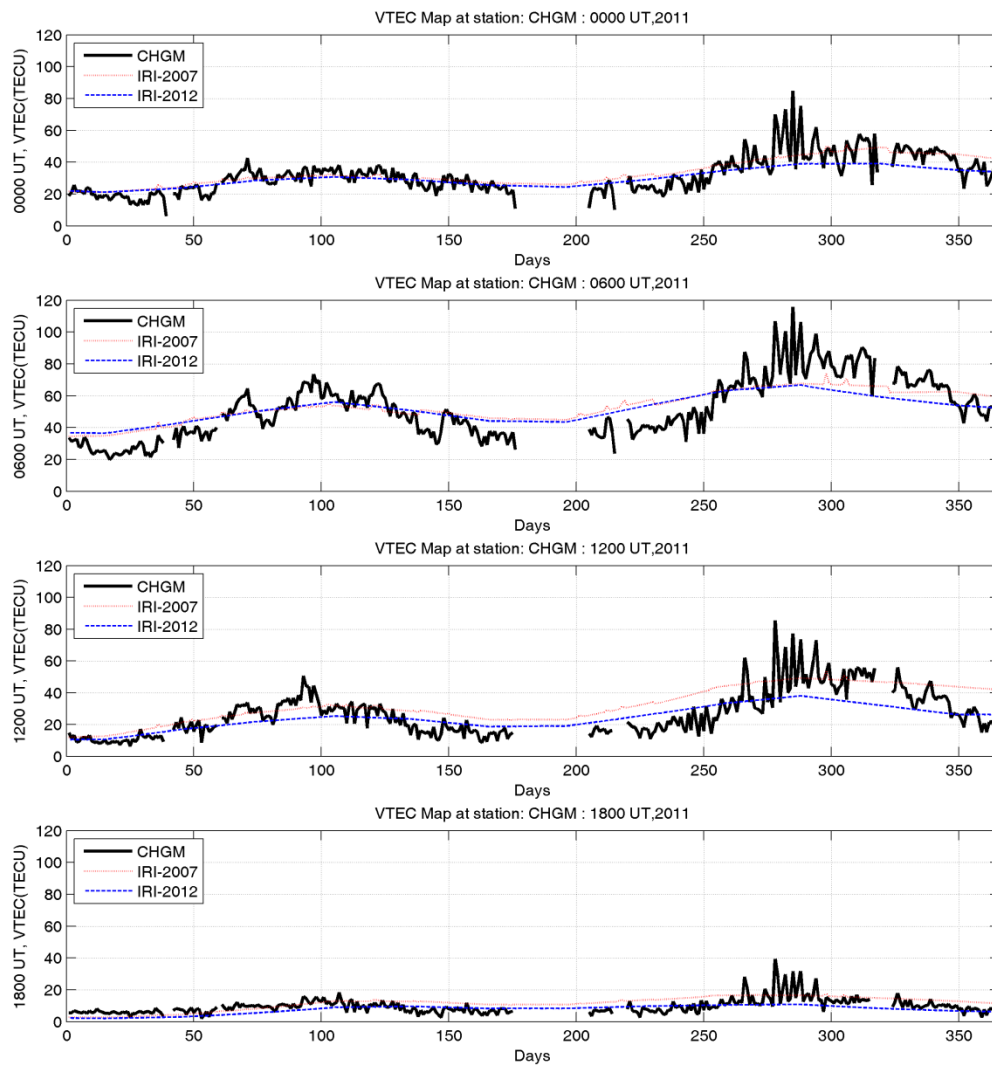
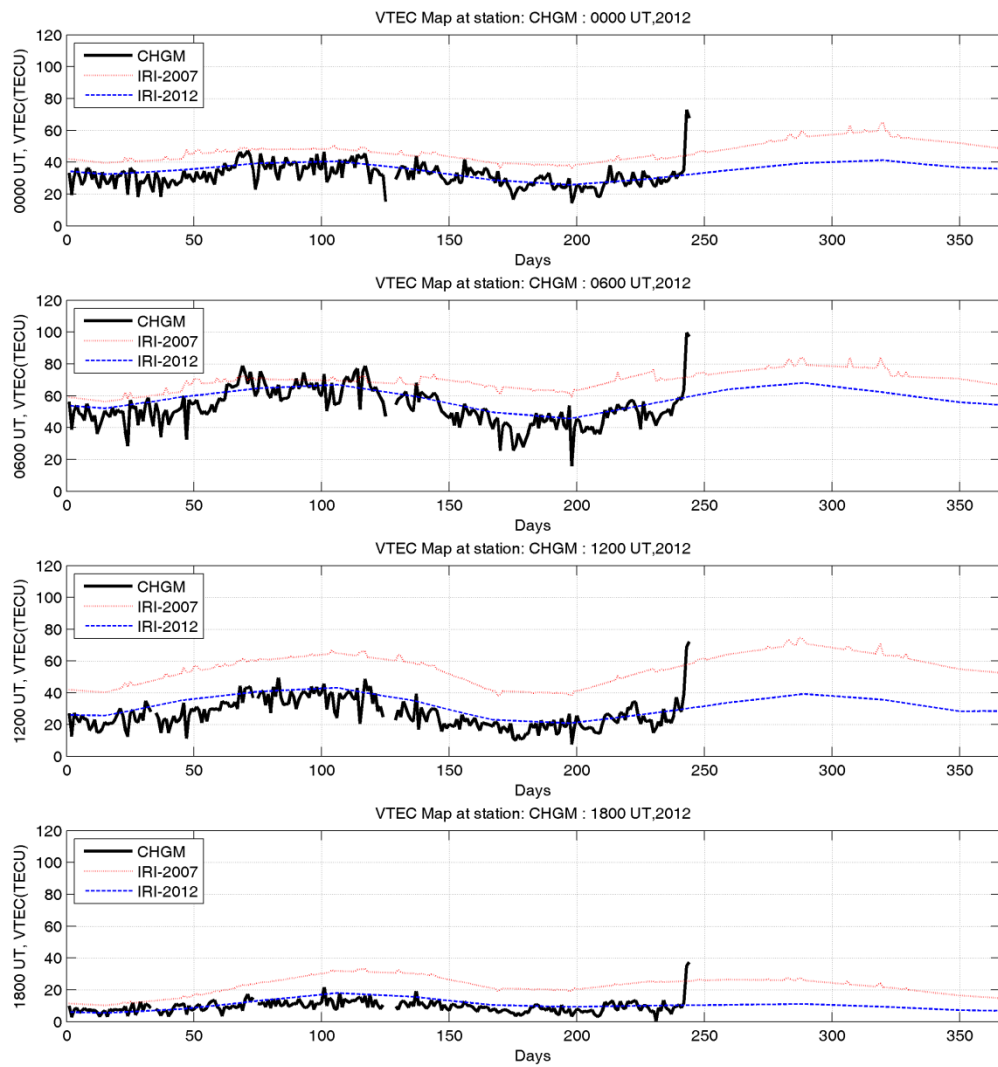


Figure 6 a & 6 b: Diurnal mean variation of the GPS TEC, TEC from the IRI-2007 model and TEC from the IRI-2012 model, for the year 2011 at CHGM & AITB respectively.





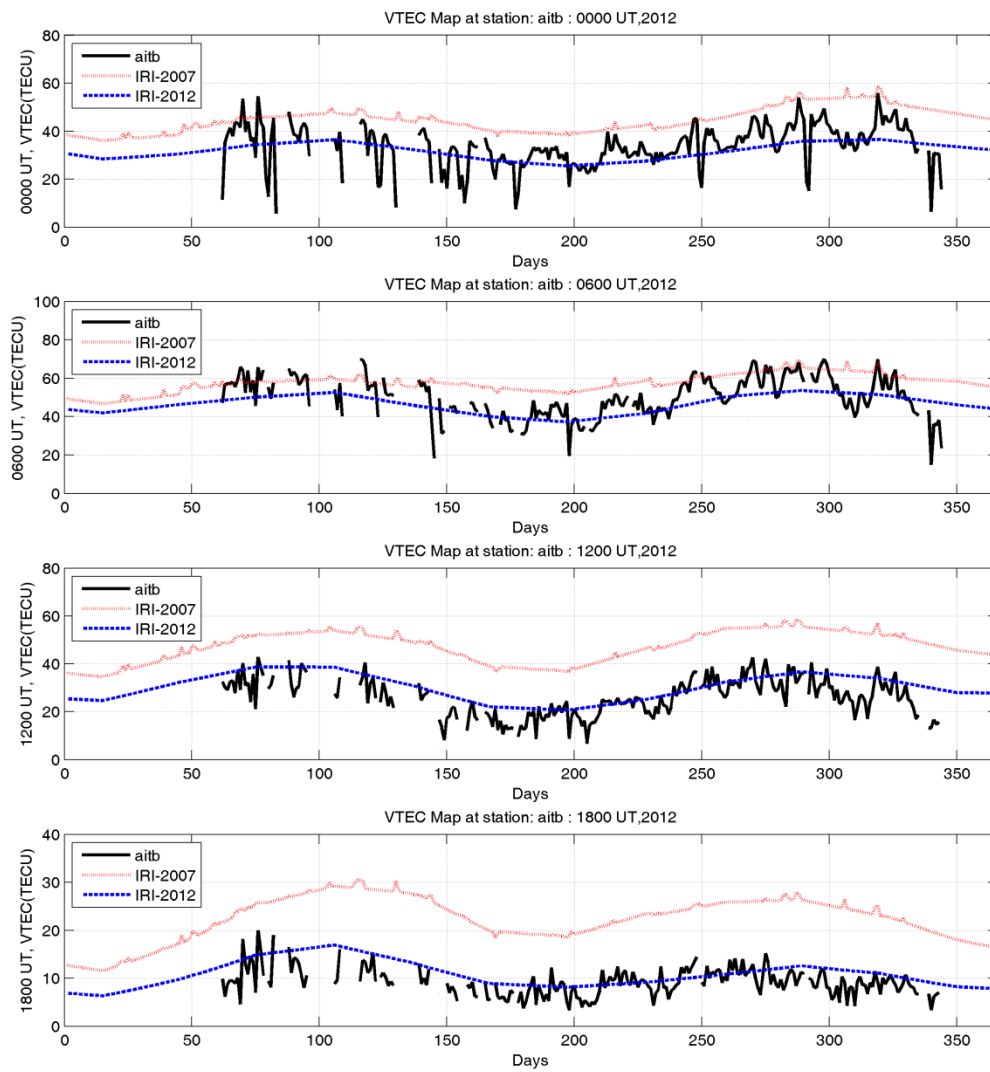


Figure 7 a & 7 b: Diurnal mean variation of the GPS TEC, TEC from the IRI-2007 model and TEC from the IRI-2012 model, from January, 2012 to August, 2012 at CHGM & AITB respectively.

### 7.3 Severe Space Weather Events of March, 2012

A coronal mass ejection (CME) was hurled into space on 7th March 2012 (00:28 UT) and hit the Earth on 8 March 2012 (1100 UT), causing a smaller geomagnetic impact than was expected. The interplanetary and geomagnetic conditions associated with this storm are shown in Table 7.1.

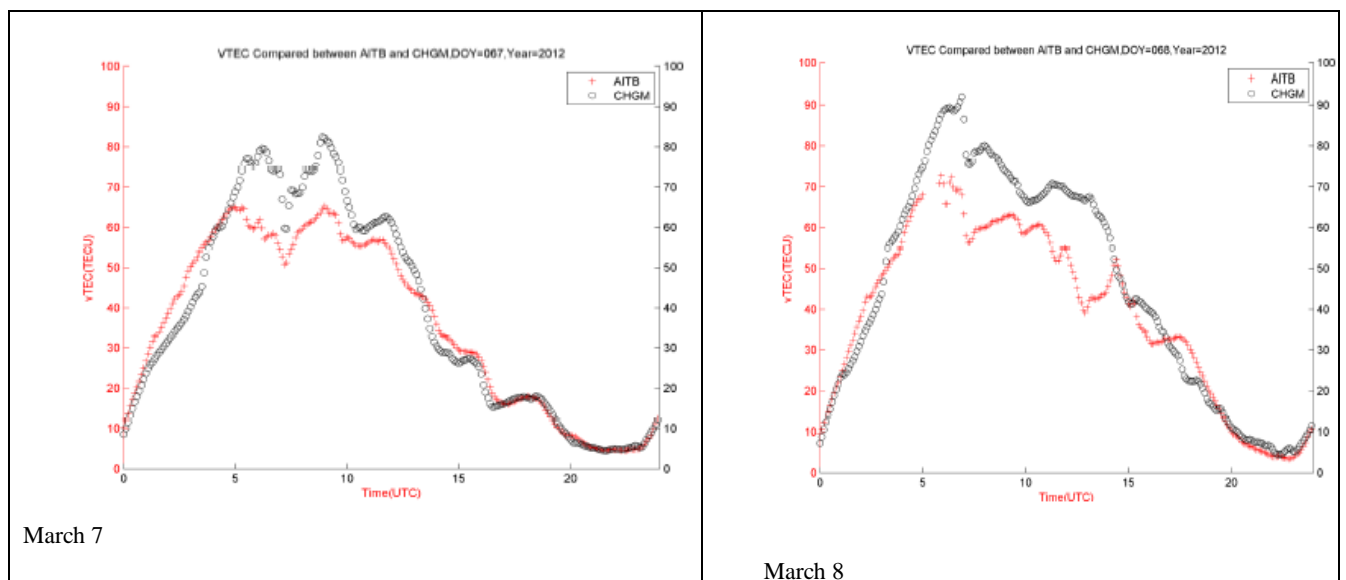
Table 7.1 Data analysis for the month of March

Data	March 7	March 8	March 9	March 10	March 11	March 12	March 13	March 14	March 15
Ap	386	197	696	153	77	269	76	65	285
Solar Wind km/s	292	291	581	476	446	674	492	496	683
Bz nT <0 South	9.6	6.9	-5.3	0.5	-0.7	-3.7	-2.6	-3.1	-1.5
Event CME Coronal hole CH	CME erupted at 00:28 UT	CME hits 11.00 UT weak	High speed CH		CME hits 11.59 UT	CME Geom ag. Storm ~09.30UT Is subsiding			CME hits 13.00 UT
Solar Flare	C2 17.35 UT X5 00.28UT	C2 19.31UT C7 0253UT	C9 20.25UT M603 .53UT	M8 17.45UT	B6 19.42UT C2 03.23UT	C1 23.00UT C2 01.55UT	M7 17.41UT	C1 18.53UT M2 15.21 UT	B8 22.14UT M1 07.52 UT
Sunspot	109	102	86	96	89	103	89	80	75
	March 6 Bz= -5.1 Auroral activity								
Highest TEC at AIT	65	72	87	71	62	69	62	65	54
Highest TEC at CMU	80	92	97	85	80	84	77	70	70
Highest S <sub>4</sub> at AIT	>0.3	0.4	0.3	0.3	>0.3	>0.3	>0.3	0.3	0.35
Highest S <sub>4</sub> at CMU	0.3	0.3	0.3	0.3	>0.3	0.5	>0.4	>0.2	0.5

With reference to the Figure 8 top left panel, on 7<sup>th</sup> March at AIT, TEC value decreased from 65 TECU at 0500 UT to 50 TECU at 0700 UT and then increased to 65 TECU at 0900 UT. A similar phenomenon was observed at the CMU station as well. At CMU, the peak TEC was observed to be 80 TECU at 0600 UT then had depleted to 65 TECU at 0700 UT and then enhanced to 82 TECU at 0900 UT. This depletion in vertical TEC can be attributed due to a geomagnetic storm at mid-latitudes at 0400 UT. The corresponding S<sub>4</sub> values obtained from PRN 12, 18, 25, 26, and 27 were >0.2, >0.2, >0.3, 0.3, and >0.3, respectively (7<sup>th</sup> March at AIT). The TEC peak value of 65 TECU on 7<sup>th</sup> March (0900 UT) increased to 72 TECU on 8<sup>th</sup> March (0600 UT) at AIT and from 80 TECU on 7<sup>th</sup> March (0900 UT) to 92 TECU on 8<sup>th</sup> March (0700 UT) at CMU. On 8<sup>th</sup> March, during 1100 UT – 1300 UT there was

a sudden decrease in TEC from 60 TECU to 40 TECU in data observed from AIT but TEC values rebounded to 52 TECU by 1420 UT. This enhancement in TEC peaks can be attributed to increased ionization of ionosphere due to CME ejections.

The PRN 3,6,16,21,25,30, and 31 were chosen to observe the severe impact of scintillations and subsequent values of  $S_4$  index observed were 0.35,0.4,>0.2,>0.2,0.4,0.3, and >0.2 respectively (on 8<sup>th</sup> March at AIT). As shown in Figure 8 top right panel, a peak TEC of 80 TECU was observed at 0800 UT and then TEC had a downfall to 68 TECU by 1100 UT and then a sudden uplift to 70 TECU at CMU. This depletion was more dominant over AIT location. Figure 8 shows the TEC and  $S_4$  values for 7<sup>th</sup> March – 8<sup>th</sup> March 2012. TEC plots compare both stations' TECU values. The scintillations observed from PRN 6,9,16,19,26,31 were >0.2,>0.2, 0.25,>0.2,0.3,0.3 respectively at CMU on 7<sup>th</sup> March 2012. And the scintillation observed from PRN 4,9,15,16,19,23,25, and 31 were 0.3,>0.2,>0.2,>0.25,>0.2,>0.25,>0.25, and 0.3 respectively at CMU on 8<sup>th</sup> March 2012. One PRN with maximum scintillations from both stations were chosen for plotting. Also, it can be observed that corresponding to TEC oscillations there are intense variations in  $S_4$  index leading to values greater than 0.3. These two stations exhibited consecutive TEC depletion and enhancement phenomenon post-1100 UT. The GPS data for the two days shows large depletions in TEC with corresponding large scintillation indices. The sudden TEC enhancement can be observed around 1500 UT at AIT station.



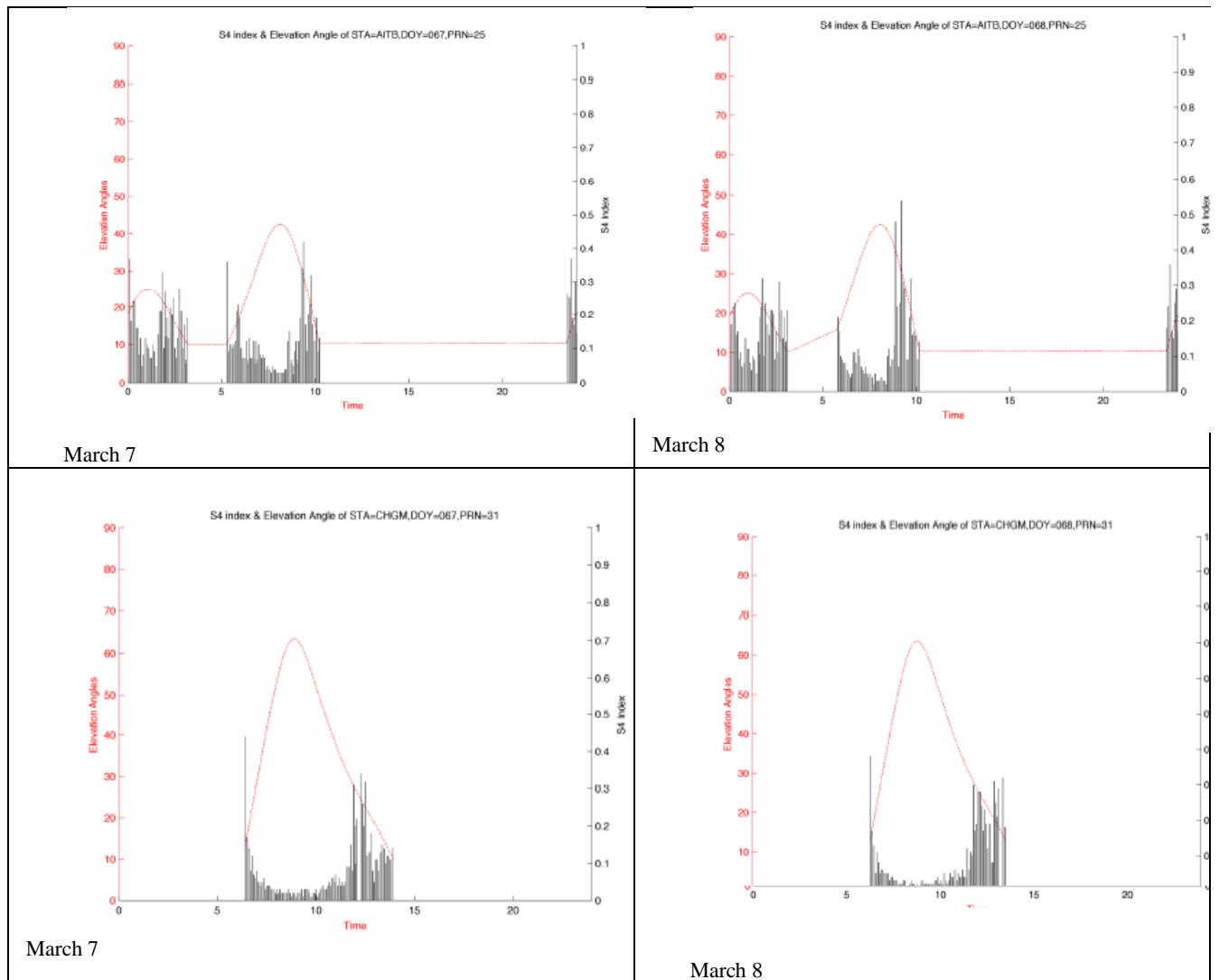


Figure 8: Variations of TEC and S4 during 7<sup>th</sup> -8<sup>th</sup> March 2012 at AIT and CMU stations.

On 9<sup>th</sup> March another strong solar flare of M6-class erupted from the Sun at 0353 UT. The corresponding space weather parameters have been tabulated in Table1. In Figure 9 a's top left panel, TEC oscillations were quite evident from both stations' TEC plot during 0600 UT – 0800 UT. Both stations exhibited their peak TEC as 87 TECU and 95 TECU at 0900 UT, respectively. The S<sub>4</sub> index observed during this particular period reached upto 0.3 for both AIT and CMU stations. As in Figure 9 a's top right panel, on 10<sup>th</sup> March, the TEC depletion process was observed at the AIT station but not at CMU during 1100 UT. The peak TEC values were observed as 71 TECU and 85 TECU at AIT and CMU, respectively. These peaks were observed to be less than previous days due to reforming of the ionosphere to normal quiet conditions. The peak S<sub>4</sub> index observed were as 0.3 for both the stations through PRN 25. As in Figure 9 a's bottom left panel, on 11<sup>th</sup> March, an interplanetary shock wave buffeted Earth's magnetic field at 1159 UT. Due to this abrupt striking, consecutive depletion and enhancements of TEC were observed from both stations. Impulsive fluctuations can be seen from TEC plots for both stations after 1200 UT. During this day, a peak TEC of 62

TECU and 80 TECU were observed at AIT and CMU stations, respectively. This depression in TEC indicates that there could have been plasma uplift due to eastward penetration electric field; and in such a case, the bottom side of the ionosphere presumably lifted and the uplifted plasma was transported away from this region along magnetic fieldlines (Basu et al., 2007; Foster and Coster, 2007; Rao et al., 2009). Also, the  $S_4$  indexes were observed as  $> 0.3$  for both stations. Subsequent plots of  $S_4$  and  $\nu$ TEC variations for both stations are shown in Figures 9 a and 9 b. Since for March 9 and March 10  $S_4$  values at CMU were very similar to those at AIT, plots for CMU have not been shown in Figure 9 b.

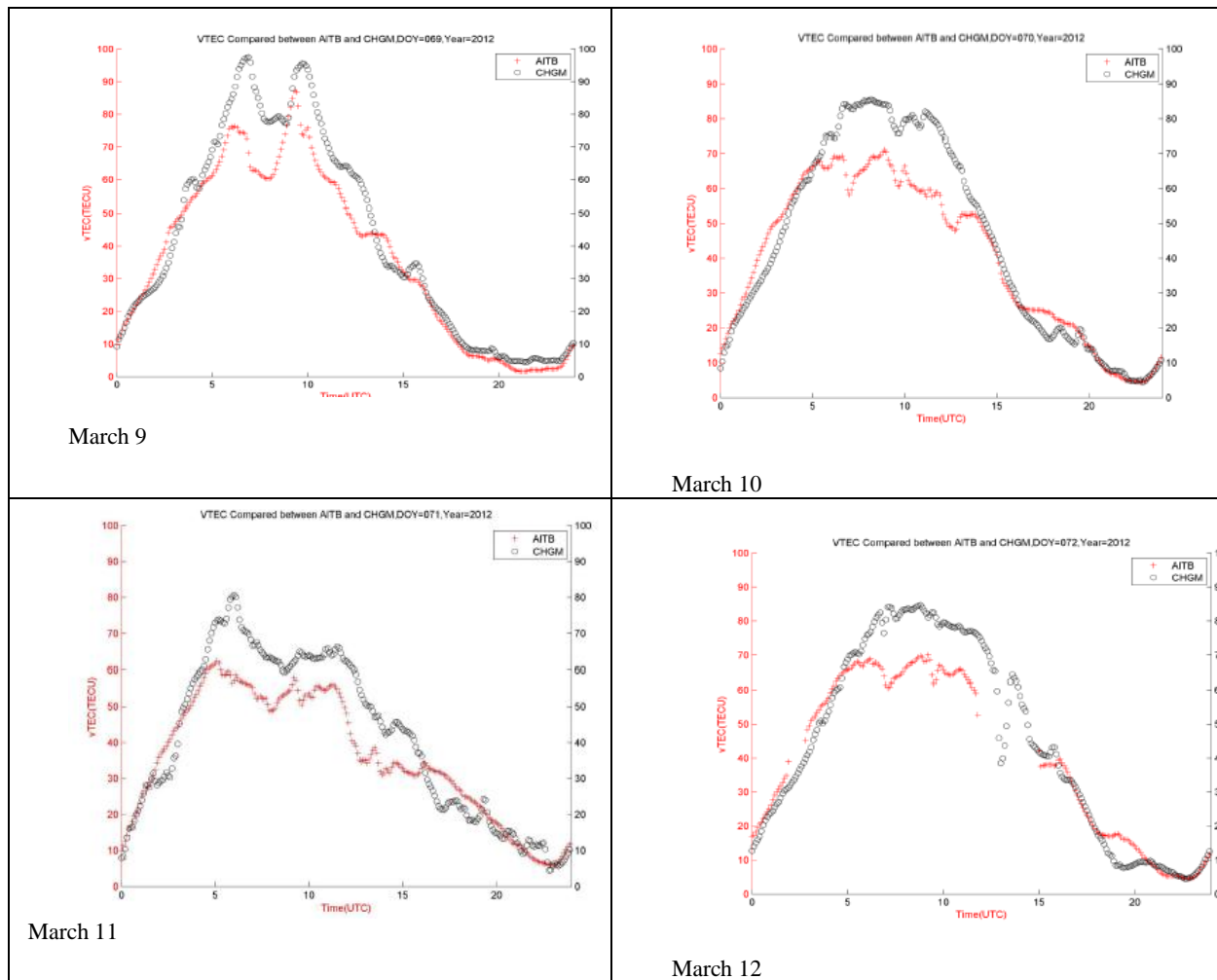


Figure 9 a: Variations of TEC during 9<sup>th</sup> -12<sup>th</sup> March 2012 at AIT and CMU stations

As in Figure 9 a's bottom right panel, on 12<sup>th</sup> March a moderate G2-class geomagnetic storm was initiated by the arrival of a CME at ~ 0930 UT. At AIT, the peak TEC was observed as 68 TECU during 0600 UT followed by a downfall to 60 TECU and then a rise to 69 TECU at 0900 UT. After this, again slight fluctuations can be seen during 1000 UT due to

CME. The corresponding scintillation observed from PRN 2, 9, 19, 22, and 27 were  $>0.3, >0.3, >0.3, >0.3$ , and  $0.3$ , respectively. At CMU, the peak TEC was observed as 82 TECU during 0630 UT followed by a minute downfall to 80 TECU during 0700 UT. Then peak rose to 84 TECU followed by small fluctuations. Observed scintillation over CMU from PRN 6, 16, and 31 were  $>0.3, 0.5$ , and  $0.3$ , respectively. The peak scintillations occurred during 1300 UT as shown in Figure 9 b's bottom right panel. The  $S_4$  index is at its minimum noise level prior to the appearance of the depletion in TEC. It suddenly shoots to a peak value of  $0.5$  coinciding with the occurrence of the TEC depletion. Thus TEC depletions can be clearly observed at both stations.

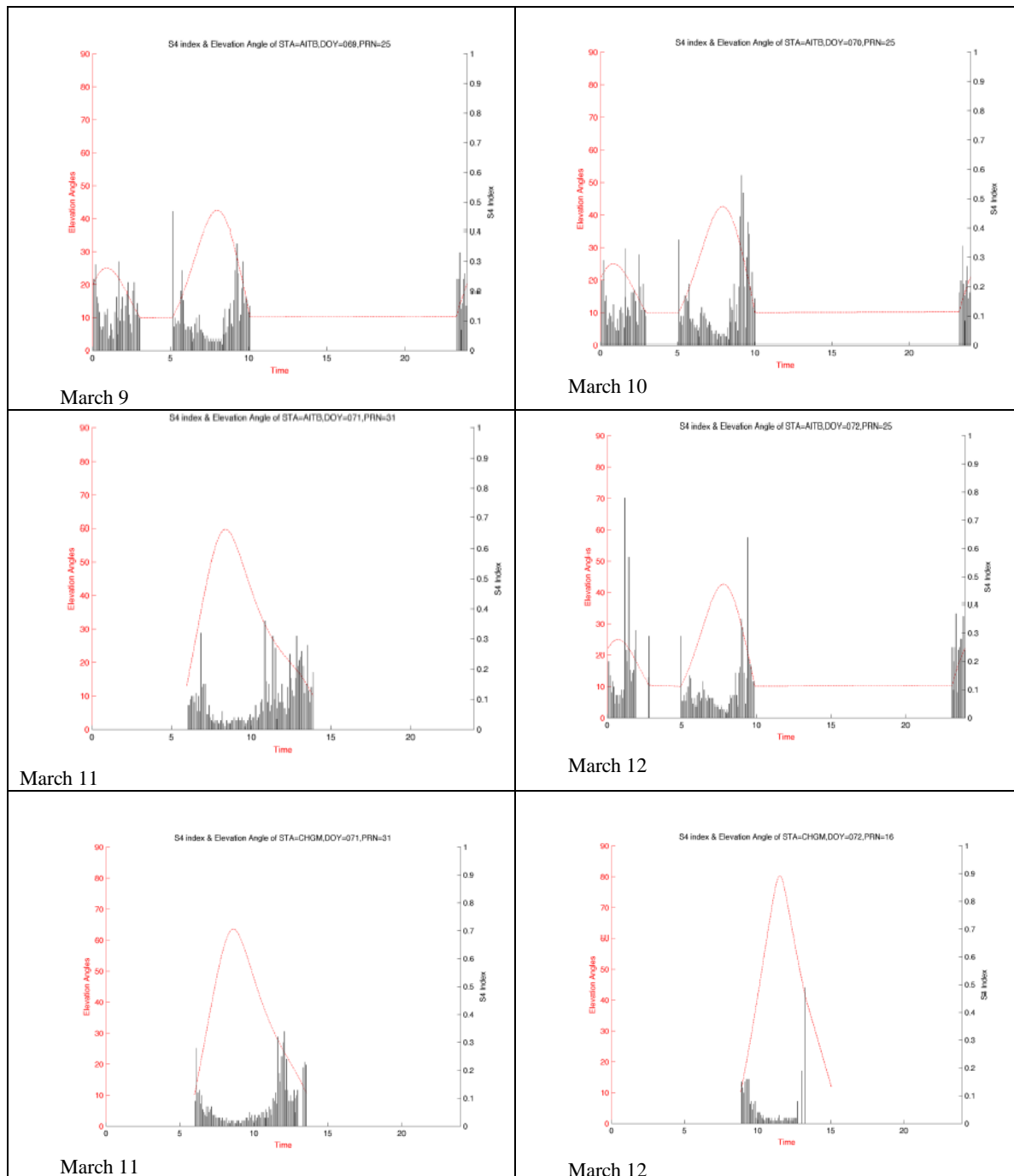


Figure 9 b: Variations of  $S_4$  during 9<sup>th</sup> - 12<sup>th</sup> March 2012 at AIT and CMU stations.

As shown in Figure 10 a's top left panel, on 13<sup>th</sup> March reduced TEC values were observed for the same reason mentioned above by Basu et al., (2007); Foster and Coster, (2007) and Rao et al., (2009). At AIT, there were a few oscillations during 0600-1200 UT leading to peak TEC of 62TECU, but post-1200 UT, TEC depletions with intense variations were observed. Scintillation observed from PRN 13,16,25,27, and 31 were  $>0.3, 0.3, >0.2, >0.2$ , and  $>0.2$ , respectively. At CMU, similar phenomenon was observed as that of AIT, except the peak led to 77 TECU at 0900 UT. A series of TEC depletions with intense turbulence was observed post-1200 UT similar to the AIT station. Both stations exhibited similar process with many sudden dynamics in TEC. At CMU, the scintillations observed from PRN 4,6,7,8,19,21, and 31 were  $0.3, >0.3, >0.2, >0.4, >0.2, >0.7$ , and  $>0.2$ , respectively. Peak  $S_4$  index of  $>0.4$  was observed during 1800 UT, which is shown in Figure 10 b's middle right panel. This corresponds to TEC depletion at the CMU station.

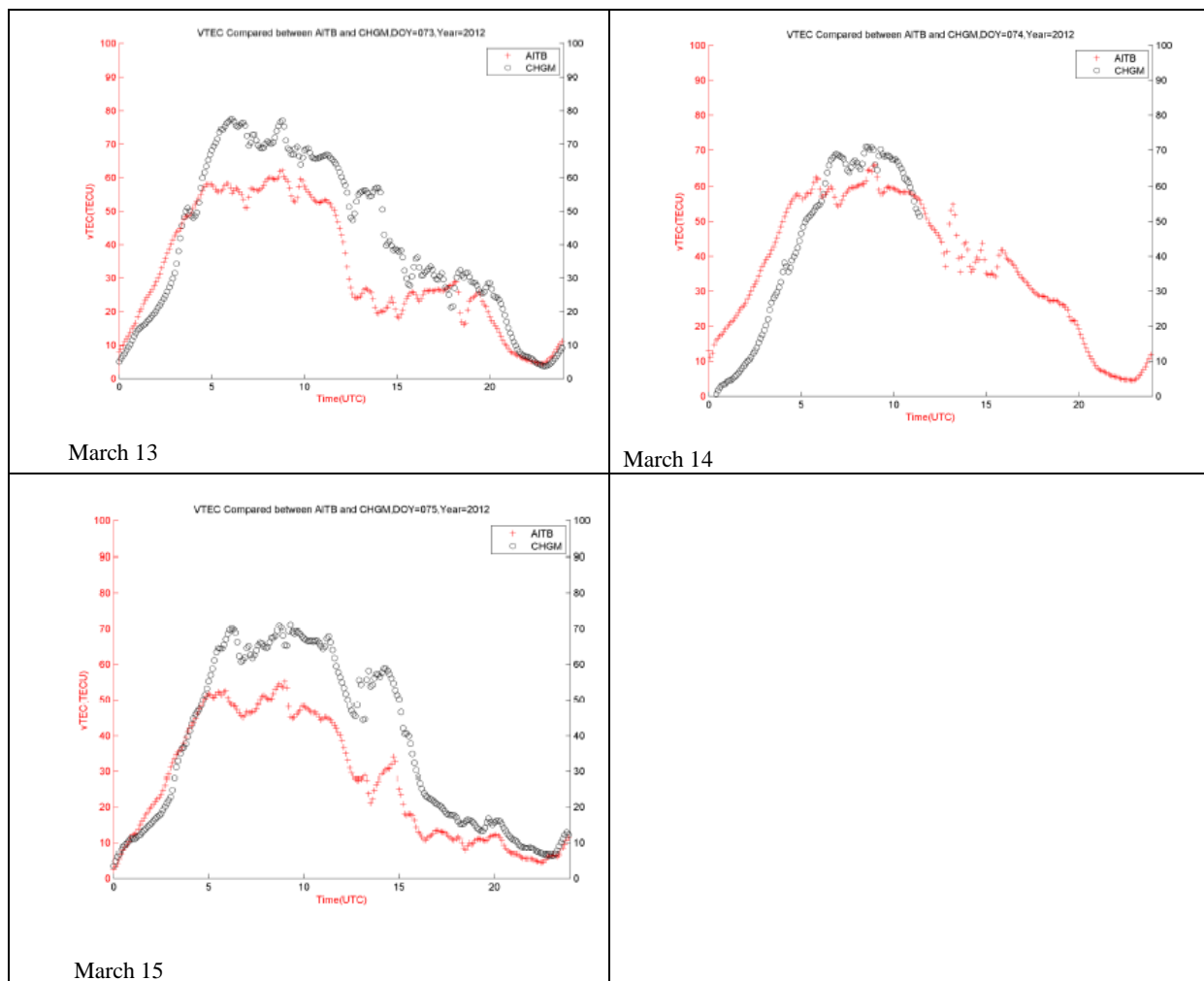


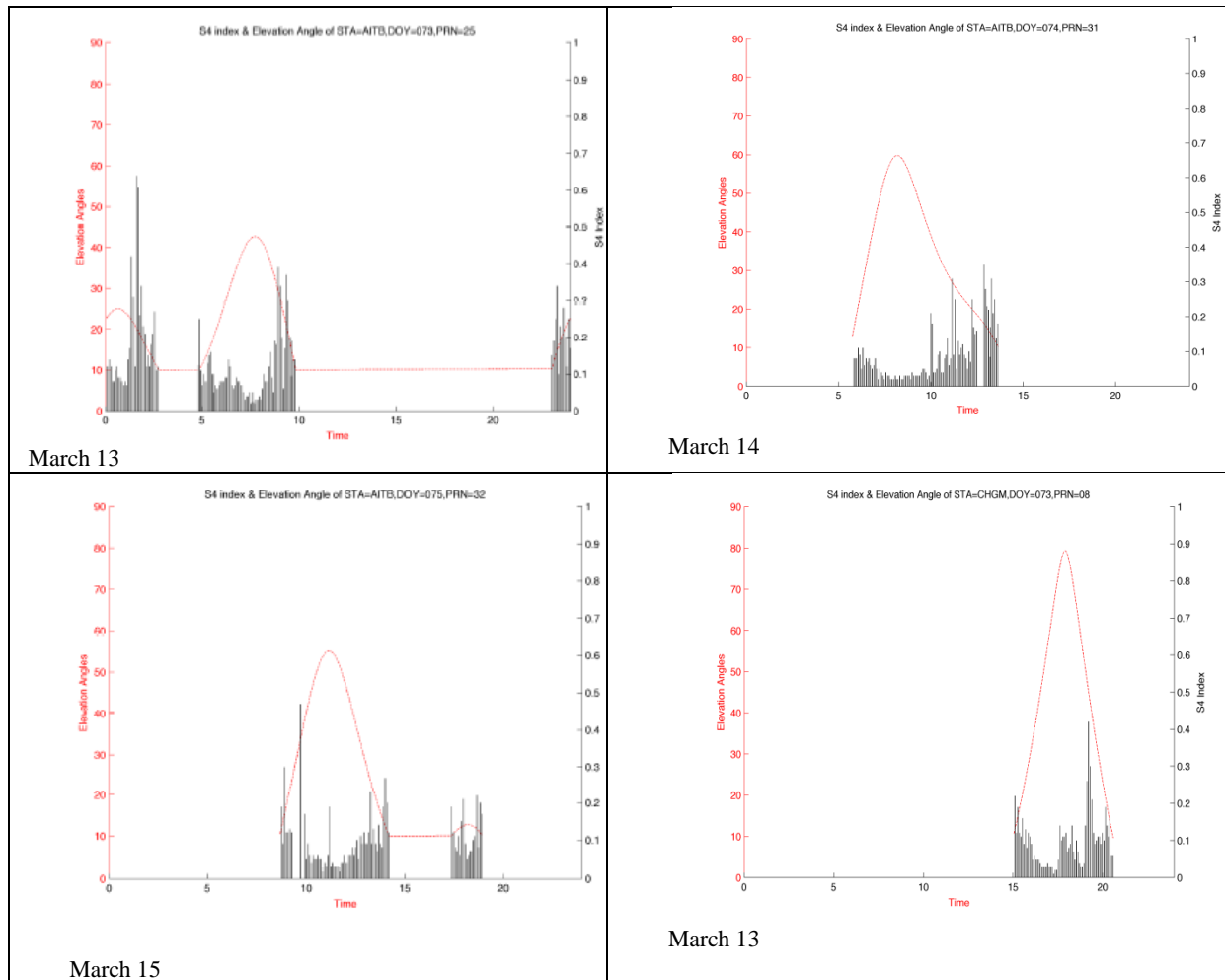
Figure 10 a : TEC variations during 13<sup>th</sup> -15<sup>th</sup> March 2012 at AIT and CMU stations

As displayed in Figure 10 a's top right panel, on 14<sup>th</sup> March at AIT a normal increase in TEC was observed during 0600-1300 UT but with few downfalls at regular intervals of 05:00, 06:00 and 07:00 UT. After 13:00 UT TEC depletions were observed until 16:00 UT, and corresponding scintillations can be observed in Figure 10 b's top right panel. Peak TEC observed was 65 TECU at 09:00 UT. The scintillations observed from PRN 1,3,5,7,9,25, and 31 were  $>0.2, 0.3, >0.2, 0.3, >0.2, >0.2$ , and  $>0.2$ , respectively. At CMU, a similar pattern with



lower TEC values was followed until 05:00 UT, then increased to 70 TECU at 09:00 UT. After 11:00 UT no data was recorded at CMU due to an outage. The scintillations observed from PRN 9 and 25 were  $>0.2$  and  $>0.2$ . Due to the outage post 11:00 UT, no significant TEC depletions were observed in the CMU station, and corresponding scintillations are not shown for this day.

In Figure 10 a's bottom left panel, on 15<sup>th</sup> March the flank of a CME hit Earth's magnetic field around 1300 UT. Due to this CME, a sudden downfall of TEC to 21 TECU with a rise back to 34 TECU within a short span of 2 hours can be observed. The peak TEC was observed as 54 TECU at 08:30 UT. The scintillations observed from PRN 1,2,3,4,6,9,14,25,31, and 32 were 0.3, $>0.2$ ,0.3, $>0.2$ ,0.35, $>0.2$ ,0.3,0.3, $>0.2$ , and 0.35, respectively. The effect of scintillations was more pronounced on 15<sup>th</sup> March compared to previous days due to the storm effect. Thus, a corresponding TEC depletion is clearly evident from the Figure 10 a's bottom left panel.



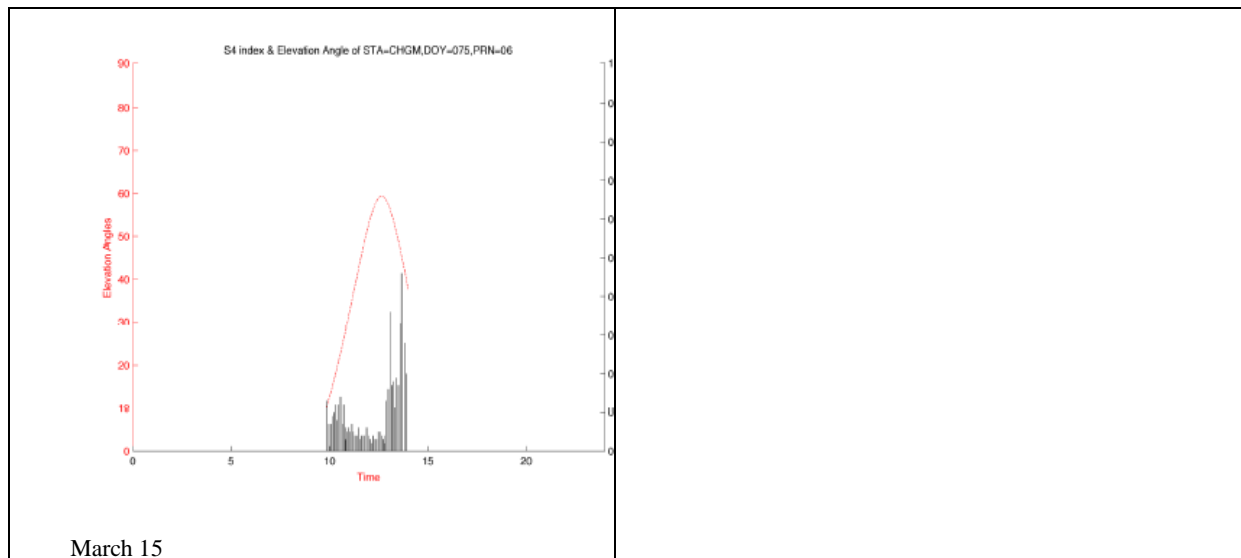


Figure 10 b : S4 during 13<sup>th</sup> -15<sup>th</sup> March 2012 at AIT and CMU stations

At CMU, the pattern of TEC was similar except the peak value was 70 TECU, and depletion was observed very similar to the AIT station. The scintillations observed from PRN 1,3,4,6,16,23,25,28, and 31 were  $>0.2, 0.4, >0.2, 0.5, >0.3, 0.3, 0.3, 0.3$ , and 0.3, respectively. Subsequent plots of  $S_4$  and  $vTEC$  variations for both stations are shown in Figures 10 a and 10 b. As mentioned earlier, one PRN with maximum scintillations for each station per day were considered for plotting as shown in Figure 10 b. Similar phenomenon of depletions and corresponding scintillations were observed from both of the stations.

#### 7.4 Higher Order Ionospheric Effects in GPS positioning

This section presents the research work carried by Mr. Sanit Arunpold during his visit at UBI, Portugal. This was mainly on monitoring location accuracy based on Ionosphere scintillation using Global Positioning System with Space & Earth Geodetic Analysis Laboratory (SEGAL).

##### Objective

- To study the ionosphere effect in point precise positioning
- To study the GPS Processing software in PPP process and few software related ionosphere analysis.

Instructor – Co-PI

Rui Manuel da Silva Fernandes, University of Beira Interior, Covilha, Portugal

## **Study Area: Singapore GPS Based Data**

### **Softwares Used and Learned**

1. GIPSY/OASIS software package, which was developed by Jet Propulsion Laboratory's (JPL's) to perform static and kinematic precise point positioning from GPS data.
2. RINEX\_HO Software was Developed by Marques, Sao Paulo, Brazil, its main objective is to improve rinex file for the correction of second and third order ionosphere effects.
3. RINEX\_GOPI, Developed from researcher in Boston College is used for analysis of slant TEC (sTEC) and it is also supported by the SCINDA format.

### **GIPSY-OASIS Software**

GIPSY is the GNSS-Inferred Positioning System and Orbit Analysis Simulation Software package. GIPSY is developed by the Jet Propulsion Laboratory (JPL), and maintained by the Near Earth Tracking Applications and Systems groups.

#### **Features:**

- Analysis of data from Global Navigation and Satellite Systems (GNSS):
  - Global Positioning System (GPS)
  - Russian GLONASS
  - French DORIS
  - Satellite Laser Ranging (SLR) system
- Precise centimeter-level GNSS-based positioning and timing:
  - Space platforms, including low-Earth orbiters and GNSS constellations
  - Airplanes
  - Terrestrial (ground) stations, static or moving
  - Time transfer
- Single high-level user interface supports majority of precise positioning applications

- Single-receiver ambiguity resolution using JPL's GPS orbit and clock products
- Documentation accompanying software modules, and [online help](#)
- Training at annual GIPSY user group classes, and [online](#)
- Hundreds of research and educational users in more than 20 countries
- Builds on more than 25 years of JPL experience with GPS data analysis

### **Applications:**

- Terrestrial positioning for geophysical research:
- Earth deformation, plate tectonics
- GNSS Networks (e.g. PBO and SCIGN)
- Ice flow
- Climate studies through observation of troposphere and ionosphere
- Reference frame (geocenter and scale) and Earth rotation parameters
- Airplane positioning
- Precise orbit determination
- Low-Earth orbiters: Topex/Poseidon, Jason-1, Jason-2/OSTM, GRACE, Champ, SAC-C, COSMIC, Space Shuttle (e.g. SRTM), Commercial Satellites
- GNSS constellations including GPS and GLONASS

### **RINEX\_HO Software**

RINEX\_HO was developed in C++ language by Haroldo Antonio Marques and uses classes from the NGS (*National Geodetic Survey*), available at <http://www.ngs.noaa.gov/gps-toolbox/rinex.htm>, to read and create a new output RINEX file. In addition, additional C++ classes were developed to compute or interpolate TEC, to compute second and third order ionospheric effects, to apply the corrections to the GPS data and subsequent storage of the corrected data in a new RINEX file. To account for the geomagnetic field subroutines in Fortran for the Corrected Geomagnetic Model (CGM) and subroutines in C for the International Geomagnetic Reference Field (IGRF11) were used. The subroutines in Fortran were mixed with C/C++ in the RINEX\_HO either through Dynamic Link Libraries (DLLs) for Windows or through “.o” files for the Linux operating system.

One can choose between calculating TEC from raw pseudoranges, from pseudoranges smoothed by phase, or from Global Ionosphere Maps (GIM). To use the TEC from the phase-smoothed pseudoranges, a cycle slip detection method, following the Turbo Edit algorithm by Blewitt (1990), was implemented. When a cycle slip is detected for a particular satellite the smoothing filter is restarted.

In the case of computing TEC from the pseudoranges the user must provide the values for the P1/P2 and P1/C1 satellite Differential Code Biases (DCBs) in the form of input files, which can be retrieved from CODE's ftp server <ftp://ftp.unibe.ch/aiub/CODE/yyyy> (where yyyy is the year of the observations). The receiver DCBs for the station being processed also must be provided when computing TEC from the pseudoranges. These can be obtained through a receiver calibration process by following, for example, Ciraolo et al (2007). However if an IGS station is being analyzed, the receiver DCB is also available from the CODE ftp server.

Concerning the geomagnetic field involved in the second order ionospheric effect, it is possible to choose from a simple dipolar approximation, a transformation using the Corrected Geomagnetic Model from PIM, or the IGRF11 model.

## **RINEX\_GOPI Software**

Dr.Gopi Krishna Seemala from Institute developed RINEX\_GOPI for Scientific Research in Boston College.

### **Features of Application:**

- Ability to batch process the input files (rinex etc) for example: all files of the month, year, all stations and files in directory.
- Gets ephemeris from IGS navigation file, has the ability to download the navigation file automatically if connected to internet; unless it finds the file in the same directory as data.
- Calculates TEC from the observation data of GPS Rinex, Novatel (reads only ID43 records), SCINDA(.scn files) and Leica (for leica formats, file name convention is yet to fix, works with our convention names now).
- Process cycle slips in phase data
- Read satellite biases from DCB IGS code files, if not available calculates them.
- Calculates the receiver bias
- Calculates the inter-channel biases for different satellites in the receiver.

- Plots the vertical TEC values on screen and writes ascii output files (\*.CMN & \*.STD) in the same directory of data file.

## Research Site and Analysis

We used data from the Singapore's SiReNT network, which is currently formed by seven stations distributed over an area of approximately 50Km by 25Km. We have compared the positioning solutions in single mode (using the GIPSY-OASIS software package with the Precise Point Positioning strategy) and in differential mode (using TBC, a commercial software). We have also compared the results obtained using a dedicated software (RINEX\_HO) developed to correct the GPS observables for second- and third-order ionosphere effects. We represent that the improvement is marginal for most positioning applications, namely for surveying, but that can slightly improve the accuracy of the derived time-series.

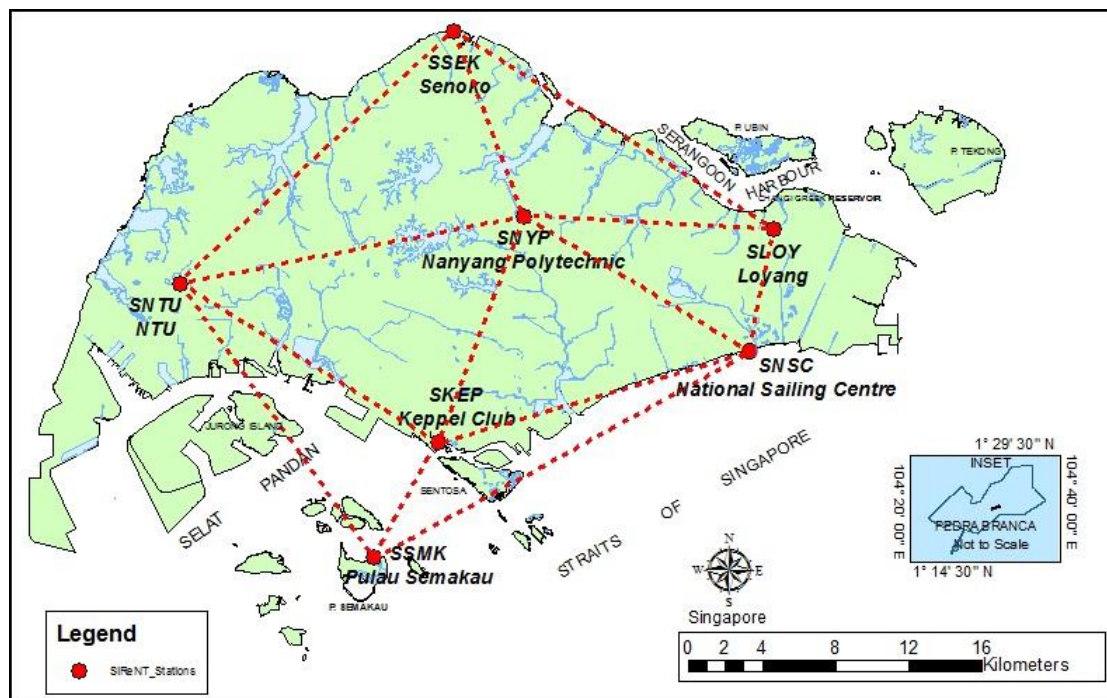


Figure 11 :SiReNT - Singapore Satellite Positioning Reference Network

### **Station ID's used for Analysis:**

SKEP, SNTU, SNYP, SLOY, SSEK

### **Duration of Observation and Analysis**

The period considered during this research is the scenario where the effect of geomagnetic activity is more than  $Kp > 4$  and  $Kp < 4$ , also to compare both and to observe & analysis the movements.

Kp index is a reasonable way to summarize the global level of geomagnetic activity, but it has not always been easy for those affected by the space environment to understand its significance. The NOAA G-scale was designed to correspond, in a straightforward way, to the significance of effects of geomagnetic storms. We use estimates of the planetary average Kp index in our operations to determine Geomagnetic Storm (NOAA Space Weather Scale) level, as follows:

<b>Kp-index</b>	<b>NOAA Space Weather Scale Geomagnetic Storm Level</b>
<b>Kp≤4</b>	<b>G0</b>
<b>Kp=5</b>	<b>G1</b>
<b>Kp=6</b>	<b>G2</b>
<b>Kp=7</b>	<b>G3</b>
<b>Kp=8</b>	<b>G4</b>
<b>Kp=9</b>	<b>G5</b>

### **Dst-Index**

The Dst or disturbance storm time index is a measure of geomagnetic activity used to assess the severity of magnetic storms. It is expressed in nanoteslas and is based on the average value of the horizontal component of the Earth's magnetic field measured hourly at four near-equatorial geomagnetic observatories. Use of the Dst as an index of storm strength is possible because the strength of the surface magnetic field at low latitudes is inversely proportional to the energy content of the ring current, which increases during geomagnetic storms. In the case of a classic magnetic storm, the Dst shows a sudden rise, corresponding to the storm sudden commencement, and then decreases sharply as the ring current intensifies. Once the IMF turns northward again and the ring current begins to recover, the Dst begins a slow rise back to its quiet time level. The relationship of inverse proportionality between the horizontal



component of the magnetic field and the energy content of the ring current is known as the Dessler-Parker-Sckopke relation. Other currents contribute to the Dst as well, most importantly the magnetopause current. The Dst index is corrected to remove the contribution of this current as well as that of the quiet-time ring current.

### Dst Index for a Major Geomagnetic Storm

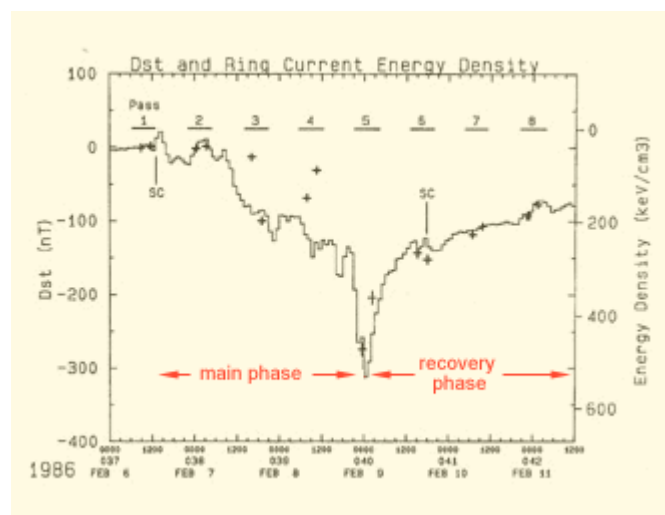


Figure 12 : Dst (nT) and Ring Current Energy Density

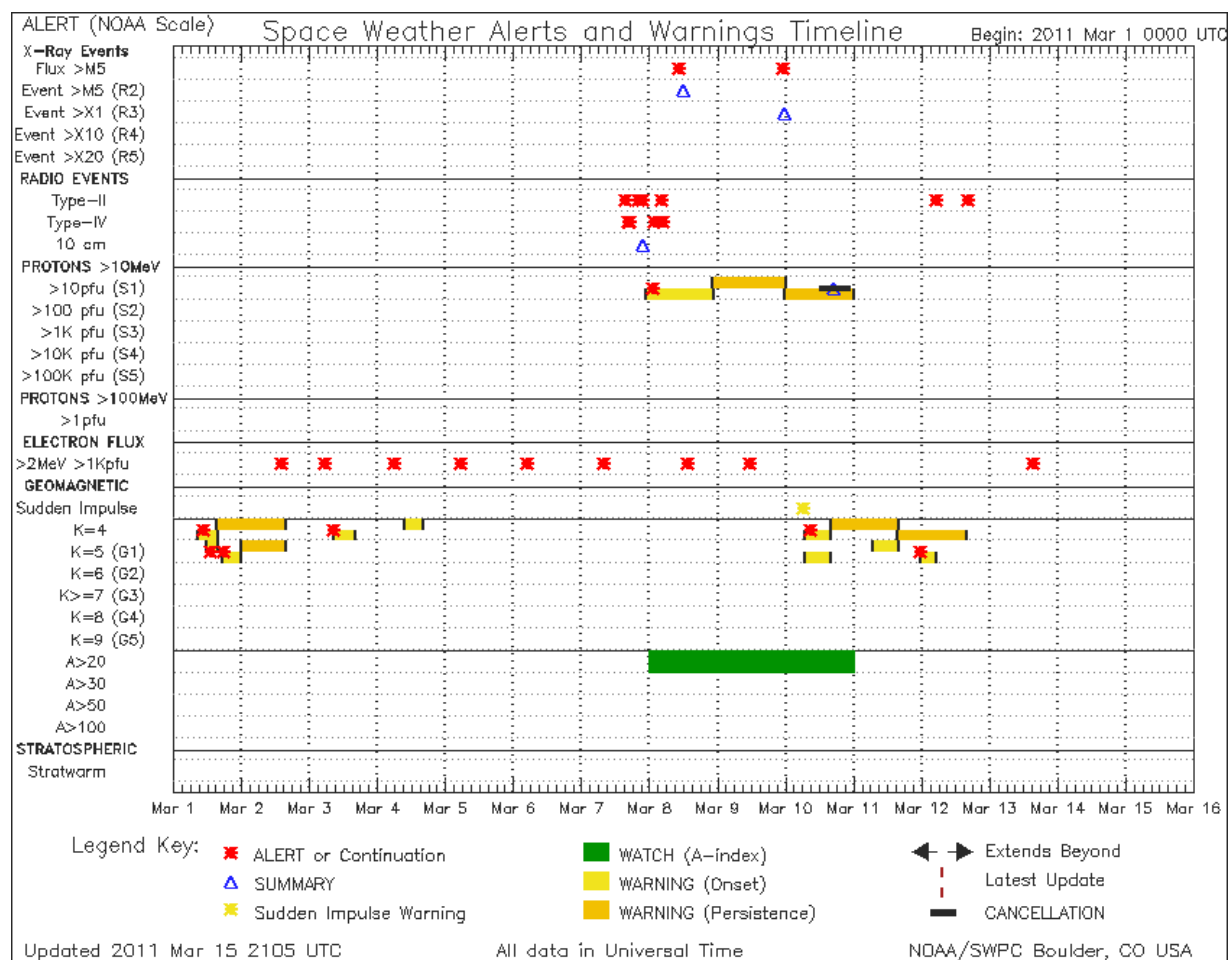
(Source: Hamilton, D. C., et al., Ring current development during the great geomagnetic storm of February 1986, J. Geophys. Res., 93, 14343, 1988.)

The plot above shows the decrease in the Dst index (solid line) and the increase in the energy content of the ring current between  $L = 3$  and 5 (crosses) observed during a major geomagnetic storm that occurred in February 1986. Following a slow two-day build-up, the storm reached maximum intensity early on February 9, by which time the energy content of the ring current had grown to nearly sixteen times its quiet-time value and the Dst had dropped to -312 nT. The sharp rise in ring current energy content during the latter part of February 8 is due to the strong injection into the ring current of ionospheric ions; the rapid

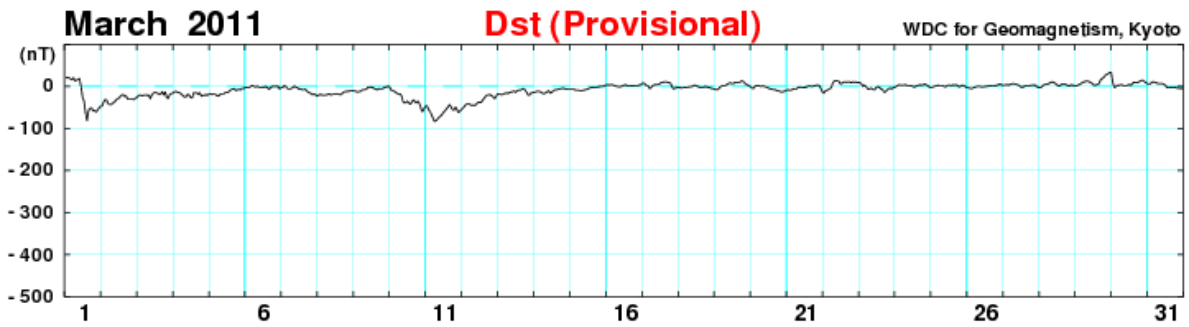
initial recovery on February 9 is due to the rapid loss of these same ions. Full recovery of the ring current to its quiet-time state required over a month.

## Data Analysis

The data for analysis has been supported by Space Weather Prediction Centre (SWPC) of NASA. Which updates all Geo-magnetic indices data , X-ray flux data for every 15 minutes. Also it has archived data of various parameters.



From above figure it is quite evident that, we have a warning issued by NASA when a geomagnetic storm of K=4 has been released onto space. And it went to next level at K=5, which states the moderate effect of that particular storm. Thus during March 1<sup>st</sup> – 16<sup>th</sup> 2011 we have two such scenarios.



The above graph gives Disturbance storm time during the month of March 2011. Which represents that there was a sudden decrease in Dst index during late 1<sup>st</sup> of March and during 11<sup>th</sup> March 2011. This indicates the severity of geomagnetic storm, during those 2 dates.

**Kp index >4 or G>0**

DOY 069 : 10 March 2011 : Kp >4

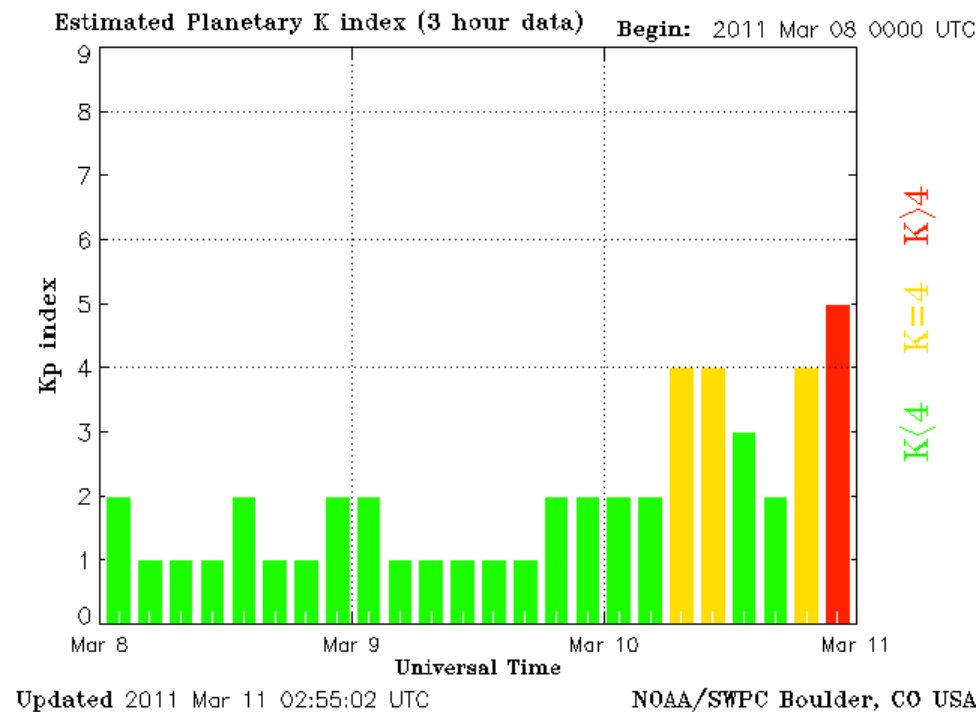


Figure : Kp index 10 Mar 2010

Space Weather Message Code: ALTK04

Serial Number: 1499

Issue Time: 2011 Mar 10 0841 UTC

ALERT: Geomagnetic K-index of 4

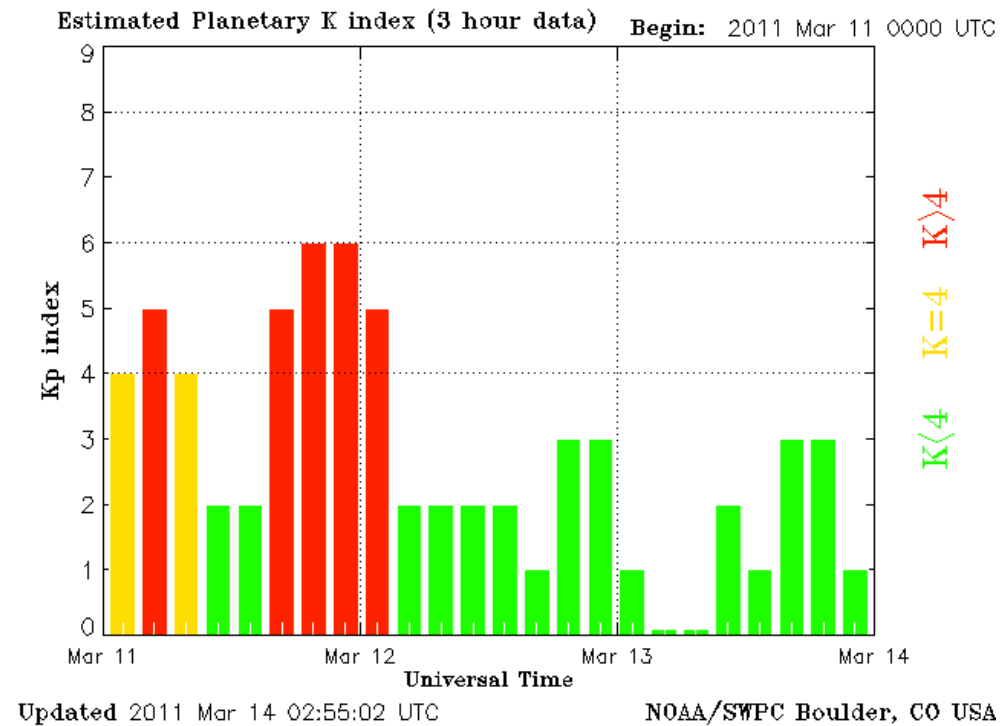
Threshold Reached: 2011 Mar 10 0840 UTC

Synoptic Period: 0600-0900 UTC

Station: Boulder

Active Warning: Yes

DOY 070 : 11 March 2011 : Kp>4



ALERT: Geomagnetic K-index of 5

Threshold Reached: 2011 Mar 11 2343 UTC

Synoptic Period: 2100-2400 UTC

Station: Boulder

Active Warning: Yes

NOAA Scale: G1 - Minor

DOY 071 : 12 March 2011 : Kp>4

Space Weather Message Code: WARK04

Serial Number: 1702

Issue Time: 2011 Mar 11 1531 UTC

EXTENDED WARNING: Geomagnetic K-index of 4 expected

Extension to Serial Number: 1701

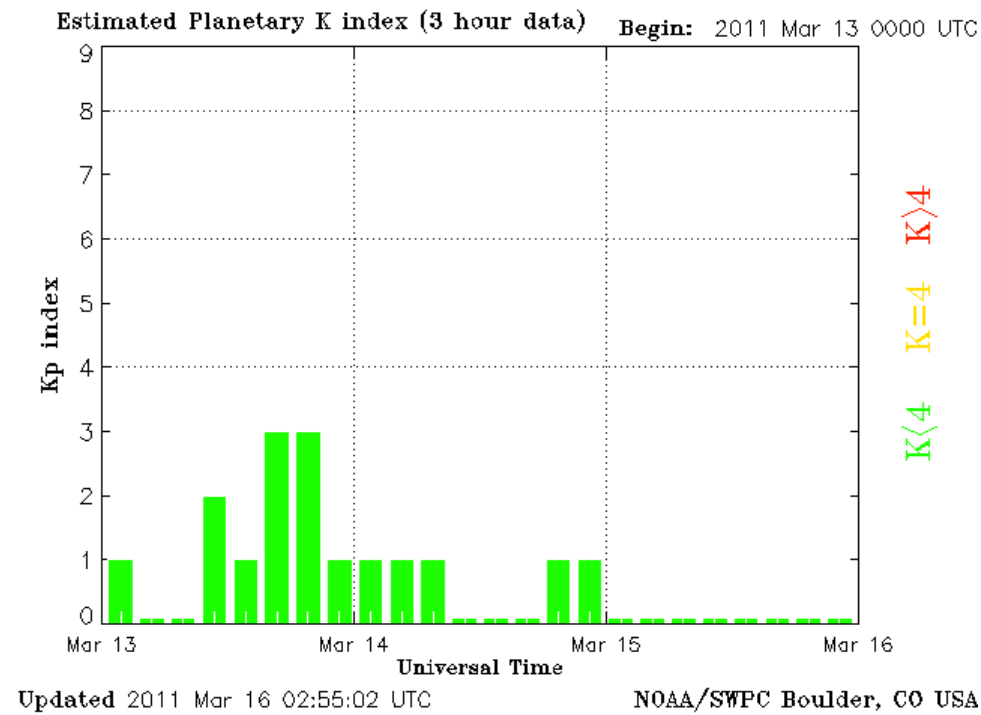
Valid From: 2011 Mar 10 0640 UTC

Now Valid Until: 2011 Mar 12 1600 UTC

Warning Condition: Persistence

DOY 072 : 13 March 2011 : Kp>4

**Kp index <4 or G=0**





The flowchart of work plan that has been followed is illustrated as below:

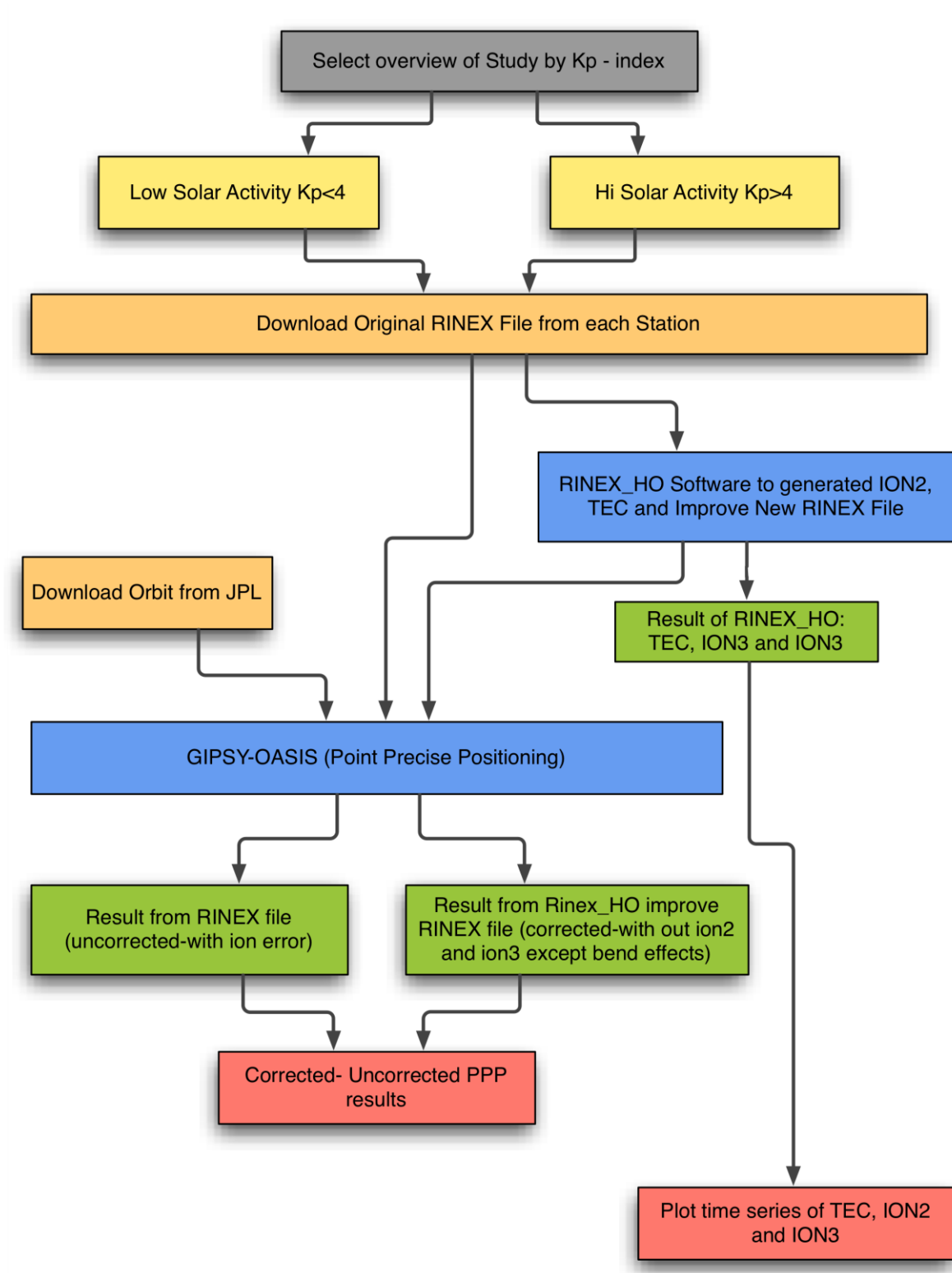


Figure 13: Flow Chart of analysis of higher order effect in positioning process

## Discussion and Results

### RINEX\_HO

```
gpserver@Gpserver-PC: ~/Documents/RINEX_HO
File Edit View Search Terminal Help
BRFT/brft2311.07o //obs file^M
BRFT/brft2311.07n //nav file^M
BRFT/brft231c.07o //new obs file^M
BRFT/brft231_Out //Start name of output files^M
4985396.638 -3954994.721 -428429.232 //Receiver coordinates (if 0.0 => Try to read coordinates from RINEX)^M
10 //Elevation Mask (means that observables under this mask won't be corrected) ^M
1 //Save output and log files (yes=1; no=0)^M
2 //0 = Tec from raw pseudorange; 1 = TEC from smoothed pseudorange by phase; 2 = TEC from GIM^M
BRFT/CODG2310.07I //Name of the CODE map: In the case before option "To use CODE map" = 1^M
6.898 //DCB (P1-P2) = receiver bias in ns (nano-segundos): In the case computing TEC from pseudorange ^M
BRFT/P1C1_190807.DCB //DCB (P1-C1) - P1C1 bias - Found in: ftp://ftp.unibe.ch/aiub/CODE/^M
BRFT/P1P2_190807.DCB //DCB (P1-P2) - P1P2 bias for satellites ^M
2 //0 = Dipolar model; 1 = CGM from PIM; 2 = IGRF model^M
BRFT/IGRF11.COF //Name of the IGRF coefficients
MANUAL.DOC
gpserver@Gpserver-PC:~/Documents/RINEX_HO$ vi script_mstation
gpserver@Gpserver-PC:~/Documents/RINEX_HO$ 1,1 All
```

Figure 14: RINEX\_HO input parameter

```
gpserver@Gpserver-PC: ~/Documents/RINEX_HO
File Edit View Search Terminal Help
echo -n "How many STATION will COMPUTE and press[ENTER]: "
read numsta
echo -n "STAID ID:"

gpserver@Gpserver-PC: ~/Documents/RINEX_HO
File Edit View Search Terminal Help
gpserver@Gpserver-PC:~/Documents/RINEX_HO$ ls
backup_env_script  CycleSlip.o  rinex_ha_param.dat  rinex_ho
BRFT               datetime.o  rinex_ho.cpp        rinex_ho
CGLALO.DAT         FilterCode  rinex_ho.cpp~       rinex_ho.cpp.save
CGM_DLL_Lahey_Fujtsu  Filter_Code.o  rinex_ho.h          rinex_ho.h~
cgm_util.mk~       Fortran_Class  rinex_ho.o          rinex_ho.o
cgm_util.o         IGRF11       rinex_ho.res        rinex.log
Class IGRF11.o     input        rinex.o             script_mstation
Class Iono         Makefile     rinex.o             script_mstation.save
Class Iono.mk      Makefile~   rinex.o             script_mstation.save.1
Class Iono.o       output      script_mstation_sort
Class TEC          precip.o    script_mstation
Class TEC.o        Rinex_Class
compilacao.txt~    rinex_ha2.inp
compiling.txt      rinex_ha.inp
Cycle_Slip         rinex_ha.inp.brtrf
gpserver@Gpserver-PC:~/Documents/RINEX_HO$ ./script_mstation
```

Figure 15 :Running RINEX\_HO Module

FUTY2870.110										
convert_rinex.bat										
AITB072-2011-03-13.Cmn										
AITB069_Out_I2L1.txt										
SKEP070_Out_I2L1.txt.orign										
SKEP071_Out_I2L1.txt.orign										
\\psf\Home\Desktop\ignnet\ignnet_OBS\287\FUTY2870.110										
			PRN03	PRN04	PRN05	PRN06	PRN07	PRN08	PRN09	PRN10
2	71.00000	Nan	0.005561	Nan	0.006050	Nan	Nan	Nan	Nan	Nan
3	71.00035	Nan	0.005589	Nan	0.006069	0.001246	Nan	Nan	Nan	Nan
4	71.00069	Nan	0.005618	Nan	0.006088	0.001265	Nan	Nan	Nan	Nan
5	71.00104	Nan	0.005646	Nan	0.006107	0.001284	Nan	Nan	Nan	Nan
6	71.00139	Nan	0.005675	Nan	0.006125	0.001303	Nan	Nan	Nan	Nan
7	71.00174	Nan	0.005703	Nan	0.006143	0.001322	Nan	Nan	Nan	Nan
8	71.00208	Nan	0.005731	Nan	0.006161	0.001341	Nan	Nan	Nan	Nan
9	71.00243	Nan	0.005759	Nan	0.006179	0.001361	Nan	Nan	Nan	Nan
10	71.00278	Nan	0.005787	Nan	0.006196	0.001381	Nan	Nan	Nan	Nan
11	71.00312	Nan	0.005816	Nan	0.006214	0.001400	Nan	Nan	Nan	Nan
12	71.00347	Nan	0.005843	Nan	0.006231	0.001420	Nan	Nan	Nan	Nan
13	71.00382	Nan	0.005871	Nan	0.006248	0.001440	Nan	Nan	Nan	Nan
14	71.00417	Nan	0.005899	Nan	0.006265	0.001460	Nan	Nan	Nan	Nan
15	71.00451	Nan	0.005927	Nan	0.006281	0.001480	Nan	Nan	Nan	Nan
16	71.00486	Nan	0.005955	Nan	0.006298	0.001501	Nan	Nan	Nan	Nan
17	71.00521	Nan	0.005982	Nan	0.006314	0.001521	Nan	Nan	Nan	Nan
18	71.00556	Nan	0.006010	Nan	0.006330	0.001541	Nan	Nan	Nan	Nan
19	71.00590	Nan	0.006037	Nan	0.006346	0.001562	Nan	Nan	Nan	Nan
20	71.00625	Nan	0.006064	Nan	0.006361	0.001583	Nan	Nan	Nan	Nan
21	71.00660	Nan	0.006092	Nan	0.006377	0.001604	Nan	Nan	Nan	Nan
22	71.00694	Nan	0.006119	Nan	0.006392	0.001625	Nan	Nan	Nan	Nan
23	71.00729	Nan	0.006146	Nan	0.006407	0.001646	Nan	Nan	Nan	Nan
24	71.00764	Nan	0.006173	Nan	0.006421	0.001667	Nan	Nan	Nan	Nan
25	71.00799	Nan	0.006200	Nan	0.006436	0.001688	Nan	Nan	Nan	Nan
26	71.00833	Nan	0.006226	Nan	0.006450	0.001710	Nan	Nan	Nan	Nan
27	71.00868	Nan	0.006253	Nan	0.006464	0.001731	Nan	Nan	Nan	Nan
28	71.00903	Nan	0.006280	Nan	0.006478	0.001753	Nan	Nan	Nan	Nan
29	71.00937	Nan	0.006306	Nan	0.006492	0.001775	Nan	Nan	Nan	Nan
30	71.00972	Nan	0.006333	Nan	0.006505	0.001797	Nan	Nan	Nan	Nan
31	71.01007	Nan	0.006359	Nan	0.006518	0.001819	Nan	Nan	Nan	Nan

Figure 16 :Result of RINEX\_HO for Ion2, Ion3 and TEC

## TEC Plot

As predefined the slant Total Electron Content(STEC) plots was generated for each station. As it is clearly visible that the TEC retrieved from SKEP station ,that TEC value slowly increased during 69-72 Day of year , which started from below 150 TECU to reached its maximum of 170TECU, which totally agrees with the effect caused on 11<sup>th</sup> March 2011. The TECU value was at its peak during 70 and 71 day of year which corresponds to 10<sup>th</sup> and 11<sup>th</sup> March,2011.

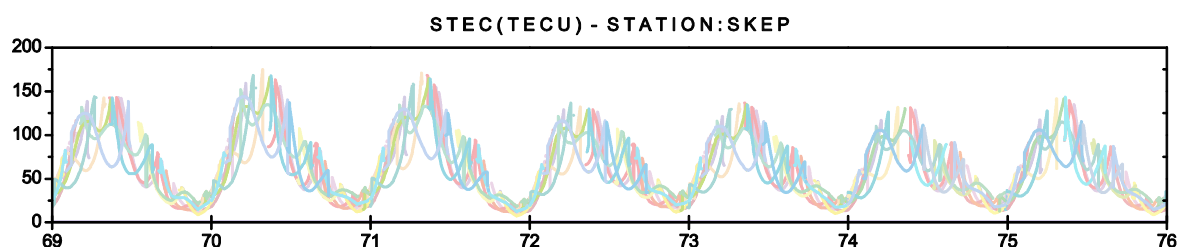


Figure 17 a: Slant-TEC for SKEP station during 69-76 doy

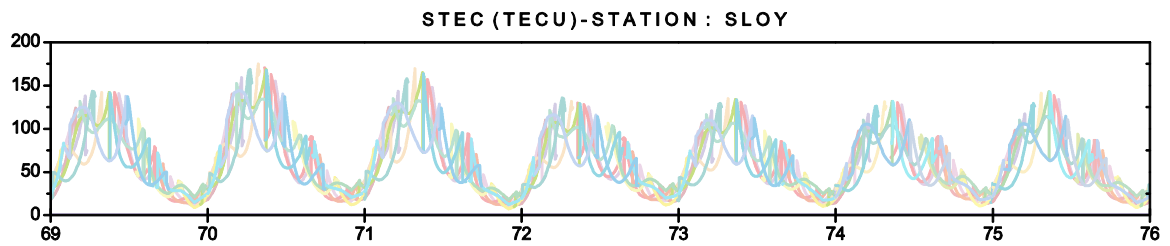


Figure 17 b: Slant-TEC for SLOY station during 69-76 day

The same pattern can be observed from SLOY station also, which also accepts the severity of the geomagnetic storm that occurred during March, 2011. It can be visible that from 72<sup>nd</sup> -76<sup>th</sup> Day of year, the TEC value decreased gradually, that makes to understand that the effect of storm has been nullified.

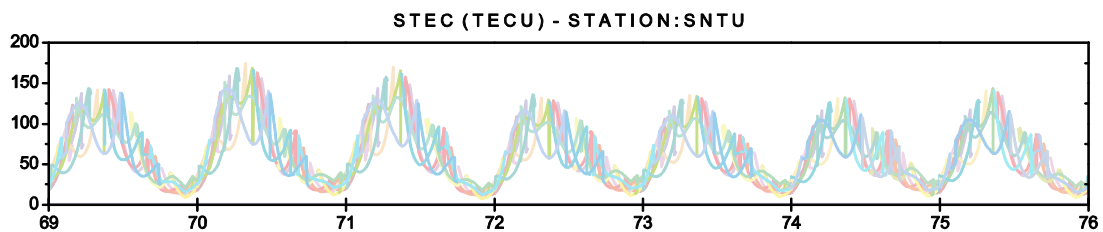


Figure 17 c: Slant-TEC for SNTU station during 69-76 day

The plot obtained from SNTU station also, agree with the same phenomenon followed by other two stations. During the off storm period value of TEC has been dropped to 120 TECU, which is quite less when compared to its values during the peak stage of storm which was more than 160 TECU.

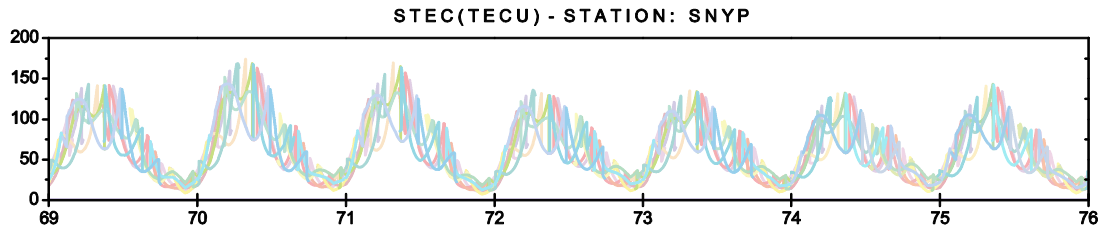


Figure 17 d: Slant-TEC for SNYP station during 69-76 day

The data obtained from SNYP station also approves with the pattern obtained and analyzed at previous stations. It can be well noted that having a TECU values above 100 leads that the ionospheric content was heavily charged due to release of this storm. And during the peak period it went beyond 150 TECU

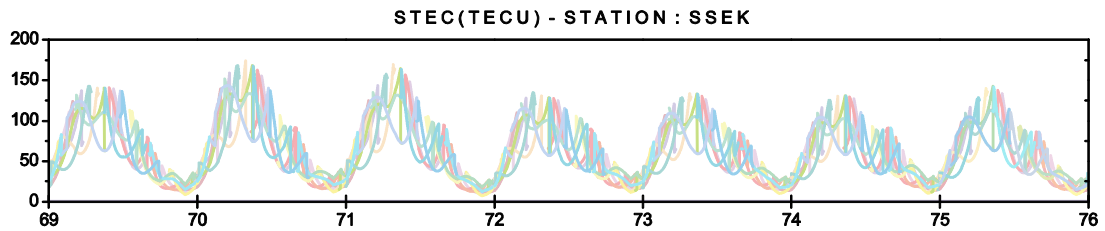


Figure 17 e: Slant-TEC for SSEK station during 69-76 day

The plots obtained from SSEK station also indicate the similar performance during the geomagnetic storm effect onto the Earth's atmosphere. It can be noted that during this period ionosphere has become more ionized and it can create more charge onto satellite and can lead to extra drag of satellite from its orbit.

### **Second order ionospheric effect on GPS carrier L1 signal during 69-76 day**

As it is well know that in a GPS signal we have 2 carrier waves L1 and L2 at 1.5GHz and 1.2 GHz respectively, that are used to encapsulate the navigation signal throughout its journey from GPS satellite to ground based receivers. Thus each of L1 and L2 signal has their own



effect by Ionosphere. The graph below illustrates the second order ionospheric effect on GPS signals during the period of March 2011.

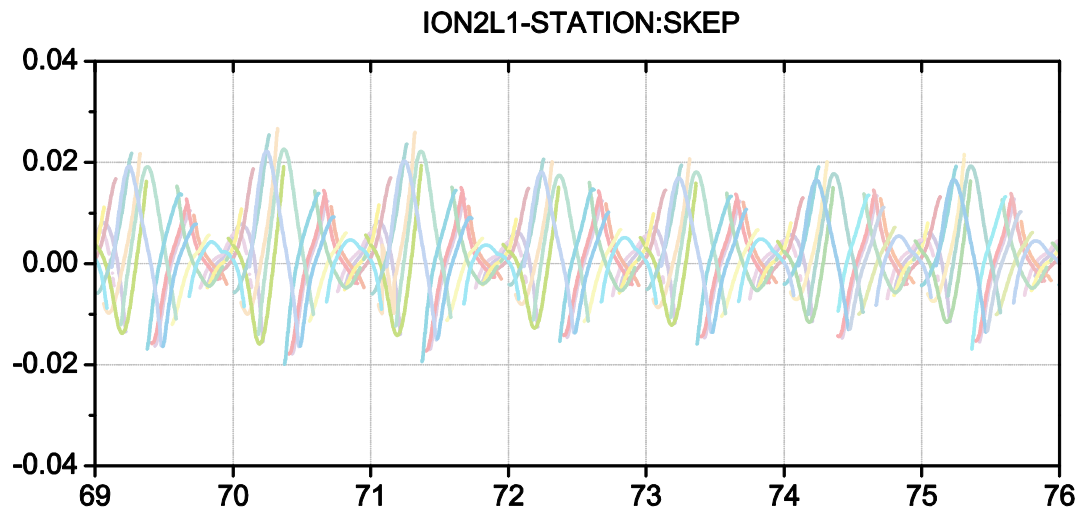


Figure 18 a: Second order ionospheric effect on GPS carrier L1 signal for SKEP station during 69-76 day

As it is evident from the graph obtained from SKEP station that, the deviation due to this geomagnetic storm is very nominal which is around +0.02m to -0.02 m during the start of the event. Whereas on the day of event, it went slightly above this value. And is also agrees with K-index and Dst-Index values.

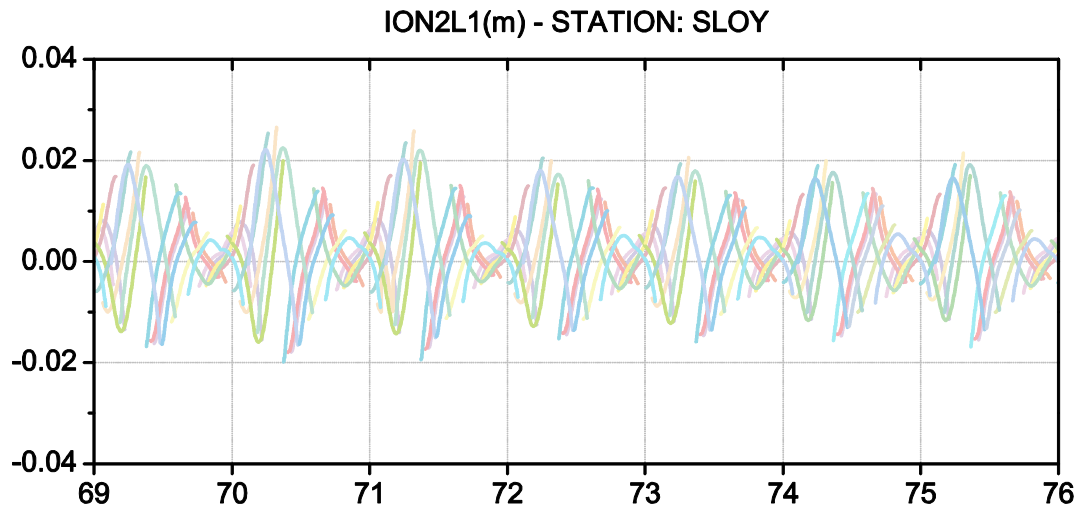


Figure 18 b: Second order ionospheric effect on GPS carrier L1 signal for SLOY station during 69-76 day

Data obtained from SLOY station, also confirms the same pattern which was obtained by SKEP station. This also illustrated the decrease in second order ionospheric effects post to occurrence of the event. As it is visible that post event days of year is again following the similar pattern of getting values below 0.02m

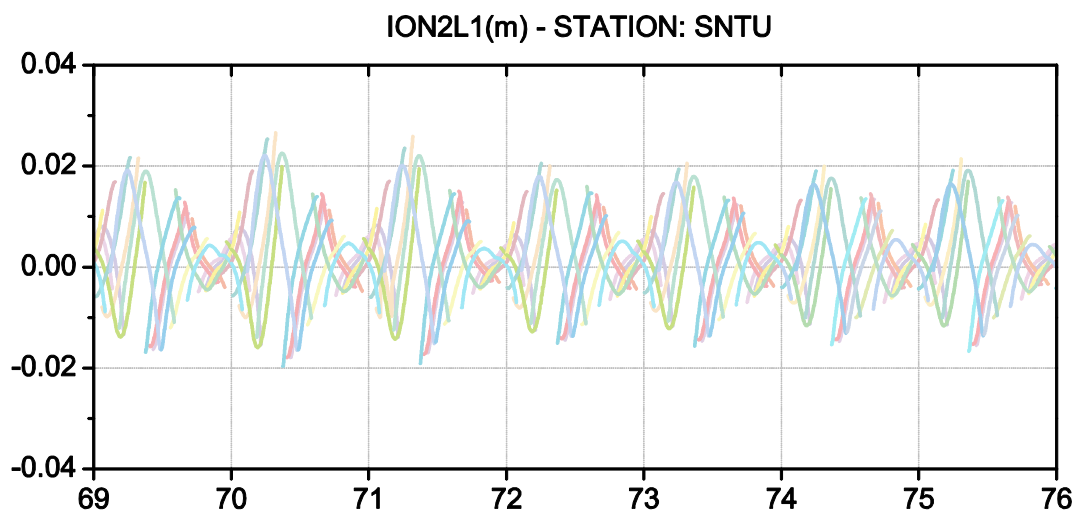


Figure 18 b: Second order ionospheric effect on GPS carrier L1 signal for SNTU station during 69-76 day

Second order Ionospheric effect derived at SNTU station on GPS L1 carrier accepts the same phenomenon which was observed in the previous stations. The Ion2 value has a slight raise during 70<sup>th</sup>-71<sup>st</sup> days of year and then they become stable during the other dates.

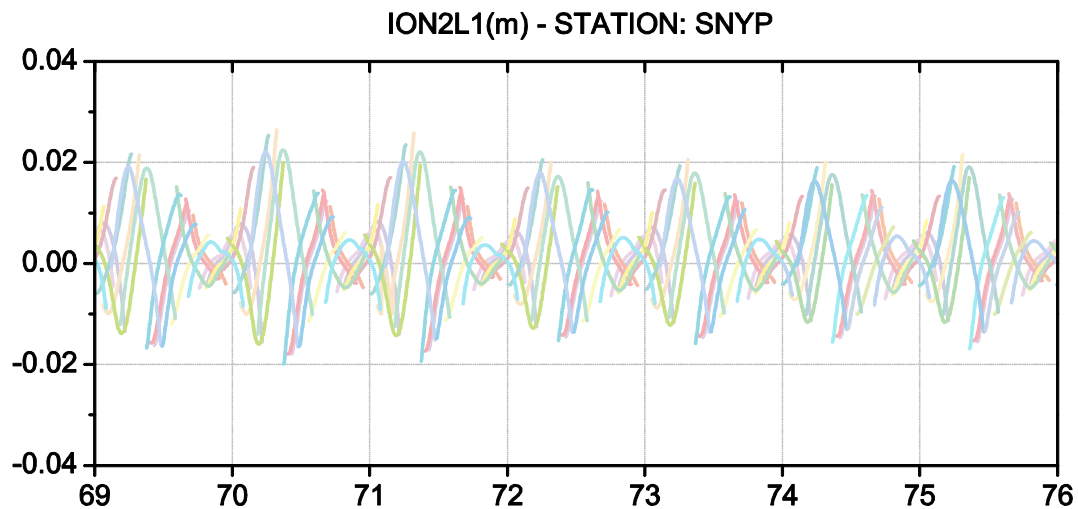


Figure 18 c: Second order ionospheric effect on GPS carrier L1 signal for SNYP station during 69-76 doy

Data obtained from SNYP station also supports the previous analysis of the second order ionospheric effects in various stations. The data obtained from all the stations are so symmetric and express the phenomenon during these day of year.

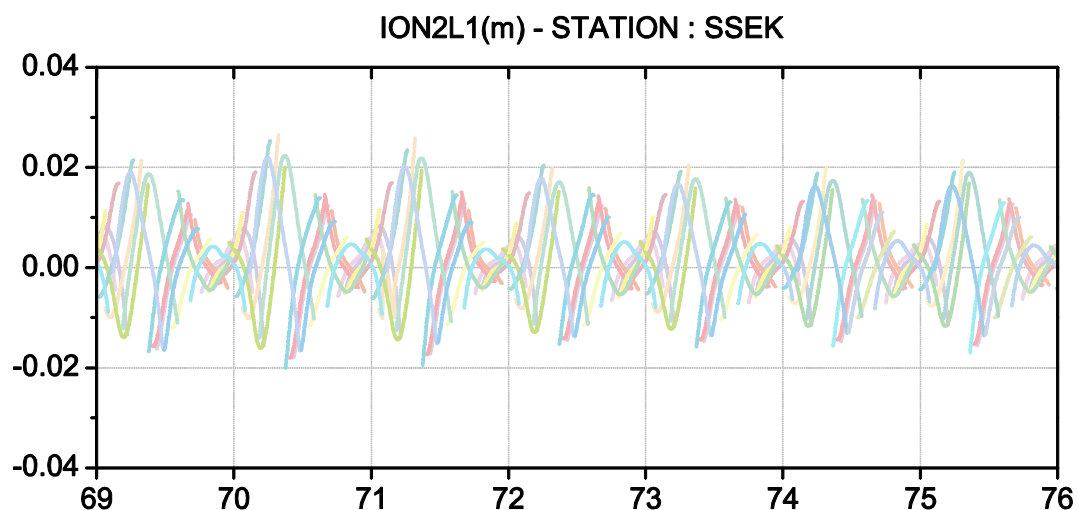


Figure 18 d: Second order ionospheric effect on GPS carrier L1 signal for SSEK station during 69-76 day

Data obtained from SSEK station also accepts the symmetry discussed for the previous stations. It can also be seen that negative values are smaller than positive values of Ion2 on L1 signal.

Thus finally, all the stations obey a particular fashion of plots which can be due to very near locations of these data deriving points. Thus observing same type of graphs and plots during this period and it confirms the precision of the data.

### Second order ionospheric effect on GPS carrier L2 during 69-76 day

As discussed that we have two carriers in the GPS signal namely L1 and L2, now we will discuss the effect of second order ionospheric on L2 signal during the 69<sup>th</sup> – 76<sup>th</sup> Day of year.

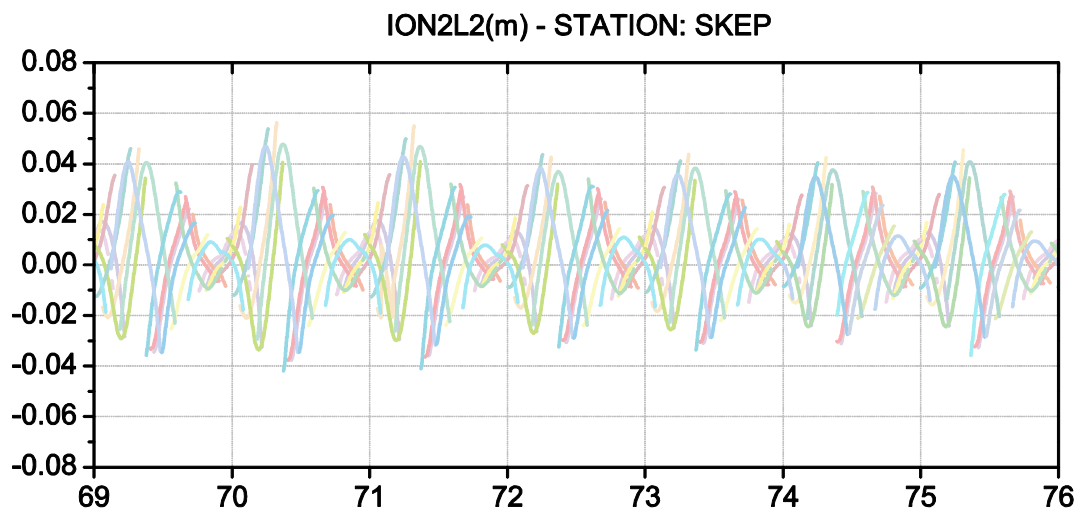


Figure 19 a: Second order ionospheric effect on GPS carrier L2 signal for SKEP station during 69-76 day

It is evident from the graphs obtained from SKEP station that second order Ionospheric effect was around 0.06 m during the peak time of event occurrence. Post event the ion2l2 value became to a stable value of around 0.04m which is twice the values obtained by second order ionospheric effect on L1.

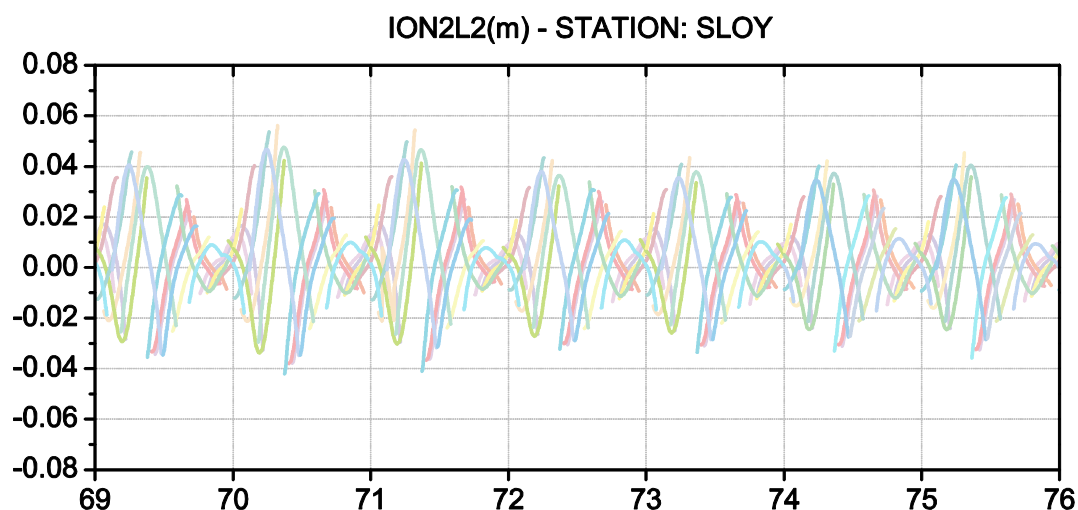


Figure 19 b: Second order ionospheric effect on GPS carrier L2 signal for SLOY station during 69-76 day

Data obtained from SLOY station proves the same pattern obtained from the previous station, the value post to event is around 0.04m is similar to values obtained at SKEP station. The value retained during the 72<sup>nd</sup> – 76<sup>th</sup> day of the year.

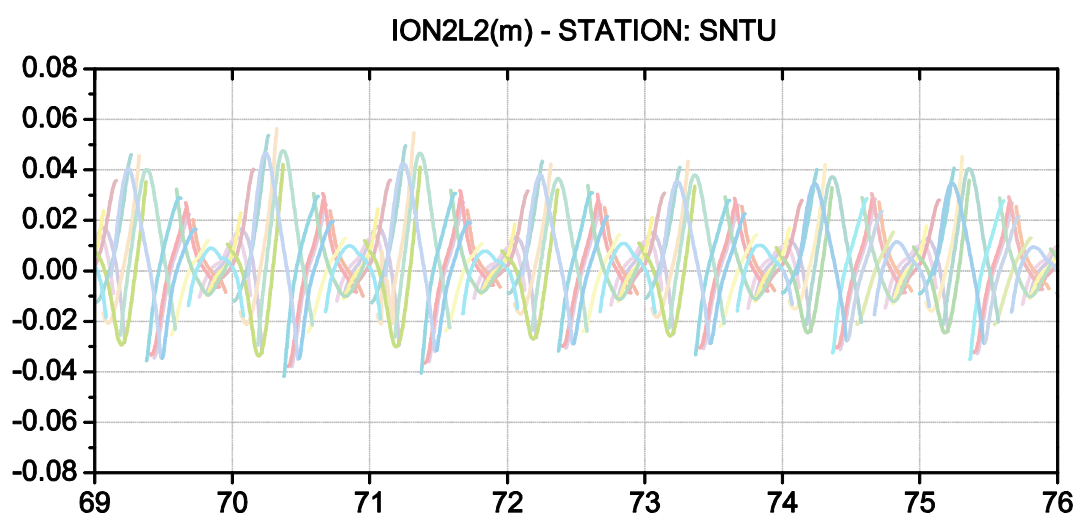


Figure 19 c: Second order ionospheric effect on GPS carrier L2 signal for SNTU station during 69-76 day



The data obtained from SNTU station also accepts the second order ionospheric effects on L2 signals which is symmetric to the data obtained from previous stations. This can be observed that the values obtained at L2 signal are much more effected than that are obtained by L1 signals.

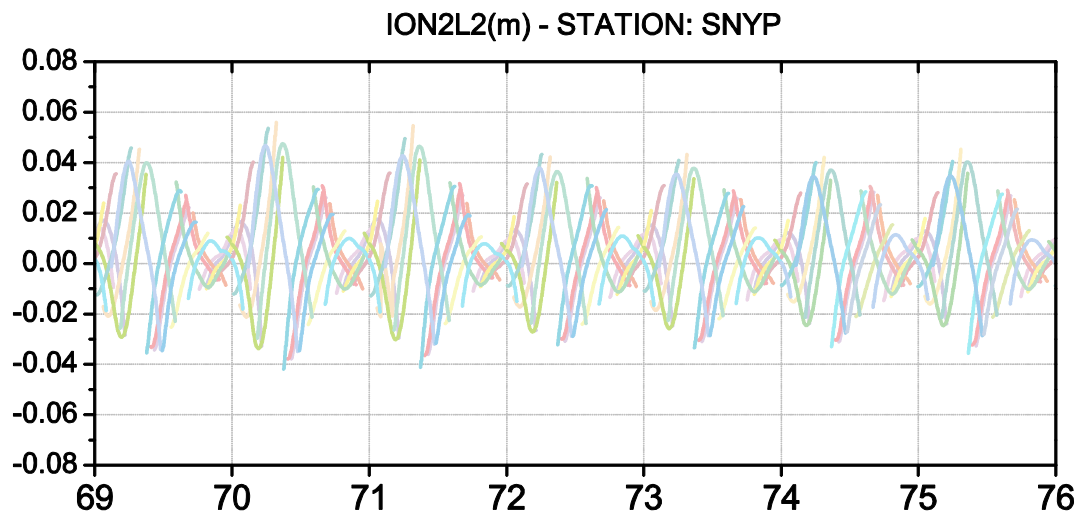


Figure 19 d: Second order ionospheric effect on GPS carrier L2 signal for SNYP station during 69-76 doy

The ionospheric effect on SNYP station represents the same pattern with that of previous stations. The values of -0.04m to +0.04m is obtained during the geomagnetic storm on 11<sup>th</sup> March 2011. Which again validates with the data obtained from SWPC and GOES-15 satellite.

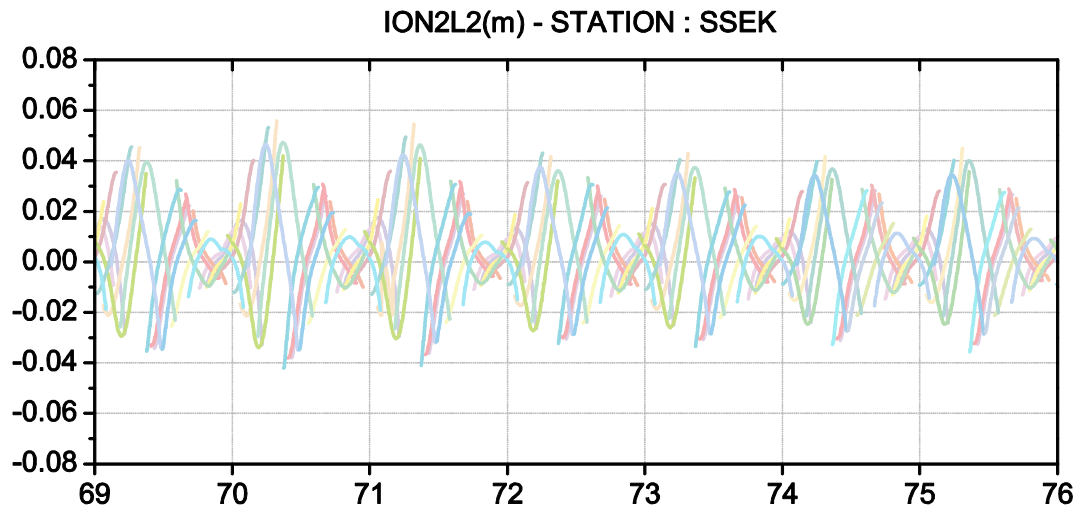


Figure 19 e: Second order ionospheric effect on GPS carrier L2 signal for SSEK station during 69-76 doy

The data obtained from SSEK station also confirms the co-orelation of data with previous stations. Here it can visualize that Ion2L2 values are more shifted towards the positive axis than the negative. As we can see maximum negative values upto -0.04m and maximum positive value upto +0.05m during the event occurrence.

Thus it can be concluded that all the stations followed a similar pattern of plots and graphs during the geomagnetic storm activity during early of March 2011. The second order ionospheric effects obtained are so symmetric and equi-valued.

### **Third order ionospheric effect on GPS carrier L1 signal during 69-76 doy**

As we have to consider second and third order ionopsheric effects on each of L1 and L2 carrier signals of GPS. Data from various stations has been generated for third order ionospheric effect.

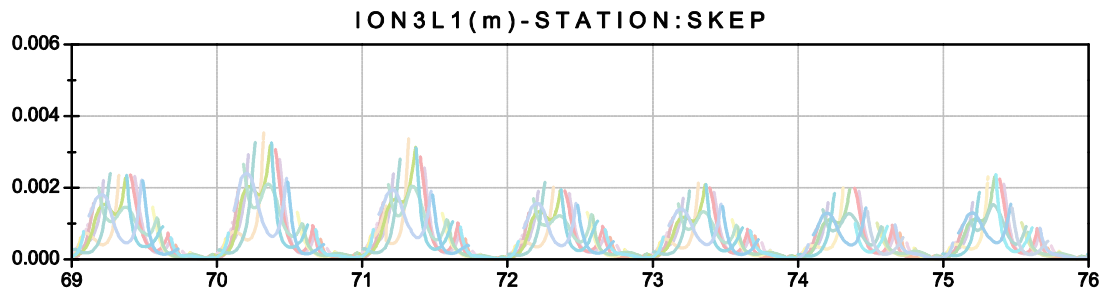


Figure 20 a: Third order ionospheric effect on GPS carrier L1 signal for SKEP station during 69-76 doy

The data obtained from SKEP station represents that third order ionosphere was effect to the limit of less than 0.004m which is the least value obtained during the whole post processing procedure. Also it can we witnessed, it has cut-off the negative values and we are left with only positive values.

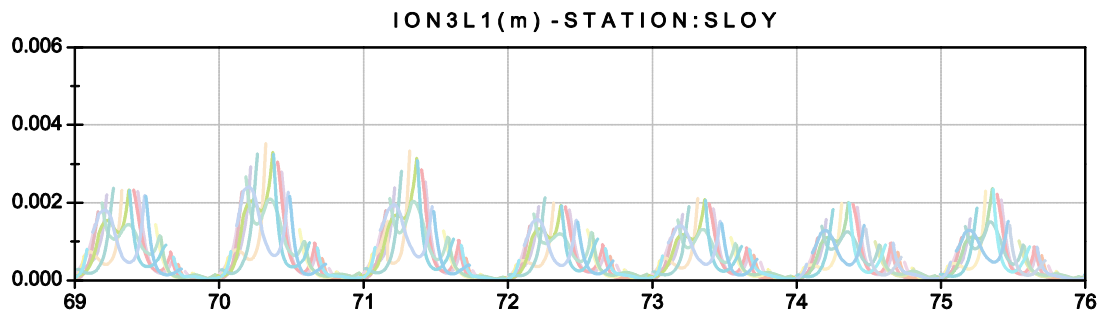


Figure 20 b: Third order ionospheric effect on GPS carrier L1 signal for SLOY station during 69-76 doy

The data obtained from SLOY station indicates that during the 70<sup>th</sup> -71<sup>st</sup> day of the year effect of geomagnetic storm was predominant which fluctuated to above 0.003m and during the post effects of third order ionospheric ion3L1 they are very smooth and in a more stable manner.

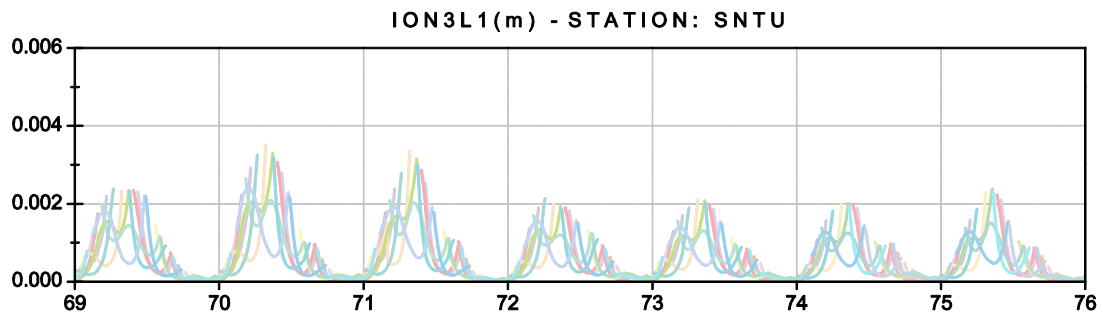


Figure 20 c: Third order ionospheric effect on GPS carrier L1 signal for SNTU station during 69-76 day

The data obtained from SNTU stations is very similar to all the previous stations as well. This can be well noticed that during the pre and post event, the value for third order ionospheric effects was very less fluctuated and there values are up to 0.002m during 72<sup>nd</sup>-76<sup>th</sup> day of the year.

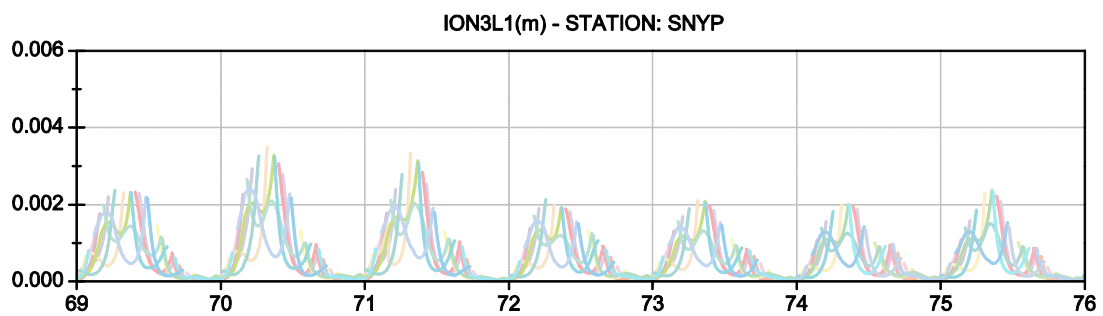


Figure 20 d: Third order ionospheric effect on GPS carrier L1 signal for SNYP station during 69-76 day

The data obtained from SNYP totally agrees with the co-relation of data with other stations and represents the same phenomenon that occurred during the geomagnetic storm. It can be easily visualized that during the first day of event i.e., on 69<sup>th</sup> day of the year, the ion3L1 has started exceeding the cut-off of 0.002m which in the later day went upto 0.004m, which is a very slight increase.

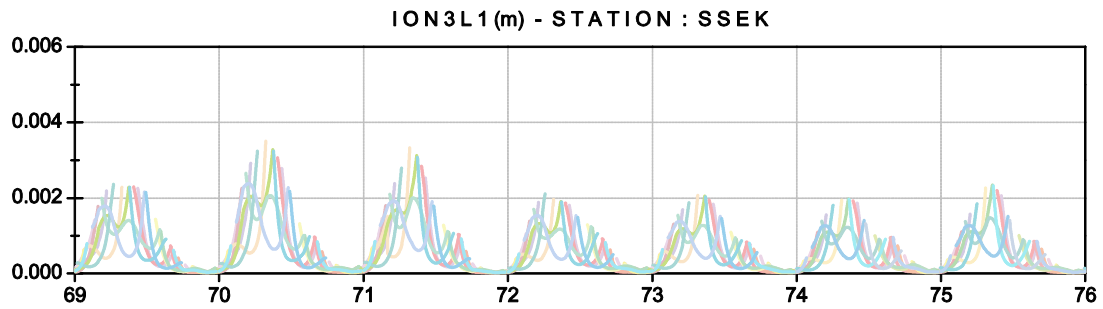


Figure20 e: Third order ionospheric effect on GPS carrier L1 signal for SSEK station during 69-76 doy

The data obtained from SSEK station about third order ionospheric scintillation is also quite resemble to previous stations due to the fact of being not far off locations with respect to each other.

Thus the data obtained by third order ionospheric effects is much clipped from the data obtained by second order ionospheric effects. Thus the distance error occurred in the positioning is also quite reduced to decimal levels. Thus improving the overall accuracy of the site.

### **Third order ionospheric effect on GPS carrier L2 signal during 69-76 doy**

Likewise we have done for GPS carrier signal L1, the data has been generated using third order ionospheric effect. The below are the graphs obtained from each stations at Singapore.

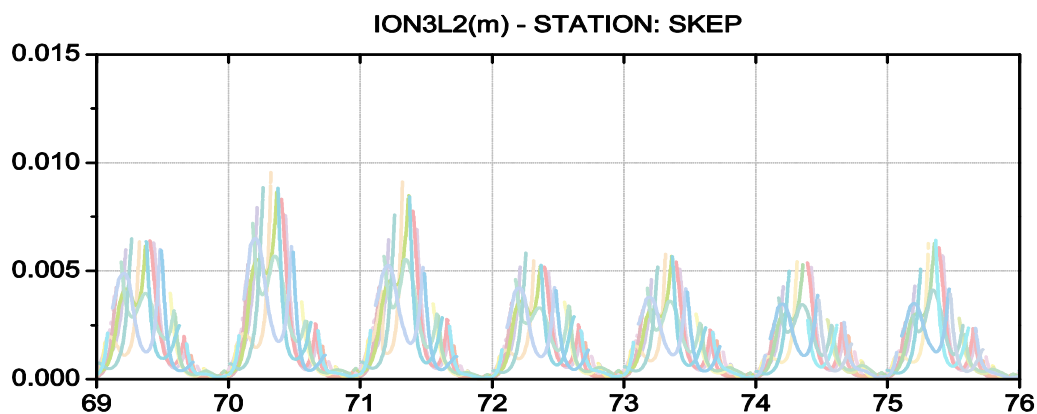


Figure: Third order ionospheric effect on GPS carrier L2 signal for SKEP station during 69-76 doy

The data obtained from SKEP station on L2 carrier signal by third order ionospheric effect is much more than that obtained by third order ionospheric effects due to L1 carrier. As we can observe the IonL2 value shoots to 0.009m during the time of occurrence of event. That continued to remain as such for the next two days.

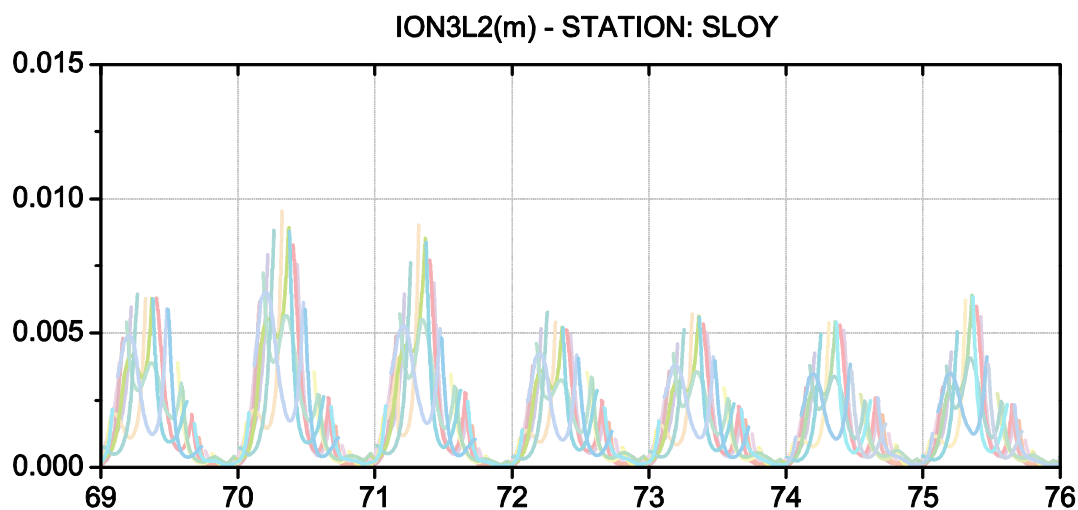


Figure 21 a: Third order ionospheric effect on GPS carrier L2 signal for SLOY station during 69-76 doy

The data obtained from SLOY station completely obey with pattern obtained at previous station. The pre event day third order ionospheric effect was around 0.007m which went to around 0.009m during the time of event and again fell down to around 0.006m in remaining days of the considered dates.



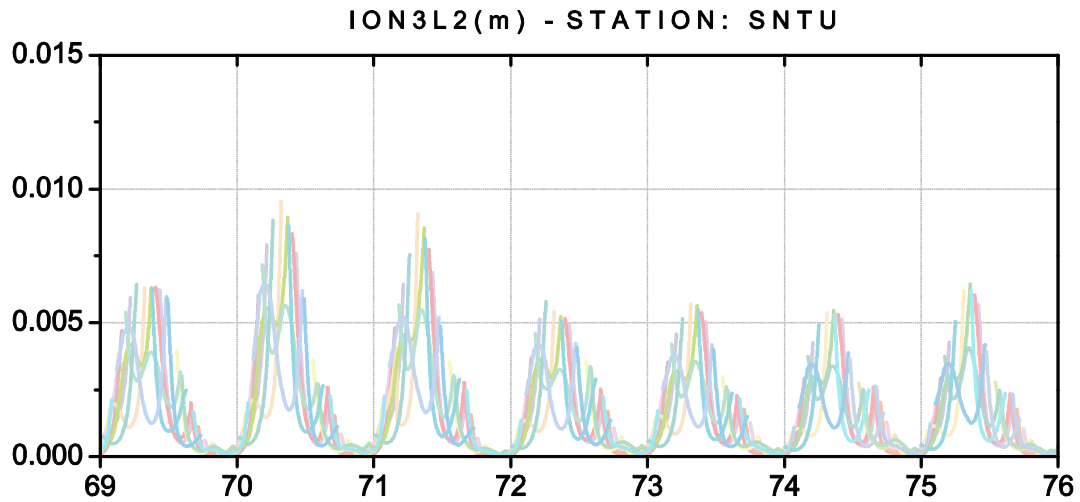


Figure 21 b: Third order ionospheric effect on GPS carrier L2 signal for SNTU station during 69-76 doy

The data obtained for the third order ionospheric effect from SNTU station agrees with deviations and fluctuations occurred due the existence of the event and totally accepts the data retrieved from SWPC and GOES-15 satellite. The whole data is again a symmetric to the data obtained from other stations.

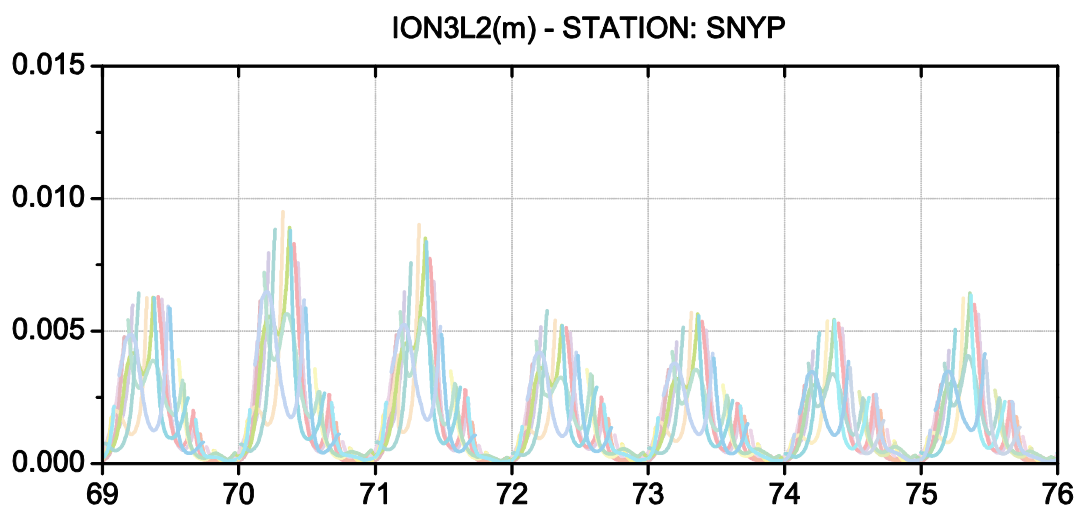


Figure 21 c: Third order ionospheric effect on GPS carrier L2 signal for SNYP station during 69-76 doy

The data obtained from SNYP station co-relates with the conditions of ionosphere during the events existence. And the third order ionospheric effect was seen quiet similar to what observed at remaining stations. A fall of ION3L2 value has been detected after the event and was again given a slight increase during the late 75<sup>th</sup> day of the year.

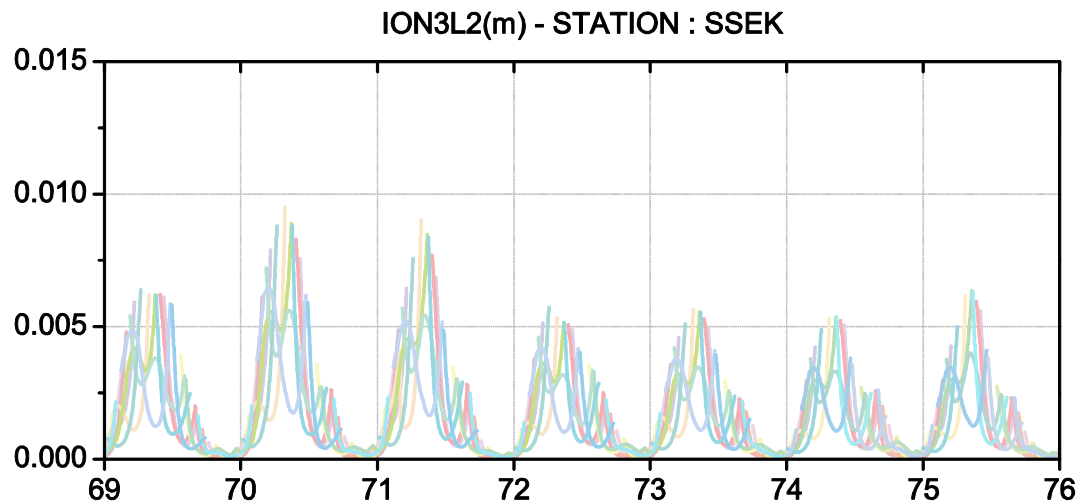


Figure 21 d: Third order ionospheric effect on GPS carrier L2 signal for SSEK station during 69-76 doy

The data obtained at SSEK station also proves to be totally agreed with data obtained at other stations. The value of third order ionospheric effect was way little compared to second order, as seen in other stations case also.

Thus, it can be verified and stated as, all data sets represent almost similar graphs and plots with same features and characteristics. So it can be concluded that all data set obtained has shown similar response to the geomagnetic storm occurred during the March 2011.

**Result from Original Rinex – Modified Rinex (from RINEX\_HO) after process by GIPSY-PPP processing**

delta X  
(cm)

DO					
Y	SKEP	SLOY	SNTU	SNYP	SSEK
69	0.041	-0.0241	-0.0238	-0.0231	-0.0195
70	-0.444	-0.0248	-0.0362	-0.0279	-0.0276
71	0.101	-0.0589	-0.0322	-0.0225	-0.025
72	-0.516	-0.0137	-0.0305	-0.0198	-0.0244
73	0.136	-0.0175	-0.0205	-0.0141	-0.0164
		0.0070		0.0077	
74	-0.0883	5	-0.0165	4	-0.0048
75	0.158	-0.0169	-0.0266	-0.0236	-0.0188

delta Y  
(cm)

DO					
Y	SKEP	SLOY	SNTU	SNYP	SSEK
69	-0.241	0.126	0.116	0.104	0.1
70	-0.964	0.129	0.135	0.136	0.125
71	0.044	0.219	0.172	0.133	0.133
72	-3.21	0.0889	0.116	0.098	0.116
73	0.0143	0.0806	0.0996	0.0764	0.0903
74	0.0962	0.0184	0.0815	0.0645	0.0484
75	-0.238	0.0675	0.0891	0.0797	0.0728

delta Z  
(cm)

DO					
Y	SKEP	SLOY	SNTU	SNYP	SSEK
69	-0.199	-0.353	-0.351	-0.356	-0.352
70	0.065	-0.397	-0.387	-0.399	-0.399
71	-0.115	-0.378	-0.367	-0.372	-0.372
72	-0.107	-0.339	-0.339	-0.340	-0.337
73	-0.046	-0.337	-0.334	0.337	-0.329
74	-0.261	-0.310	-0.323	-0.3270	-0.325
75	-0.099	-0.314	-0.322	-0.331	-0.328

The tabular shown here represents the day of year with respect to each station's response obtained after the post processing by GIPSY-PPP. The table above denotes the delays occurred during the event and the considered day of the year and how each station is being effect with this. The data is sub classified into 3-axis, for the ease of presentation.

## **8. List of Publications and Student Research Support**

### **8.1 List of Publications**

#### Journal Papers Submitted

1. Comparison of GPS TEC measurements with IRI-2007 and IRI-2012 TEC at the Equatorial latitude station, Bangkok, Thailand -- second revision undergoing , "Journal of Atmospheric and Terrestrial Physics". (Revised after review and submitted)
2. Comparison of GPS TEC measurements with IRI-2007 and IRI-2012 TEC prediction at the Equatorial Anomaly Region, Thailand -- First revision submitted and is under review, "Earth, Planets and Space" (date of submission March 30, 2014)
3. Variations of Total Electron Content in the Equatorial Anomaly Region in Thailand --- submitted to journal, "Advances in Space Research" (date of submission February 25, 2014)

#### International Conferences

1. Nitin K Tripathi, V Rajesh Chowdhary, Sanit Arunpold, Durairaju K Raju , 2013, "Ionospheric Scintillations during increasing Solar Activities using GPS" , in Asian Congress on Citizen & Environment Safety & Security, U-Town, Singapore, 5th - 7th June 2013.
2. V Rajesh Chowdhary, Nitin K Tripathi, Sanit Arunpold, Durairaju K Raju, 2012, "Study of low-latitude Ionospheric Scintillations during increasing solar activities using GPS – SCINDA data" as a author, in 4th International Conference on Geographic Information Technology for Natural Disaster Management, Colombo, Sri Lanka, 7th-8th November 2012.

## 8.2 Student Research Support

RISA project has given ample scope of performing research for the student. Two doctoral students have been pursuing their dissertation on the ionospheric studies and space weather events and their impacts.

Name: Sanit Arunpold (Doctoral Student)

Title: Probabilistic Determination of Natural Event Occurrences using Scintillation in GPS Observations

### **Abstract:**

Global Positioning System (GPS) which was developed by the United States, Department of Defense enables positioning and navigation in three dimensional spaces as its primary function. The system was designed to have 24 satellites in operation and each of it continuously transmits two high frequency carrier waves L1 and L2 of which the magnitudes are 1575.42 MHz and 1227.60 MHz, respectively (Getting, 1993). Therefore, GPS determined positioning accuracies are directly depends on the accuracies of calculated pseudo-ranges to at least four satellites (Jan, 2001). Most of the presently available GPS receivers are utilizing almost all the technical improvements in GPS hardware and processing software algorithms. However, still these GPS receivers, especially inexpensive receivers, are suffering comparatively large positioning errors due to signal propagation delays through ionosphere and troposphere, satellite and receiver clock errors, bias on ephemeris data, multipath, and receiver and measurement noises (Bradford, et al., 1996); (Xu, 2003). The GPS measurement error generally classified as either common or non-common mode errors. The common mode errors (e.g. ionosphere delay, troposphere delay, satellite clock and bias on ephemeris data) are identically affect on all the receiver measurements which operate in a limited geographical area. Noncommon mode errors (e.g. multipath, receiver and measurement noises) are distinctive and the amount of influence is dependent on the surrounding obstructions at the observation site and the technical specification of receiver hardware and software (Misra, et al., 2004).

On the other hand, the GPS error and propagation is not only for effect to positioning but can be describe some of earth phenomena also. The signals of the GPS satellites must travel through the earth's ionosphere on their way to GPS receivers on or near the earth's surface. The ionospheric scintillation is high effect to positioning of GPS. By the way, The previous study of ionospheric scintillation, show that they have some correlation between ionospheric parameter such as TEC, dst-index and S4-index with natural occurrences such as earthquake, magnetic storm, and some huge tropical storm. One of the most importance parameter to determine and show the most correlation with natural occurrence is Total Electron Content (TEC) that can derive from equation of relation to determine estimation of total electron in square meter. As the previous study confirm that during the period before and after 3-5 day of natural occurrence (Z. Yiyan., 2009) GPS station detected the TEC and another parameter have high amplitude of data.

The ultimate goal of this study is to investigate the probability estimation of natural occurrence such as earthquake, magnetic storm, and tropical storm. In order to achieve this goal, following specific objectives are to be accomplished.

- Combination of Positioning, TEC, VHF Data, S4 and related parameters to determined parametercorrelation with natural occurrence.
- Probability of natural event position / Error-Distance (PeED- Profile) for each observations stations.
- Using Neural Network method to improve accuracy in forecasting natural event occurrences byintegrating methodology data with ionospheric scintillations.



Name of the student: V Rajesh Chowdhary (Doctoral Student)

Title: Ionospheric Impact of Severe Space Weather Events on GNSS Measurements from Thailand Region

**Abstract:**

As the sun is approaching its solar maximum, the solar activity is observed to be increasing rapidly due to its 11 year solar cycle. The increase in solar activity adversely affects Earth's Ionosphere and GPS signals reaching ground based receivers. That can be a major threat to GPS users worldwide. This dissertation presents a study of effects of solar activities on ionosphere's Total Electron Content (TEC) using GPS-SCINDA station's data from Thailand region. The data used are the vertical TEC (vTEC) observed at the *Bangkok (AIT, 14.079 N, 100.612 E)* and *Chiang Mai University (CMU, 18.480 N, 98.570 E)*. AIT and CMU stations are located at 0.71° W and 0.87° W magnetic latitude respectively, a region of intense equatorial ionospheric disturbances. This study is based on data from both stations for the period July 2010 –December 2012. A brief comparison of both stations vTEC variations has been presented. During the period of study new sunspot regions were observed to be forming on the surface of the sun. Also the geomagnetic indices have exhibited an intense phenomenon due to severe space weather events. The phenomenon of TEC depletions and enhancements were observed and studied in depth during the period of research. This research also contributed to analyze the longitudinal and latitudinal variations of vTEC in the study region. The result shows very intense variations in TEC were during severe events. Also, diurnal, seasonal and annual variations of vTEC for both stations for the period of study were modelled and analyzed. And newly introduced International Reference Ionosphere-2012 (IRI-2012) model data has been utilized and compared to the GPS TEC data obtained at the both stations. Data comparison lead to the Model validation of newly released IRI-2012 version and also able to foresee the issues occurring when dealt with data over equatorial ionospheric anomaly (EIA) region.

Name of the New Student: Ms. Pragyan Parmita Das (Master's Student)

Title: Analysis of integrated GPS and QZSS signals for Ionospheric Scintillation over Equatorial Anomaly region.

**Work will start from August 2014 as the student is still completing the course work**

## 9.0 Conclusion

This report describes the activities performed in the framework of the mission carried out as part of the densification and maintenance of the SCINDA network in South East Asia. RISA project objectives were achieved as two SCINDA stations at AIT and CMU were surveyed installed and made operational since year 2010. AIT RISA team developed the capability to overcome some problems when systems were down and made it operational again. Few other sites were visited and surveyed and three locations in Timor Leste, Philippines, Phuket and Sri Lanka were surveyed for SCINDA new sites. It is a very encouraging outcome that by the end of this project the third station at Timor Leste and Phuket were installed by AIT Team and made operational.

As part of the study the data from the Singaporean SiReNT network, which currently is formed by seven stations distributed over an area of approximately 50Km by 25Km was used for analysis. The study compared the positioning solutions in single mode (using the GIPSY-OASIS software package with the Precise Point Positioning strategy) and in differential mode (using TBC, a commercial software). In addition the analysis compares the results obtained using dedicated software (RINEX\_HO) developed to correct the GPS observables for second- and third-order ionosphere effects. We show that the improvement is marginal for most positioning applications, namely for surveying, but that can slightly improve the accuracy of the derived time-series.

In this work, we also have presented the results of the analysis of vTEC and  $S_4$  calculated using GPS-SCINDA station's data from AIT, Bangkok and CMU, Chiang Mai in Thailand region, during January- August 2012. Of all the severe events considered for this study, the most severe event occurred in the month of March 2012. During this period TEC went to its peak by reaching 97 TECU which is the highest peak ever observed during other severe space weather events considered in the period of study. Both stations are susceptible to TEC depletion as both lies under ionization crest. From this study it can be stated that there exists a substantial influence of solar flare photons or CME related geomagnetic storms on the behaviour of total electron content over Thailand region. Since all these events were occurred during the solar

maximum cycle, both stations exhibited the increment in TEC as the ionosphere was highly altered.

RISA objective to generate scientific knowledge was also achieved. Two students are in final phase of their PhD thesis using the data from SCINDA stations. One more Masters student has been involved to continue the research and strengthen the research and bring out the knowledge using other extension in Phuket and also new systems like QZSS and GAGAN, These new possibilities of research have risen due to the RISA outcome.

## 10.0 Future Recommendations

RISA has given possibilities that **a research centre** may continue at AIT to keep the SCINDA stations at AIT, CMU and Phuket keep going. This will be possible by supporting the Master and Doctoral research work and also conduct seminars and workshops. Some of the recommendations came based on the input received during RISA meetings with visiting experts were:

### Extension of the RISA project

*The RISA (Research of Ionospheric Scintillation in Asia) project contributed for the development of Ionospheric studies in South-East Asia by using space-geodetic systems, in particular by analyzing data acquired using dedicated GNSS (Global Navigation Satellite Systems) networks. The results of the study are detailed in the final report (enclosed here with). RISA intends to improve the scientific knowledge on ionosphere research and GNSS data processing of the partners that are collaborating with AFRL in the region. This proposal intends to contribute directly for the current activities carried out in the framework of the RISA project .RISA will further investigate on the effects of scintillation in dense GNSS networks and the potential correlation with extreme events. The following tasks were identified to carry out under the proposed extension of the RISA project.*

- 1. Development of centralized SCINDA data archive and visualization with reception of regional data located in AIT Bangkok*
- 2. Emphasis on real time data collection and assimilation*
- 3. Perform ionosphere model validation and comparison*

## References

- Adewale, A.O., Oyeyemi, E.O., Cilliers, P.J., McKinnell, L.A., Adeloye, A.B. Low solar activity variability and IRI 2007 predictability of equatorial Africa GPS TEC. *Adv. Space Res.* 49, 316–326, 2012.
- Ackah, J.B., Obroul, O. K., Zaka, Z., Mene, M.N., Groves, K. “Study of Equatorial Ionospheric scintillation and TEC characteristics at Solar minimum using GPS-SCINDA data”, in *Sun and Geosphere*, 2011, pg. No. 23-26.
- Appleton, E.V. Two anomalies in the ionosphere. *Nature* 157, 691, 1946.
- Bhattacharya, S., Purohit, P.K., Gwal, A.K. Ionospheric time delay variations in equatorial anomaly region during low solar activity using GPS. *Indian J. Radio Space Phys.* 38, 266–274, 2009.
- Bhuyan, P.K., Borah, R.R. TEC derived from GPS network in India and comparison with the IRI. *Adv. Space Res.* 39, 830–840, 2007.
- Bilitza, D., M. Hernandez-Pajares, J. M. Juan, and J. Sanz, Comparison between IRI and GPS-IGS derived electron content during 1991-97: first results, *Phys. Chem. Earth*, 24(4), 311–319, 1998.
- Bilitza, D. International Reference Ionosphere 2000: Examples of improvements and new features. *Adv. Space Res.* 31, 151–167, 2003.
- Bilitza, D. and B. W. Reinisch, International Reference Ionosphere 2007: Improvements and new parameters, *Adv. Space Res.*, 42, 599–609, 2008.
- Basu, S., Basu, S., Rich, F.J., Groves, K.M., MacKenzie, E., Coker, C., Sahai, Y., Fagundes, P.R., Guedes, F.B. Response of the equatorial ionosphere at dusk to penetration electric fields during intense magnetic storms. *J. Geophys. Res.* 112, A08308, 2007.
- Carrano, C., Groves, k. The GPS Segment of the AFRL-SCINDA Global Network and the Challenges of Real-Time TEC Estimation in the Equatorial Ionosphere. *ION NTM 2006*, Monterey, CA, 18-20 January 1036-1047, 2006.
- Cervera, M. A., R. M. Thomas, K. M. Groves, A. G. Ramli, and Effendy (2001), Validation of wbmmod in the southeast asia region, *Radio Science*, 36 (6), 1559–1572.
- Chauhan, Vishal., Singh, O.P. A morphological study of GPS-TEC data at Agra and their comparison with the IRI model. *Adv. Space Res.* 46, 280–290, 2010.
- De La Beaujardiere, O., et al. (2004), C/nofs: a mission to forecast scintillations, *Journal of Atmospheric and Solar Terrestrial Physics*, 66 (17), 1573–1591.
- Datta-Barua, S., P. H. Doherty, S. H. Delay, T. Dehel, and J. A. Klobuchar (2003), Ionospheric scintillation effects on single and dual frequency gps positioning, in *Proceedings of ION GPS/GNSS 2003*, Institute of Navigation.

Evans, C. (2005), Ionospheric scintillation effects on gps performance and weapon's effectiveness, in 18th International Technical Meeting, Institute of Navigation; IONGNSS 2005, pp. 690–696, Institute of Navigation, Fairfax, VA.

Eranna, U., Murthy, B. R., Prasad, B.K., Manjula, R. “Effects of geomagnetic storms on VHF scintillations over near equatorial station Annapur” Ubiquitous Computing and Communication Journal, Volume 3 Number 3 pp. 55- 64, 2010.

Ezquer, R., C. Jadur, and M. Mosert, IRI95 TEC predictions for the South American peak of the equatorial anomaly, *Adv. Space Res.*, 22(6), 811–814, 1998.

Ezquer, R., C. Brunini, M. Mosert, A. Meza, R. del V. Oviedo, E. Kiorcheff, and S. M. Radicella, GPS-VTEC measurements and IRI predictions in the South American sector, *Adv. Space Res.*, 34, 2035–2043, 2004.

Groves, K., Carrano, C. 2009 Scintillation impact on GPS. Satellite Navig. Sci and Tech for Africa Workshop (23<sup>rd</sup> March – 9<sup>th</sup> April 2009, ICTP, Trieste, Italy).

Groves, K. M., et al. (1997), Equatorial scintillation and systems support, *RadioScience*, 32 (5), 2047–2064.

Huang, X. and B. W. Reinisch, Vertical electron content from ionograms in real time, *Radio Sci.*, 36(2), 335–342, 2001.

Jakowski, N., E. Sardon, and S. Schluter, GPS-Based TEC observations in comparison with IRI95 and the European TEC model NTCM2, *Adv. Space Res.*, 22(6), 803–806, 1998.

Jodogne, J. C., H. Nebdi, and R. Warnant, GPS TEC and ITEC from digisonde data compared with NEQUICK model, *Adv. Space Res.*, 2, 269–273, 2004.

Knight, M., M. Cervera, and A. Finn (1999), A comparison of predicted and measured gps performance in an ionospheric scintillation environment., in Proceedings of IONGPS-99, 12th International Technical Meeting of the Satellite Division of the Institute of Navigation, pp. 1437–1450, Institute of Navigation, Institute of Navigation, Fairfax VA.

Kenpankho, P., K. Watthanasangmechai, K., Supnithi, P., Tsugawa, T., and Maruyama, T. Comparison of GPS TEC measurements with IRI TEC prediction at the equatorial latitude station, Chumphon, Thailand. *Earth Planets Space*, 63, 365–370, 2011.

Luhr, H., Xiong, C. IRI-2007 model overestimates electron density during the 23/24 solar minimum. *Geophys. Res. Lett.* 37, L23101, [http:// dx.doi.org/10.1029/2010GL045430](http://dx.doi.org/10.1029/2010GL045430), 2010.

Maeda, H., Horizontal wind systems in the ionospheric E region deduced from the dynamo theory of geomagnetic Sq variation, Part I, *J. Geomag. Geoelectr.*, 7, 121–132, 1955.

Malik, Rakhee., Sarkar, Shivalika., Mukherjee, Shweta., Gwal, A.K. Study of ionospheric variability during geomagnetic storms. *J. Ind. Geophys. Union* 14 (1), 47–56, 2010.

Martyn, D.F. Atmospheric tides in the ionosphere. I. Solar tides in the F2 region. *Proc. Royal Soc. London A* 189, 241–260, 1947.



Maruyama, Takashi., Ma, Guanyi., Nakamara, Maho. Signature of TEC storm on 6 November 2001 derived from dense GPS receiver network and ionosonde chain over Japan. *J. Geophys. Res.* 109, A10302, [http:// dx.doi.org/10.1029/2004JA010451](http://dx.doi.org/10.1029/2004JA010451), 2004

Martyn, D. F., The Physics of the Ionosphere, *The Physical Society, London*, 260, 1955.

Matsushita, S., Campbell, Wallace H. Physics of Geomagnetic Phenomena, vols. 1-2. Academic Press, New York and London, 1967.

Mitra, S.K. Geomagnetic control of region F2 of the ionosphere. *Nature* 158, 608–669, 1946.

Misra, P., Enge, P. Global Positioning System Signals, Measurements, and Performance, second ed Ganga-Jamuna Press, 2006.

Mosert, M., R. Ezquer, C. Jadur, and R. del V. Oviedo, Time variation of total electron content over Tucuma, Argentina, *Geof. Int.*, 43(2), 143– 151, 2004.

Mosert, M., Gende, M., Brunini, C., Ezquer, R., Altadill, D. Comparisons of IRI TEC predictions with GPS and digisonde measurements at Ebro. *Adv. Space Res.* 39, 841–847, 2007.

Olwendo, J.O., Baki, P., Cilliers, P.J., Mito, C., Doherty, P. Comparison of GPS TEC measurements with IRI-2007 TEC prediction over the Kenyan region during the descending phase of solar cycle. *Adv Space Res.* 49, 914–921, 2012.

Pandey, R., Dashora, N, Observations in equatorial anomaly region of total electron content enhancements and depletions. *Ann. Geophys.* 23, 2449–2456, 2005.

Rama Rao, P.V.S., Gopi Krishna, S., Niranjana, K., Prasada, D.S.V.D. Temporal and spatial variations in TEC using simultaneous measurement from the Indian GPS network of receivers during low solar activity period of 2004–2005. *Ann. Geophys.* 24 (12), 3279–3292, 2006.

Rao, P.V.S.R., Krishna, S.G., Prasad, J.V., Prasad, S.N.V.S., Prasad, D.S.V.V.D, Niranjana, K. Geomagnetic storm effects on GPS based navigation. *Ann. Geophys.* 27, 2101–2110, 2009.

Rastogi, R. G., The diurnal development of the anomalous equatorial belt in the F2 region of the ionosphere, *J. Geophys. Res.*, 64, 727–732, 1959.

Rino, C. L. (1979b), A power law phase screen model for ionospheric scintillation, 2. strong scatter, *Radio Science*, 14.

Sardon, E., Rius, A., Zarraoa, N. Estimation of the transmitter and receiver differential biases and the ionospheric total electron from global position system observation. *Radio Sci.* 29 (3), 577–586, 1994.

Sardon, E., Zarraoa, N. Estimation of total electron content using GPS data: How stable are the differential satellite and receiver instrumental biases? *Radio Sci.* 32 (5), 1899–1910, <http://dx.doi.org/10.1029/97RS01457>, 1997.

Scida, L.A., Ezquer, R.G., Cabrera, M.A., Mosert, M. IRI 2001/90 TEC predictions over a low latitude station. *Adv. Space Res.* 44, 736–741, 2009.

Seemala, G.K., Valladares, C.E. Statistics of total electron content depletions observed over the South American continent for the year 2008. *Radio Sci.* 46, RS5019, doi:10.1029/2011RS004722, 2008.

Sethi, N.K., Dabas, R.S., Sarkar, S.K. Validation of IRI-2007 against TEC observations during low solar activity over Indian sector. *J. Atmos. Solar-Terr. Phy.* 73, 751–759, 2011.

Theodore, L.B., Paul, M.K. Simultaneous global positioning system observations of equatorial scintillations and total electron content fluctuations. *J. Geophys. Res.* 104 (A10), 22,553–22,565, 1999.

Thomas, R.M., et al. (2001), A regional gps receiver network for monitoring equatorial scintillation and total electron content, *Radio Science*, 36 (6), 1545–1557.

Thomas, R. M., M. A. Cervera, A. G. Ramli, Effendy, P. Totarong, K. M. Groves, and P. J. Wilkinson (2004), Seasonal modulation of gps performance due to equatorial scintillation, *Geophysical Research Letters*, 31 (18), doi: 10.1029/2004GL020581.

Tsurutani, B.T., Verkhoglydova, O.P., Mannucci, A.J., Araki, T., Sato, A., Tsuda, T., Yumoto, K. Oxygen ion uplift and satellite drag effects during the 30 October 2003 Daytime super fountain event. *Ann. Geophys.* 25, 569–574, 2007.

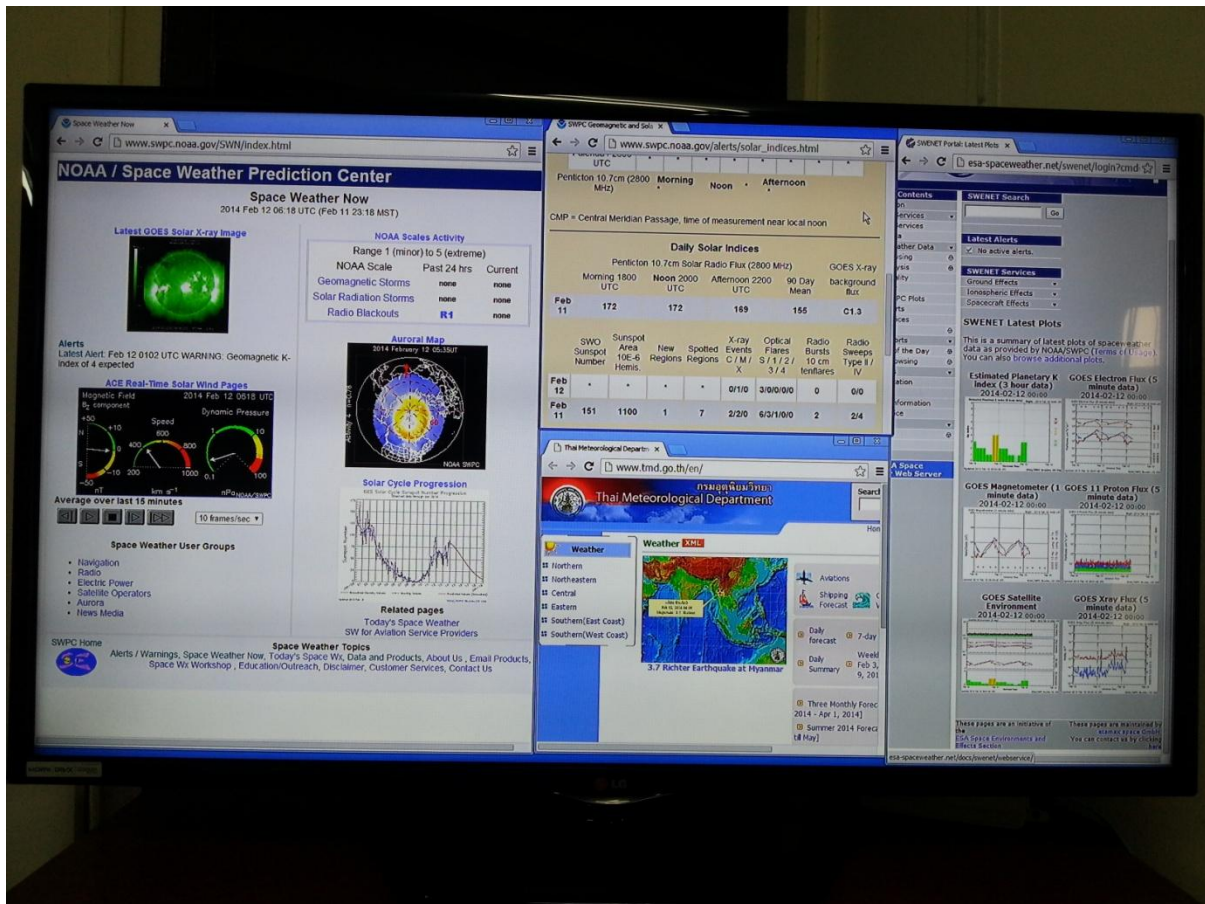
Tsurutani, B.T., Mannucci, A., Iijima, B., Abdu, M.A., Sobral, J.H.A., Gonzalez, W.D., Guarnieri, F.L., Tsuda, T., Saito, A., Yumoto, K., Fejer, B., Fuller-Rowell, T.J., Kozyra, J., Foster, J.C., Coster, A.J., Vasyliunas, V.M. Global dayside ionospheric uplift and enhancement associated with interplanetary electric fields. *J. Geophys. Res.* A08302, <http://dx.doi.org/10.1029/2003JA010342>, 2004.

Valladares, C.E., Villalobos, J., Hei, M.A., Sheehan, R., Basu, Su., Mackenzie, E., Doherty, P.H., Rios, V.H. Simultaneous observation of travelling ionospheric disturbances in the Northern and Southern hemisphere's. *Ann. Geophys.* 27, 1501–1508, 2009.

Xu, Zhenzhong, Weimin, Wang., Nan, Zhou., Xiaofei, Song., Haotian, Zh.u. Variability study of ionospheric total electron content at crest of equatorial anomaly in China from 1997 to 2007. *Adv. Space Res.* 50, 70–76, 2012.

## Appendix-A

### Photo of Monitor in RISA Project Room



## Asian Institute of Technology

School of Engineering and Technology

Remote Sensing and GIS FoS

Milton Bender Auditorium

17 October 2012

### Workshop

#### Ionospheric Scintillations Monitoring using GPS



You are kindly invited to joint

workshop between AIT and ICAO (International Civil Aviation Organisation) on Ionospheric Scintillation Monitoring using GPS.

#### Schedule

Time	Item
10:00	ICAO Ionospheric Studies Task Force (ISTF) arrives AIT
10:10	Welcome by Dean- SET
10:15	Brief presentation by ISTF on the scope of the work being carried out by ISTF
10:35	Presentation by AIT
11:10	Visit to the data collection site and other relevant facilities Discussions and development of a consensus for cooperation/coordination
11:30	Lunch

Pl. confirm by e-mail to [nitinkt@ait.asia](mailto:nitinkt@ait.asia).

Dr. Nitin Kumar Tripathi

Associate Dean, School of Engg and Technology

Coordinator, Remote Sensing and GIS, Asian Institute of Technology

P.O. Box:44, Klong Luang, Pathumthani 12120, Thailand

Phone: +66-81751 8384 (Mobile), +66-2-524 6392(Office),

e-mail: [nitingis@gmail.com](mailto:nitingis@gmail.com), [nitinkt@ait.asia](mailto:nitinkt@ait.asia)



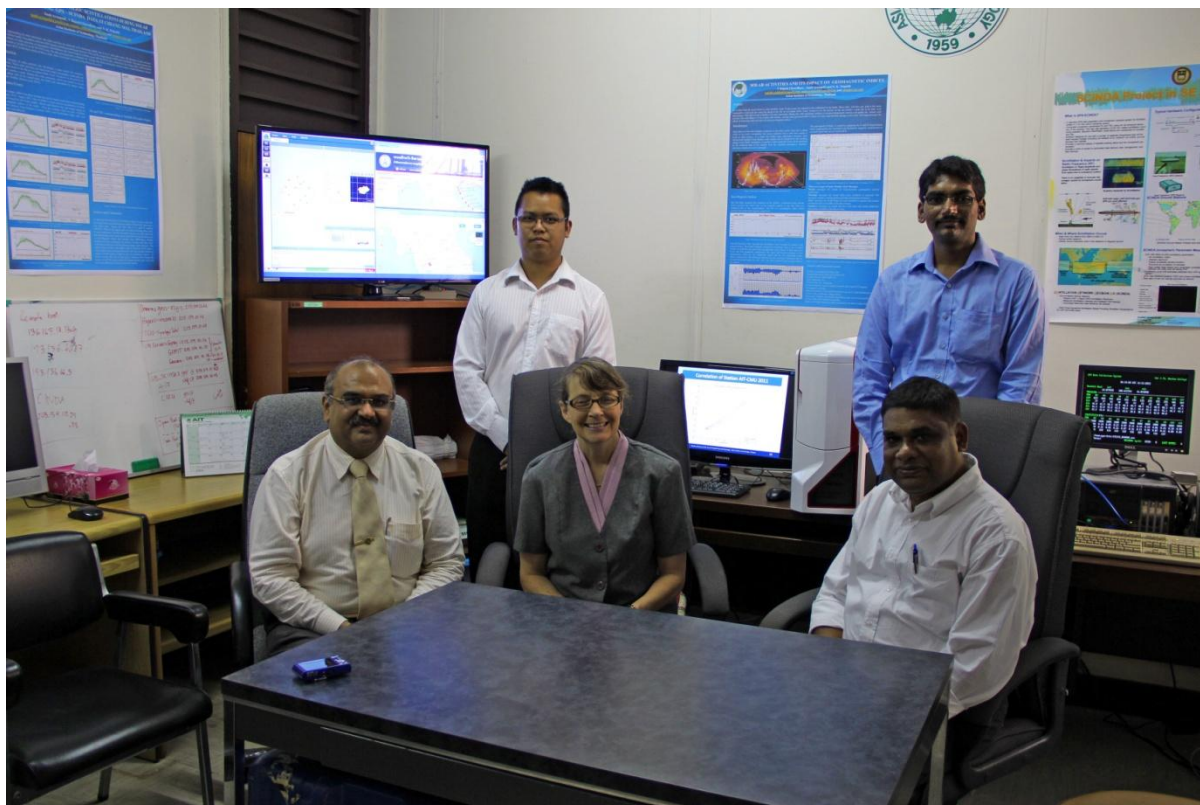






## Appendix-C

### Visit of Dr Ingrid Wysong, Program Officer, AORD for RISA Project Meeting in 2013



## Appendix-D

### Summary Meeting with Dr.Susumo @ NUS, Singapore

**Date: 11-02-2014**

#### **An Agenda following the meeting as following:**

- Welcome and Overview of meeting : Dr.Raju
- Present RISA Project and current Work : Sanit
- Online skype meeting with Dr.Nitin and Mr. Rajesh @ AIT
- Discuss Topic:
  - About Workshop on March 2014
  - Collaboration with join knowledge and Data Sharing
  - Opening Discussion Issues and problem of study

#### **Summary**

Welcome message and overview of meeting, Dr.Raju explained about SCIDA Project , site reference data archived, station and the framework. Then followed the RISA project with currently work done. Then Mr.Sanit presented about his research over the SCINDA project and RISA project following the objective study as following:

1. The research aims to monitor diurnal, seasonal and annual variations of TEC and S4 in the GPS-SCINDA stations { AIT Bangkok, CMU Chiang Mai }
2. To monitor the correlations and variations in TEC and S4 during severe space weather events at various SCINDA stations.
3. To calculate the positioning errors during severe space weather events.
4. IRI-2007,IRI-2012 and AIT & CMU TEC data comparison and model validation.
5. To model TEC and S4 data into real time maps.

Then Dr.Susumo recommended about the study in phenomena about physical concept of plasma bubble. Healso suggestd about the selection of site and parameters for identification of space weather event should be separated in High, Mid and Low latitude.

